

AN EXPERIMENTAL INVESTIGATION OF THE EFFECTS
OF VARYING WORKING CONDITIONS ON THE CHARAC-
TERISTICS OF EXPLOSIVE COMBUSTION IN A GAS
ENGINE.

-----oOo-----

By

James Small

-oOo-

February 1930.

ProQuest Number: 13905321

All rights reserved

INFORMATION TO ALL USERS

The quality of this reproduction is dependent upon the quality of the copy submitted.

In the unlikely event that the author did not send a complete manuscript and there are missing pages, these will be noted. Also, if material had to be removed, a note will indicate the deletion.



ProQuest 13905321

Published by ProQuest LLC (2019). Copyright of the Dissertation is held by the Author.

All rights reserved.

This work is protected against unauthorized copying under Title 17, United States Code
Microform Edition © ProQuest LLC.

ProQuest LLC.
789 East Eisenhower Parkway
P.O. Box 1346
Ann Arbor, MI 48106 – 1346

1.

An experimental investigation of the effects of
Varying Working Conditions on the Characteristics of
Explosive Combustion in a Gas Engine.

Introduction.

In most thermodynamic analyses of the gas engine working cycle, it is found that the period of combustion is left out of account, and, in the infrequent cases in which it is dealt with, such results as may be obtained from it are regarded as unreliable because of the very great uncertainty which exists about the condition of the gaseous charge during the burning period. This is due to the very special difficulties which are to be overcome in any attempt to find out what is happening in the cylinder of the engine during the explosive stage.

A related problem is that of knowing within what limits in the cycle that state of thermal instability which follows ignition may be assumed to exist.

No examination of the process of combustion in gas engines is likely at the present stage to lead to a mastery of its characteristics, for at the instant of combustion the burning mass is equally outside the experience of the chemist, the physicist and the engineer. It is composed of a number of chemical "complexes"—that is to say, gaseous matter of no recognised chemical form—the structural system of which is in a state of intense vibration giving rise to radiation of long or of short wave lengths, or of both. Its thermodynamic condition is not satisfactorily expressible since the number of molecules of the gas ~~initially~~, and the quantity and the quality of the energy radiated during the combustion period/

period are variable with respect to time and with respect to the composition of the initial charge.

The investigator therefore can do little more than record his observations of the effects of varying factors and thus contribute to the framework of facts upon which a comprehensive theory may ultimately be built.

Investigations of the explosive combustion of gases have fallen roughly into three categories. The first is the observation of the effects of varying combustion conditions upon engine performance, embracing a study of turbulence and speed of combustion; the second contains experiments on the heat losses and the changes in temperature, ~~the~~ pressure and ~~the~~ specific heat of gases exploded in a stationary closed vessel. The third comprises all the visual observations upon flame - speed and luminosity of combustion in glass vessels.

These categories are represented respectively by Clerk's Experiments on the speed of inflammation with and without turbulence; by Hopkinson's and David's experiments on explosion temperatures and heat losses by conduction and radiation; and by the photographic work of Dixon, Ellis and Wheeler, and Bone and his associates.

From the engineer's point of view the disadvantage of work such as Hopkinson's and David's is that it was carried out at comparatively low pressures in a stationary vessel under non-turbulent conditions and with the cylinder walls at the atmospheric temperature.

The/

(1) B.A.Gaseous Explosions Committee. Fifth Report.
(2) Proc.Roy.Soc. A77. 1906 p.387.
(3) Phil.Frans.Roy.Soc. A211 p.375.
Proc.Inst.Mech.Engrs. Vol.II. 1924 p.741.
(4) Vide "Flame and Combustion in Gases" Bone and Townend.
(5) Journal of Chem.Socy.Feb. 1927.
(6) Vide "Flame and Combustion in Gases" Bone and Townend.

The speed of propagation of the flame was low and the rates of cooling could not be considered as closely comparable with those in a gas engine.

The photographic experiments - perhaps the most remarkable examples of which are those recently reported by Bone and Fraser ⁽¹⁾ - suffer from the disadvantage that they are necessarily carried out at low pressure and also that there are no simultaneous records of pressure or temperature changes.

There is, however, considerable value in photographic records as an indication of the mode of propagation of combustion in an exploded mass of gas. It would be much better, therefore, if simultaneous pressure and temperature records were available to enable the observer to co-relate the visual phenomena with the thermal and physical changes which accompany them.

In some of the work herein described the attempt has been made to do this for the combustion of the gaseous charge in the gas engine.

Among the points about which there has been some discussion and divergence of view is whether the instant at which maximum pressure is reached corresponds (assuming a spherical vessel with the igniting spark at the centre) to the instant at which the flame front reaches the walls. ⁽²⁾ And another point at issue is whether chemical stability is complete by the time the flame reaches the walls of the vessel. The record of the luminous part of the combustion in conjunction with that of pressure changes, has a bearing on these matters.

The/

(1) Phil. Trans. Roy. Socy. 1929. Vol. 228A, p. 197.

(2) Hopkinson Proc. Roy. Socy. Vol. 77A 1906.

Wheeler and Payman Trans. Chem. Socy. 123 (1923).

"Flame and Combustion in Gases" Bone and Townend, p. 136.

The duration of the luminous condition has been found in the present tests to vary with certain working conditions other than the air/gas ratio. The manner of this variation is of considerable interest from the point of view of heat lost by radiation from the burning charge. It will be seen that visual examination of the explosion, simultaneously with the taking of pressure and other records, has an important bearing on the subject of "after-burning" - a conception of the combustion process which gave rise to much divergence of view when put forward by Clerk many years ago and is still a subject of serious discussion among chemists and engineers. (1) The bearing of these tests upon this subject led to inclusion in this experimental work of an application of Clerk's "zig-zag Diagram" method (2) to the determination of heat losses in an engine cylinder in order to test his deductions. This is the first attempt as far as the writer knows to repeat Clerk's experiment in its entirety.

Perhaps the most fruitful part of the work herein described is that in which careful observations of the radiations in the red band of the spectrum were made by means of a polarising pyrometer during the combustion stage under different conditions of spark-angle and of air/gas ratio. These provide ground for speculation on the distribution of temperature throughout the gaseous mass and on the factors controlling the general radiation during combustion.

Arrangement/

(1) Vide "Heat Loss in Gas Engines" by W.T.David. Proc. Inst.of Mech.Eng. 1924 Vol.II.

(2) Proc.Roy.Socy. Vol.77A 1906.

Arrangement of the Report.

If the tests were described strictly in the chronological order in which they were performed there would be an apparent lack of cohesion. On the other hand it is highly desirable that the work in general should be described in the order in which it developed so that modifications made to the apparatus may be more readily understood. A compromise seems to be called for and the arrangement of the report adopted is as follows:

- I. A discussion of the displaced or out-of-phase indicator diagram, its geometry and transformation (this was used in all the tests).
- II. A description of the apparatus devised by the writer for all the tests in general and of the apparatus designed for the photographic records in particular.
- III. An examination of photographic records of combustion obtained under noted conditions, and some auxiliary tests of collateral effects on exhaust temperature, etc.
- IV. A description of tests made to examine the effects of working conditions on the indicator diagram, and a suggested method of obtaining an approximate figure for the rate of loss of heat from the working substance during the combustion.
- V. A review of Clerk's "zig-zag diagram" method for obtaining rates of heat loss and specific heats, and a commentary on his results.
- VI. A description of the apparatus used and the tests made in examining the characteristic changes in the radiation of the red band of the spectrum during the combustion in the engine under different working conditions.

SECTION I

THE "OUT-OF-PHASE" INDICATOR DIAGRAM.

The ordinary indicator diagram taken from an internal combustion engine has the disadvantage that the ignition and combustion processes take place near the end of the stroke where the piston speed is nearly zero. The result is a crowding together of important pressure-volume changes in such a way as to render them obscure. It has become a common practice, for certain purposes, to put the indicator drive out of phase with the crank so that the piston displacement scale is opened up and the changes near the crank dead-centre are more easily traced by the observer. For accurate quantitative and analytical work, however, this type of diagram has not, as far as the writer knows, been seriously used. For the investigations later described, an out-of-phase indicator drive was necessary since it was the aim to measure time and crank angles during the explosion period. But the diagram has advantages apart from its property of magnifying the volume changes at the dead centre. The errors due to the drum friction and to drum inertia are most pronounced in their effects on the length of the drum cord at the ends of the diagram. By the displacement of the diagram, these effects are removed from the record of the combustion process.

Geometry of the Diagram. If the ratio of the length (l) of the connecting rod to the length (r) of the crank is denoted by n it may be shown that for any position of the crank at an angle β to the inner dead centre (see Fig. 1) the piston displacement (s) from the beginning of its stroke is given by

$$s = r(1 - \cos\beta) + l\left(1 - \frac{1}{n}\sqrt{n^2 - \sin^2\beta}\right) \text{-----} (1)$$

Now/

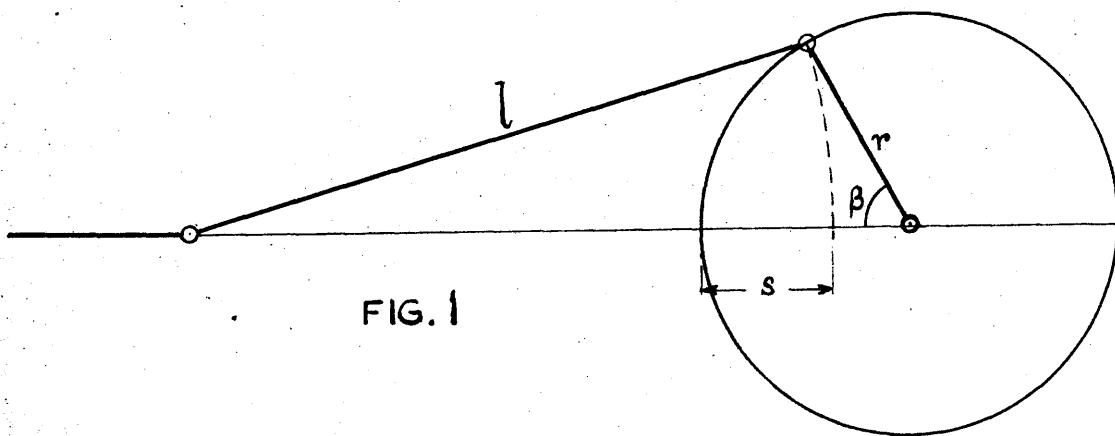


FIG. 1

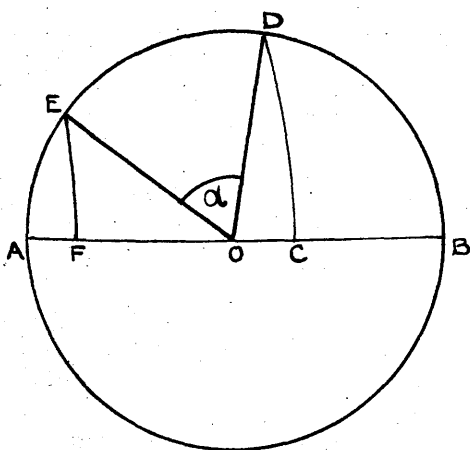


FIG. 2

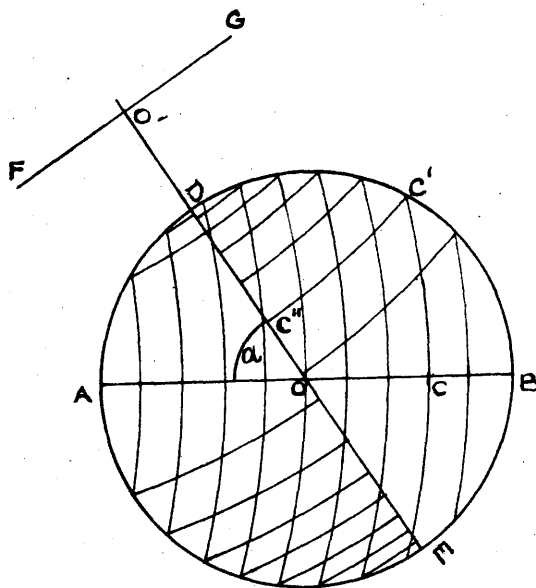
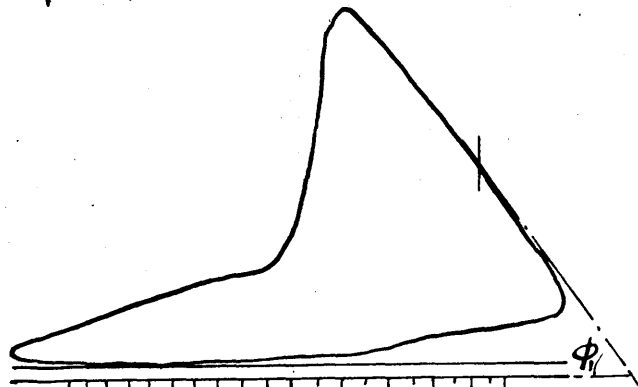
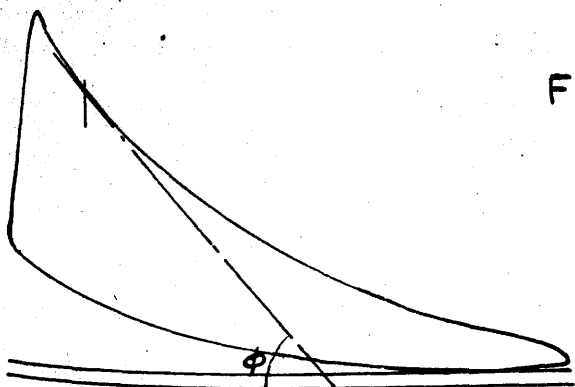


FIG. 3

FIG. 5



-40 -30 -20 -10 0 10 20 30 40
 SCALE OF ANGLES FOR UPPER BOUNDARY

Now if the connecting rod and crank in question are those of the auxiliary gear driving the indicator, and if this auxiliary crank is set at an angle α in advance of that of the engine we can express the displacement of one in terms of the displacement of the other. This is what is required in transforming the displaced diagram into the ordinary diagram. The stroke is $2r$ and therefore the fractional displacement (from equation (1)) is

$$f = \frac{s}{2r} = \frac{1}{2} - \frac{\cos\beta}{2} + \frac{n}{2} - \frac{1}{2} \sqrt{n^2 - \sin^2\beta} \quad \text{--- (2)}$$

Solving for β we have,

$$\begin{aligned} \sqrt{n^2 - \sin^2\beta} &= 1 - \cos\beta + n - 2f \\ n^2 - \sin^2\beta &= 1 + \cos^2\beta + n^2 + 4f^2 - 2\cos\beta + 2n - 4f - 2n\cos\beta + 4f\cos\beta - 4fn \\ &= (n+1-2f)^2 - 2\cos\beta(1+n-2f) \\ \cos\beta &= \frac{(n+1-2f)^2 - (n^2-1)}{2(n+1-2f)} = \frac{n+1-2f}{2} - \frac{n^2-1}{2(n+1-2f)} \quad \text{--- (3)} \end{aligned}$$

As a check on this result we note that $\cos\beta = 1$ when $f = 0$ and $\cos\beta = -1$ when $f = 1$.

The symbol f denotes the fractional displacement of some point on the out-of-phase diagram. Solve for β .

Substituting $(\beta-\alpha)$ for β in the above expression we get two values for f which are values of the corresponding alternative displacements on the true diagram. One of the two roots applies to the forward stroke and the other to the return stroke of the piston.

Writing θ for $(\beta-\alpha)$ and f' for the true fractional displacement of the piston we have from (2).

$$\begin{aligned} f' &= \frac{1}{2} \left\{ 1 - \cos\theta + n - \sqrt{n^2 - \sin^2\theta} \right\} \\ &= \frac{n+1}{2} - \frac{1}{2} \left\{ \cos\theta + \sqrt{n^2 - \sin^2\theta} \right\} \quad \text{--- (4)} \end{aligned}$$

Choice of phase angle. The common practice is to make $\alpha = 90^\circ$. This has the great advantage of simplifying the relationship so that the two roots of (2) are equal/

equal. But it will be seen that when the crank of the engine is on its inner dead centre the corresponding displacement on the displaced diagram is greater than half the stroke. That is to say, the motion of the engine piston through more than half of its stroke from the inner dead centre is recorded on the displaced diagram by considerably less than half the length of the diagram. For the particular purpose to which the displaced diagram was applied in the investigations reported later, this was a definite difficulty. A value of α less than 90° had to be chosen. What was considered the next best choice was that angle which made the mid-point of the displaced diagram coincide with the inner dead centre. To find this angle, α , put r for s in equation (1).

$$r = r(1 - \cos\alpha) + l\left(1 + \frac{1}{n} \sqrt{n^2 - \sin^2\alpha}\right)$$

$$\cos\alpha = n\left(1 - \frac{1}{n} \sqrt{n^2 - \sin^2\alpha}\right)$$

$$\text{or } n - \cos\alpha = \sqrt{n^2 - \sin^2\alpha}$$

$$\text{Squaring } \cos^2\alpha - 2n \cos\alpha + n^2 = n^2 - \sin^2\alpha$$

$$\therefore 2n \cos\alpha = 1 \quad \text{or} \quad \cos\alpha = \frac{1}{2n}$$

In the engine under review $l = 41.35$ ins and $r = 7.5$ ins so that $n = \frac{41.35}{7.5} = 5.5133$.

Substituting this in (4) we get $\alpha = 84^\circ 48'$.

The crank angle corresponding to maximum piston speed is very nearly 80° . Indicator drum cord effects are therefore at a minimum near the mid-point of the displaced diagrams.

When the more troublesome calculations involved in using an odd phase angle are once made and tabulated it has the very definite advantage that a simple bisection of the displaced diagram provides us at once with the conditions at the inner dead centre of the piston.

Calculated/

Calculated transforming values.

When the phase angle was fixed, the fractional displacements on the true diagram corresponding to fortieths and fiftieths of the stroke on the displaced diagrams were calculated. These are collected in Table 1. The values are given to more than the practical degree of accuracy; but the table, the figures on which were run out on a calculating machine, is now standard for the engine. A perusal of the values gives a very clear idea of the manner in which they vary.

Geometrical construction for transforming diagram.

Referring to Fig. 2, p. 7, let OD represent the displaced crank driving the indicator while OE, at an angle α behind it, represents the crank of the engine. The horizontal diameter AB represents the stroke. With a radius equal to n times OD or OE and with centres on BA produced, draw arcs DC and EF. Now the fractional displacement on the displaced diagram is $\frac{AC}{AB}$, corresponding to the true fractional displacement of the piston $\frac{AF}{AB}$. It is clear how a displacement AC on the displaced diagram may be transformed to the displacement AF on the true diagram.

A chart constructed in the following manner, however, affords a means of transforming rapidly the one diagram to the other, with a sufficient degree of approximation. In Fig. 3, p. 7 the horizontal diameter AB again represents the stroke. Draw DE at α to AB as shown. Now divide DE into as many equal parts as may be desired. With radius equal to n times OA, and centre on BA produced, draw arcs from the point of division, such as C, to cut the circumference of the circle/

TABLE I

TABLE I

FRACTION OF STROKE	DISPACED STROKE DIAGRAM	FRACTION OF STROKE	$\theta = \beta - 84.48'$		$\sin \theta_1$	$\sin \theta_2$	$\cos \theta_1$	$\cos \theta_2$	$\sin^2 \theta_1$	$\sin^2 \theta_2$	$\sin^2 \theta_1 \sin^2 \theta_2$	$\theta_1 - \sin^2 \theta_1$	$\theta_2 - \sin^2 \theta_2$	$\theta_1^2 - \sin^2 \theta_1^2$	$\theta_2^2 - \sin^2 \theta_2^2$	$\sqrt{\theta_1^2 - \sin^2 \theta_1^2}$	$\sqrt{\theta_2^2 - \sin^2 \theta_2^2}$	$\cos \theta_1 + \sqrt{\theta_1^2 - \sin^2 \theta_1^2}$	$\cos \theta_2 + \sqrt{\theta_2^2 - \sin^2 \theta_2^2}$	$\cos \theta_1 + \sqrt{\theta_1^2 - \sin^2 \theta_1^2}$	$\cos \theta_2 + \sqrt{\theta_2^2 - \sin^2 \theta_2^2}$	FRACTION OF STROKE
			θ_1	θ_2																		
0	0	0	84° 48'	84° 48'	0.99588	0.99588	0.00663	0.00663	0.99178	0.99178	0.99178	29.40470	29.40470	5.42261	5.42261	5.42261	5.42261	5.1324	5.1324	5.1324	5.1324	0.50000
0.02	0.02	0.02	84° 50'	84° 50'	0.99586	0.99586	0.00664	0.00664	0.99176	0.99176	0.99176	29.40534	29.40534	5.42255	5.42255	5.42255	5.42255	5.1324	5.1324	5.1324	5.1324	0.62921
0.025	0.025	0.025	84° 51'	84° 51'	0.99584	0.99584	0.00665	0.00665	0.99174	0.99174	0.99174	29.40598	29.40598	5.42249	5.42249	5.42249	5.42249	5.1324	5.1324	5.1324	5.1324	0.63399
0.03	0.03	0.03	84° 52'	84° 52'	0.99582	0.99582	0.00666	0.00666	0.99172	0.99172	0.99172	29.40662	29.40662	5.42243	5.42243	5.42243	5.42243	5.1324	5.1324	5.1324	5.1324	0.68849
0.035	0.035	0.035	84° 53'	84° 53'	0.99580	0.99580	0.00667	0.00667	0.99170	0.99170	0.99170	29.40726	29.40726	5.42237	5.42237	5.42237	5.42237	5.1324	5.1324	5.1324	5.1324	0.70065
0.04	0.04	0.04	84° 54'	84° 54'	0.99578	0.99578	0.00668	0.00668	0.99168	0.99168	0.99168	29.40790	29.40790	5.42231	5.42231	5.42231	5.42231	5.1324	5.1324	5.1324	5.1324	0.71861
0.045	0.045	0.045	84° 55'	84° 55'	0.99576	0.99576	0.00669	0.00669	0.99166	0.99166	0.99166	29.40854	29.40854	5.42225	5.42225	5.42225	5.42225	5.1324	5.1324	5.1324	5.1324	0.74246
0.05	0.05	0.05	84° 56'	84° 56'	0.99574	0.99574	0.00670	0.00670	0.99164	0.99164	0.99164	29.40918	29.40918	5.42219	5.42219	5.42219	5.42219	5.1324	5.1324	5.1324	5.1324	0.77627
0.055	0.055	0.055	84° 57'	84° 57'	0.99572	0.99572	0.00671	0.00671	0.99162	0.99162	0.99162	29.40982	29.40982	5.42213	5.42213	5.42213	5.42213	5.1324	5.1324	5.1324	5.1324	0.80495
0.06	0.06	0.06	84° 58'	84° 58'	0.99570	0.99570	0.00672	0.00672	0.99160	0.99160	0.99160	29.41046	29.41046	5.42207	5.42207	5.42207	5.42207	5.1324	5.1324	5.1324	5.1324	0.82025
0.065	0.065	0.065	84° 59'	84° 59'	0.99568	0.99568	0.00673	0.00673	0.99158	0.99158	0.99158	29.41110	29.41110	5.42201	5.42201	5.42201	5.42201	5.1324	5.1324	5.1324	5.1324	0.82988
0.07	0.07	0.07	84° 59'	84° 59'	0.99566	0.99566	0.00674	0.00674	0.99156	0.99156	0.99156	29.41174	29.41174	5.42195	5.42195	5.42195	5.42195	5.1324	5.1324	5.1324	5.1324	0.83951
0.075	0.075	0.075	85° 0'	85° 0'	0.99564	0.99564	0.00675	0.00675	0.99154	0.99154	0.99154	29.41238	29.41238	5.42189	5.42189	5.42189	5.42189	5.1324	5.1324	5.1324	5.1324	0.84914
0.08	0.08	0.08	85° 0'	85° 0'	0.99562	0.99562	0.00676	0.00676	0.99152	0.99152	0.99152	29.41302	29.41302	5.42183	5.42183	5.42183	5.42183	5.1324	5.1324	5.1324	5.1324	0.85877
0.085	0.085	0.085	85° 1'	85° 1'	0.99560	0.99560	0.00677	0.00677	0.99150	0.99150	0.99150	29.41366	29.41366	5.42177	5.42177	5.42177	5.42177	5.1324	5.1324	5.1324	5.1324	0.86840
0.09	0.09	0.09	85° 1'	85° 1'	0.99558	0.99558	0.00678	0.00678	0.99148	0.99148	0.99148	29.41430	29.41430	5.42171	5.42171	5.42171	5.42171	5.1324	5.1324	5.1324	5.1324	0.87803
0.095	0.095	0.095	85° 2'	85° 2'	0.99556	0.99556	0.00679	0.00679	0.99146	0.99146	0.99146	29.41494	29.41494	5.42165	5.42165	5.42165	5.42165	5.1324	5.1324	5.1324	5.1324	0.88766
0.1	0.1	0.1	85° 2'	85° 2'	0.99554	0.99554	0.00680	0.00680	0.99144	0.99144	0.99144	29.41558	29.41558	5.42159	5.42159	5.42159	5.42159	5.1324	5.1324	5.1324	5.1324	0.89729
0.105	0.105	0.105	85° 3'	85° 3'	0.99552	0.99552	0.00681	0.00681	0.99142	0.99142	0.99142	29.41622	29.41622	5.42153	5.42153	5.42153	5.42153	5.1324	5.1324	5.1324	5.1324	0.90692
0.11	0.11	0.11	85° 3'	85° 3'	0.99550	0.99550	0.00682	0.00682	0.99140	0.99140	0.99140	29.41686	29.41686	5.42147	5.42147	5.42147	5.42147	5.1324	5.1324	5.1324	5.1324	0.91655
0.115	0.115	0.115	85° 4'	85° 4'	0.99548	0.99548	0.00683	0.00683	0.99138	0.99138	0.99138	29.41750	29.41750	5.42141	5.42141	5.42141	5.42141	5.1324	5.1324	5.1324	5.1324	0.92618
0.12	0.12	0.12	85° 4'	85° 4'	0.99546	0.99546	0.00684	0.00684	0.99136	0.99136	0.99136	29.41814	29.41814	5.42135	5.42135	5.42135	5.42135	5.1324	5.1324	5.1324	5.1324	0.93581
0.125	0.125	0.125	85° 5'	85° 5'	0.99544	0.99544	0.00685	0.00685	0.99134	0.99134	0.99134	29.41878	29.41878	5.42129	5.42129	5.42129	5.42129	5.1324	5.1324	5.1324	5.1324	0.94544
0.13	0.13	0.13	85° 5'	85° 5'	0.99542	0.99542	0.00686	0.00686	0.99132	0.99132	0.99132	29.41942	29.41942	5.42123	5.42123	5.42123	5.42123	5.1324	5.1324	5.1324	5.1324	0.95507
0.135	0.135	0.135	85° 6'	85° 6'	0.99540	0.99540	0.00687	0.00687	0.99130	0.99130	0.99130	29.42006	29.42006	5.42117	5.42117	5.42117	5.42117	5.1324	5.1324	5.1324	5.1324	0.96470
0.14	0.14	0.14	85° 6'	85° 6'	0.99538	0.99538	0.00688	0.00688	0.99128	0.99128	0.99128	29.42070	29.42070	5.42111	5.42111	5.42111	5.42111	5.1324	5.1324	5.1324	5.1324	0.97433
0.145	0.145	0.145	85° 7'	85° 7'	0.99536	0.99536	0.00689	0.00689	0.99126	0.99126	0.99126	29.42134	29.42134	5.42105	5.42105	5.42105	5.42105	5.1324	5.1324	5.1324	5.1324	0.98396
0.15	0.15	0.15	85° 7'	85° 7'	0.99534	0.99534	0.00690	0.00690	0.99124	0.99124	0.99124	29.42198	29.42198	5.42099	5.42099	5.42099	5.42099	5.1324	5.1324	5.1324	5.1324	0.99359
0.155	0.155	0.155	85° 8'	85° 8'	0.99532	0.99532	0.00691	0.00691	0.99122	0.99122	0.99122	29.42262	29.42262	5.42093	5.42093	5.42093	5.42093	5.1324	5.1324	5.1324	5.1324	0.99322
0.16	0.16	0.16	85° 8'	85° 8'	0.99530	0.99530	0.00692	0.00692	0.99120	0.99120	0.99120	29.42326	29.42326	5.42087	5.42087	5.42087	5.42087	5.1324	5.1324	5.1324	5.1324	0.99285
0.165	0.165	0.165	85° 9'	85° 9'	0.99528	0.99528	0.00693	0.00693	0.99118	0.99118	0.99118	29.42390	29.42390	5.42081	5.42081	5.42081	5.42081	5.1324	5.1324	5.1324	5.1324	0.99248
0.17	0.17	0.17	85° 9'	85° 9'	0.99526	0.99526	0.00694	0.00694	0.99116	0.99116	0.99116	29.42454	29.42454	5.42075	5.42075	5.42075	5.42075	5.1324	5.1324	5.1324	5.1324	0.99211
0.175	0.175	0.175	85° 10'	85° 10'	0.99524	0.99524	0.00695	0.00695	0.99114	0.99114	0.99114	29.42518	29.42518	5.42069	5.42069	5.42069	5.42069	5.1324	5.1324	5.1324	5.1324	0.99174
0.18	0.18	0.18	85° 10'	85° 10'	0.99522	0.99522	0.00696	0.00696	0.99112	0.99112	0.99112	29.42582	29.42582	5.42063	5.42063	5.42063	5.42063	5.1324	5.1324	5.1324	5.1324	0.99137
0.185	0.185	0.185	85° 11'	85° 11'	0.99520	0.99520	0.00697	0.00697	0.99110	0.99110	0.99110	29.42646	29.42646	5.42057	5.42057	5.42057	5.42057	5.1324	5.1324	5.1324	5.1324	0.99100
0.19	0.19	0.19	85° 11'	85° 11'	0.99518	0.99518	0.00698	0.00698	0.99108	0.99108	0.99108	29.42710	29.42710	5.42051	5.42051	5.42051	5.42051	5.1324	5.1324	5.1324	5.1324	0.99063
0.195	0.195	0.195	85° 12'	85° 12'	0.99516	0.99516	0.00699	0.00699	0.99106	0.99106	0.99106	29.42774	29.42774	5.42045	5.42045	5.42045	5.42045	5.1324	5.1324	5.1324	5.1324	0.99026
0.2	0.2	0.2	85° 12'	85° 12'	0.99514	0.99514	0.00700	0.00700	0.99104	0.99104	0.99104	29.42838	29.42838	5.42039	5.42039	5.42039	5.42039	5.1324	5.1324	5.1324	5.1324	0.98989
0.205	0.205	0.205	85° 13'	85° 13'	0.99512	0.99512	0.00701	0.00701	0.99102	0.99102	0.99102	29.42902	29.42902	5.42033	5.42033	5.42033	5.42033	5.1324	5.1324	5.1324	5.1324	0.98952
0.21	0.21	0.21	85° 13'	85° 13'	0.99510	0.99510	0.00702	0.00702	0.99100	0.99100	0.99100	29.42966	29.42966	5.42027	5.42027	5.42027	5.42027	5.1324	5.1324	5.1324	5.1324	0.98915

circle as in C'. With the same radius but with centres on ED produced now draw arcs from such points as C' to meet the diameter DE in such points as C". The displacement AC on the out-of-phase diagram corresponds to the true displacement DC"; for the angle AOC' = β, and (β-α) which is the angle of the engine crank, = DOC'. If a point O' be chosen on ED produced such that O'D represents the clearance volume to the same scale as DE represents the stroke volume, then O'C" represents the total volume corresponding to the point C on the base of the displaced diagram.

Fig. 4 is the chart constructed in this way for the engine in question, showing crank displacement angles.

The direct transformation of gradients.

(See Fig. 5 p.). On differentiating equation (1) we get

$$\frac{ds}{d\beta} = r \sin \beta + r \frac{\sin \beta \cos \beta}{\sqrt{n^2 - \sin^2 \beta}}$$

$$= r \left(\sin \beta + \frac{\sin \beta \cos \beta}{\sqrt{n^2 - \sin^2 \beta}} \right) \text{----- (5)}$$

Where β has the value (β-α), as for the engine crank,

$$\frac{ds}{d\beta} = r \left\{ \sin(\beta-\alpha) + \frac{\sin(\beta-\alpha) \cos(\beta-\alpha)}{\sqrt{n^2 - \sin^2(\beta-\alpha)}} \right\} \text{----- (6)}$$

Now at a particular point on the displaced diagram let the gradient be given by $\frac{\delta p}{\delta s_1}$. Suppose the element of displacement δs_1 on the displaced diagram to correspond with δs on the true diagram; but in both the increment of pressure δp is the same and so also is the increment of angle $\delta \beta$. The true gradient on the true diagram is $\frac{\delta p}{\delta s}$.

$$\frac{\text{True gradient}}{\text{Apparent gradient}} = \frac{\tan \phi}{\tan \phi_1} = \frac{\frac{\delta p}{\delta s}}{\frac{\delta p}{\delta s_1}} = \frac{\delta s_1}{\delta s} = \frac{\frac{\delta s_1}{\delta \beta}}{\frac{\delta s}{\delta \beta}}$$

And/

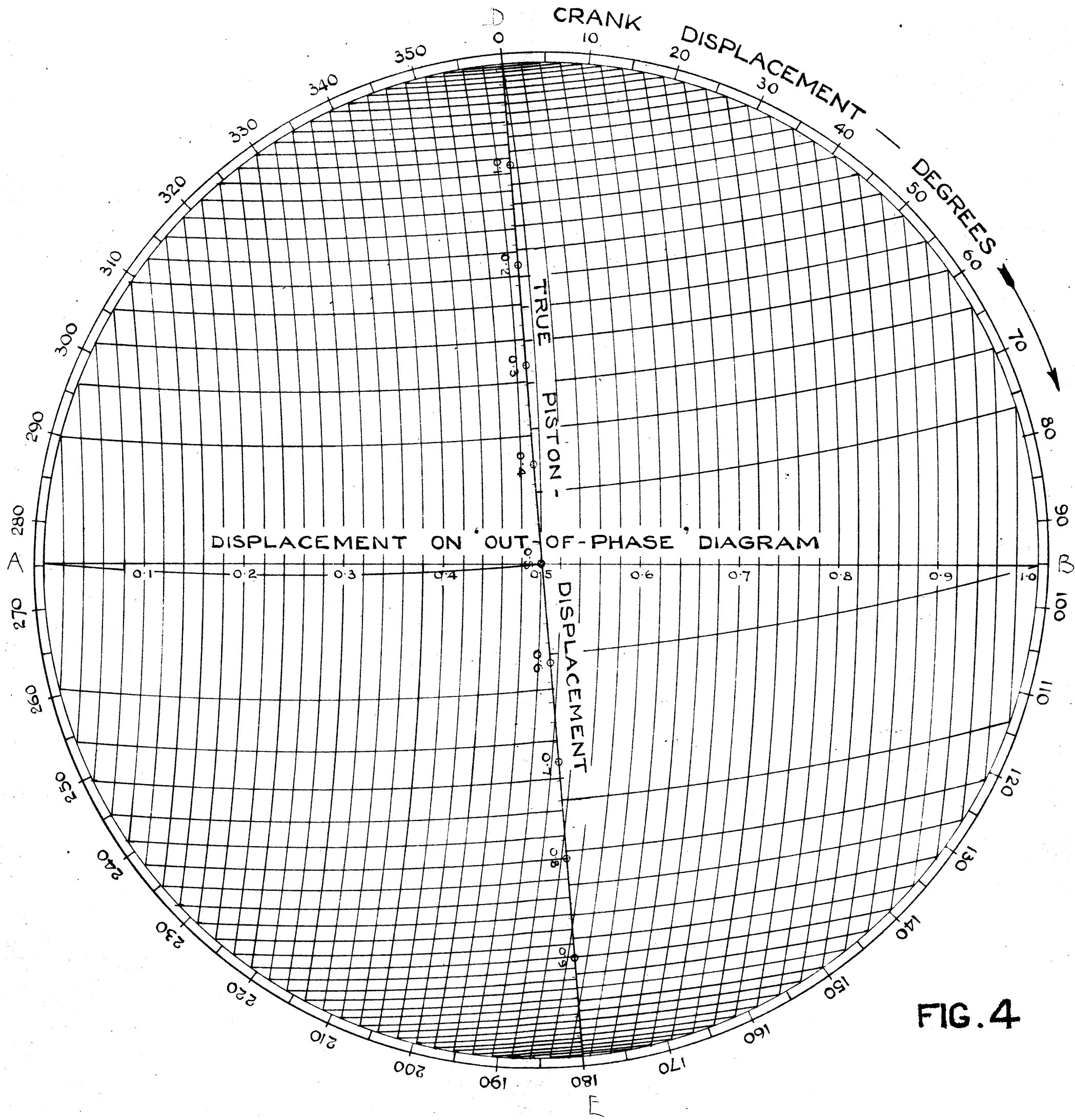


FIG. 4

And this in the limit is

$$\frac{\frac{ds_1}{d\beta}}{\frac{ds}{d\beta}} = \frac{\sin \beta + \frac{\sin \beta \cos \beta}{\sqrt{n^2 - \sin^2 \beta}}}{\sin(\beta - \alpha) + \frac{\sin(\beta - \alpha) \cos(\beta - \alpha)}{\sqrt{n^2 - \sin^2(\beta - \alpha)}}$$

$$\tan \phi = \frac{\sin \beta + \frac{\sin \beta \cos \beta}{\sqrt{n^2 - \sin^2 \beta}}}{\sin(\beta - \alpha) + \frac{\sin(\beta - \alpha) \cos(\beta - \alpha)}{\sqrt{n^2 - \sin^2(\beta - \alpha)}}} \cdot \tan \phi_1$$

The indicator reducing gear used throughout the tests described in the following pages was of the "eccentric and strap" form as adapted by Professor Goudie for the prime movers in the James Watt Laboratories.

Fig. 7 ^{p.14} illustrates the mechanical arrangement of the gear.

-----oOo-----

SECTION II.THE APPARATUS.

The engine in use was a Crossley of about 9 rated B.H.P. at 200 revs/min. governed by a hit-and-miss mechanism, and having a bore of 7ins. and a stroke of 15ins. It had been fitted originally with hot-tube ignition; but this was superseded by battery ignition, operated by an adjustable contact in the cam shaft working on the primary circuit. It was at first considered desirable, however, to have a single igniting spark in each cycle. For this reason a magneto was arranged as an alternative means of ignition.

The combustion chamber of the engine is shown in section in Fig. 6 (P.14) It was roughly spherical and the aperture 1 lay on the axis. This aperture which was $\frac{3}{8}$ " in diameter was part of the original hot-tube ignition system, in which it served along with a timing valve to make communication between the combustion chamber and the hot-tube. It proved of great use in the present tests in accommodating a glass window by means of which the centre of the chamber could be observed during the combustion period. The cover casting which fitted into the large aperture 2 carried both the indicator and the spark plug. The extended poles of the latter were so arranged that the spark-gap was in line with the aperture 1.

The special apparatus which had to be devised by the writer for the first tests included (a) a spark indicator to show exactly at what point in each cycle the spark took place, (b) a window in the cylinder and an adjustable camera lens, (c) a photographic box in which to have the luminous period photographically recorded, (d) a magneto from which to obtain a single igniting spark per cycle and (e)/

FIG. 6

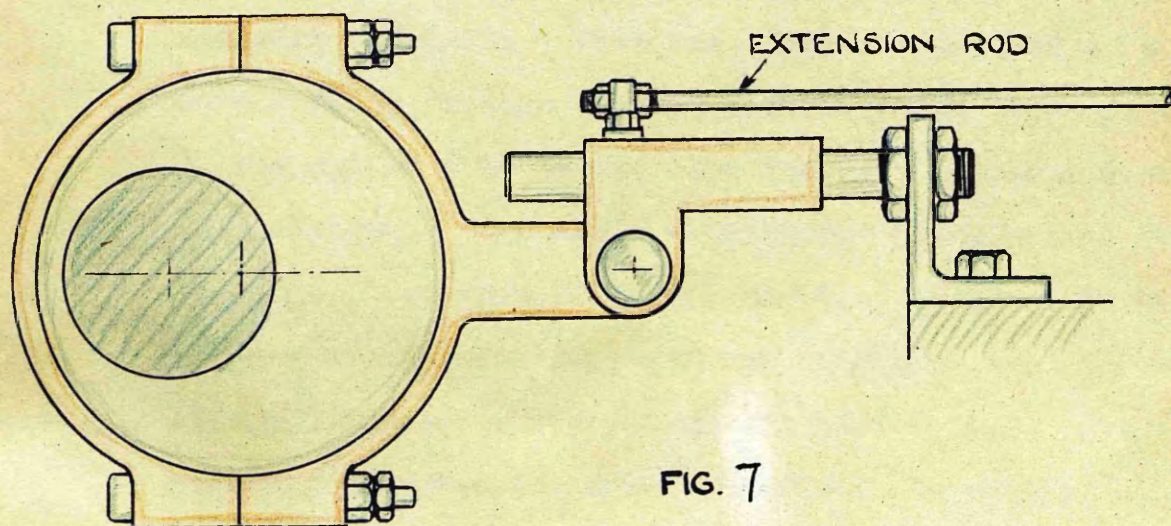
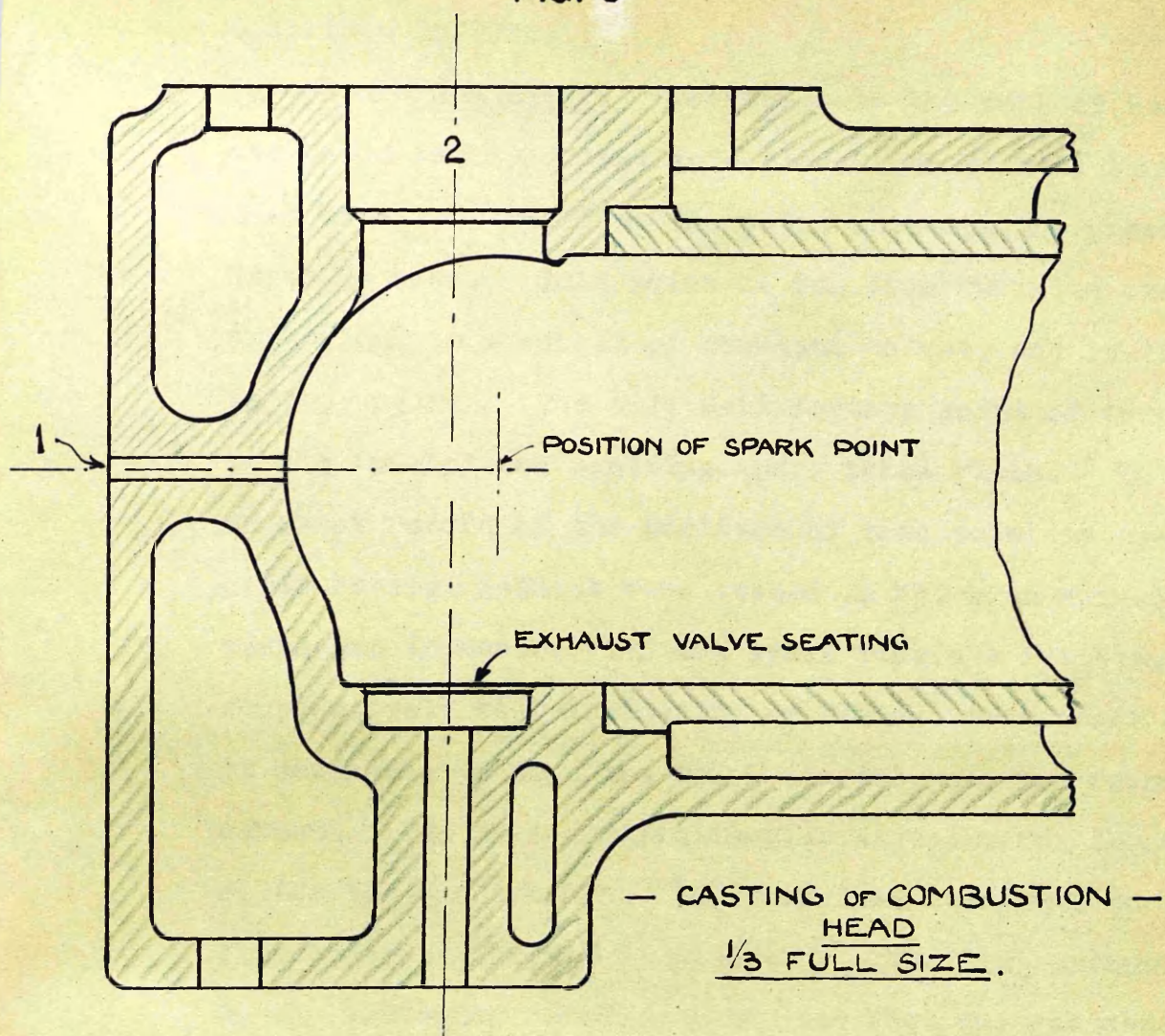


FIG. 7

(e) a spark plug with extended poles. These will be described in turn.

(a) Spark Indicator. Reference to the work of Hopkinson and David on explosions in a closed vessel will show that they measured time from the point at which the pressure began to rise. This point is far from definite even for explosions in a vessel of constant volume, and is less so in the engine. The only satisfactory point of zero time is the instant the igniting spark takes place. To obtain an exact record of the position of this point in the engine cycle, several methods were tested in which an auxiliary spark-gap in series with the spark plug was fitted. The comparatively weak luminosity of the electric spark rendered it desirable to have the spark carried near the recording screen. The most satisfactory arrangement for the purpose of the tests which will be described was found to be that illustrated in Figs. 8, 9 & 10, pp. 16 & 17. The long extension rod on the indicator reducing gear (see Fig. 7, p. 14) was made to pass through a wooden camera box, and inside the box it carried the auxiliary spark apparatus. This consisted of a small vulcanite chamber 1 (Fig. 8) carrying the two brass sparking points 2. This was fitted to the end of a short tube 3 which in turn carried another short telescopic tube 4. At the end of this latter tube was fitted a lens 5 of short focal length. The whole arrangement was attached to a carriage piece clamped to the rod 6. An image of the spark passing at the auxiliary gap was thrown on the ground glass screen 7 fitted to the end of the camera box. The indicator reducing gear was set out-of-phase by the desired angle.

In work of this kind it is Professor Goudie's practice to have the circumference of the fly-wheel marked off in degrees against an index and the dead centre positions carefully noted. This was found to be a great advantage throughout the tests in making angular measurements and in the/

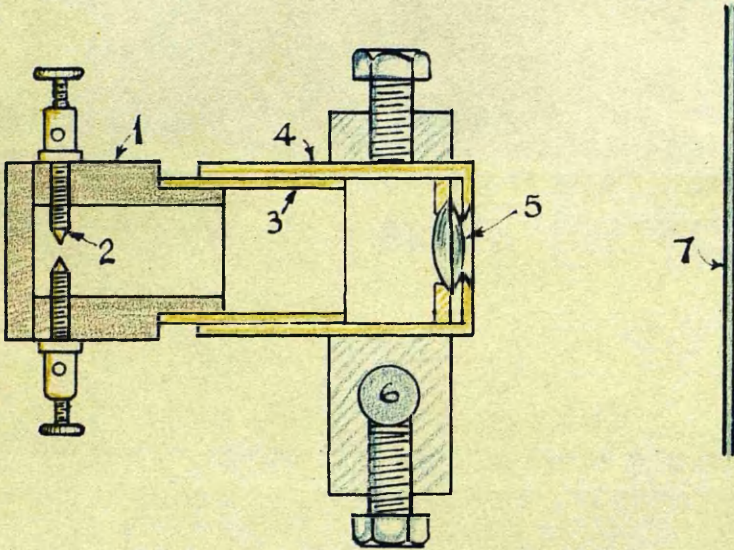
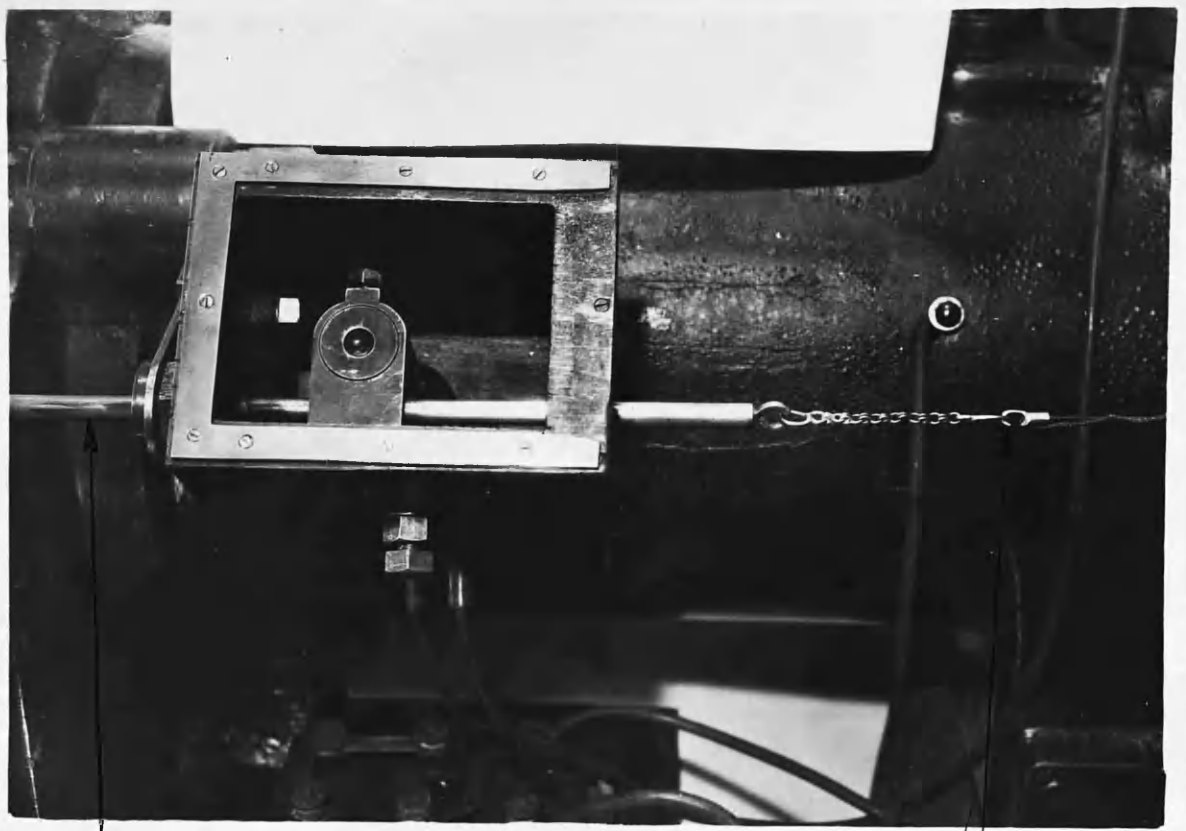


FIG. 8



EXTENSION ROD. SEE FIG. 7 PL 4

FIG. 9

CORD ATTACHMENT FOR INDICATOR AND PHOTOGRAPHIC DRUM

— GROUND GLASS SCREEN IN POSITION WITH SCALE OF CRANK ANGLES. —

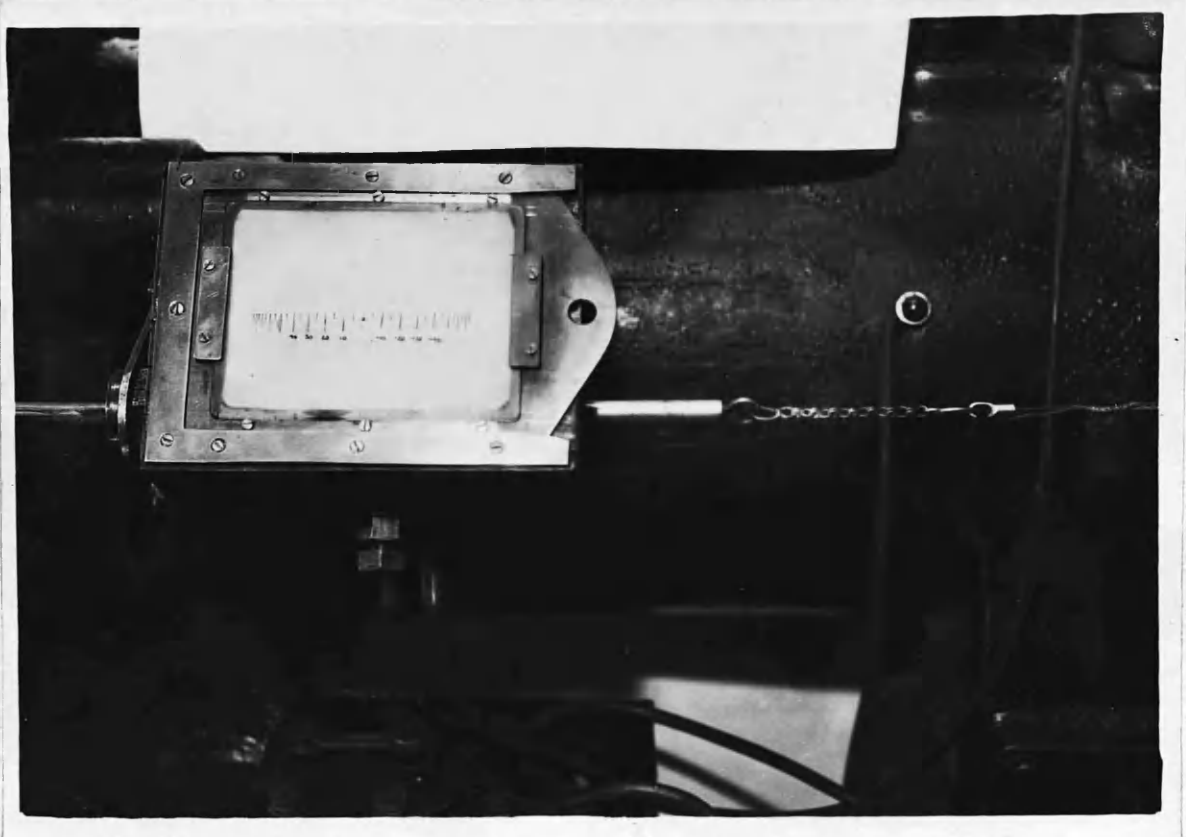


FIG. 10

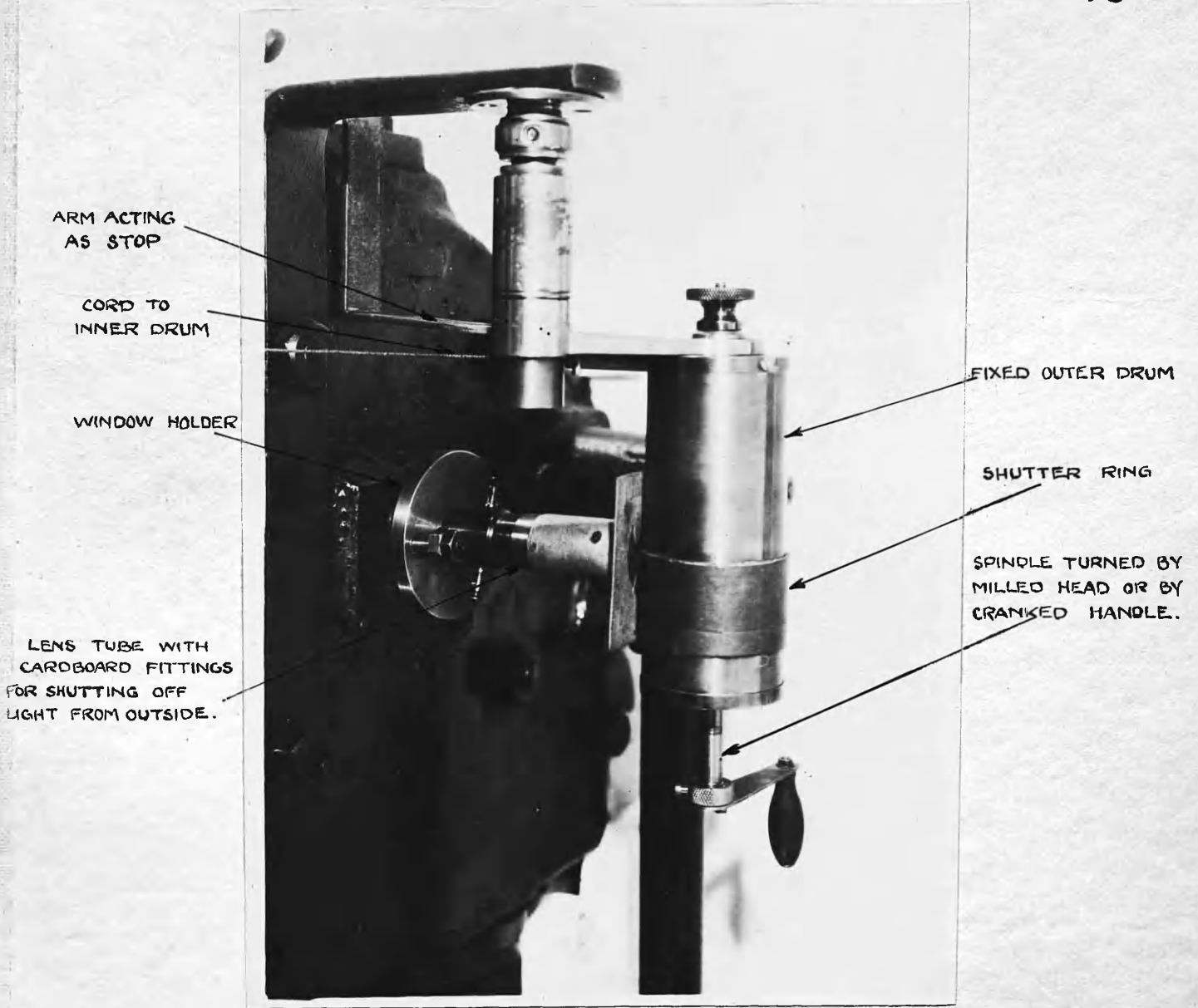


FIG. 11

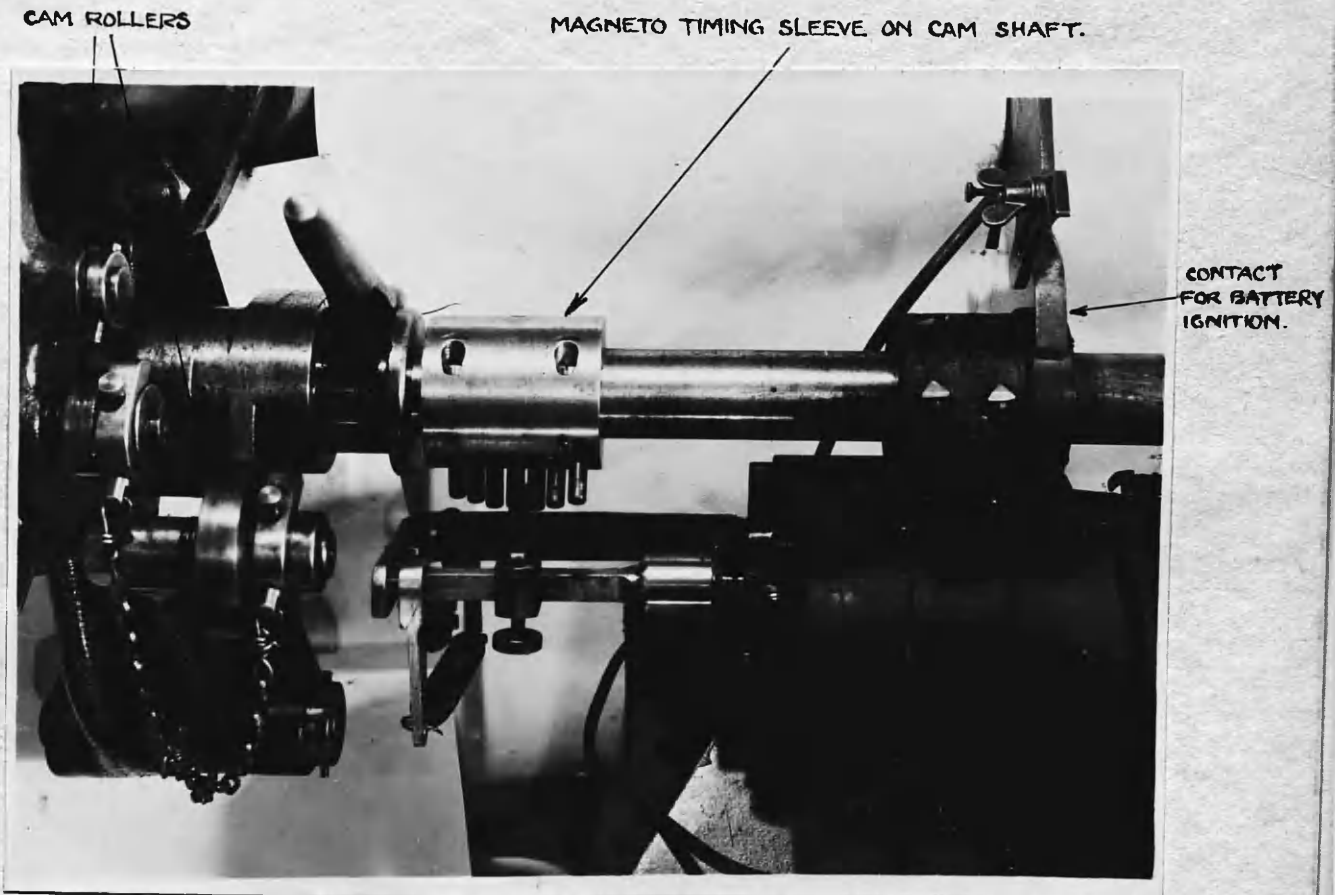


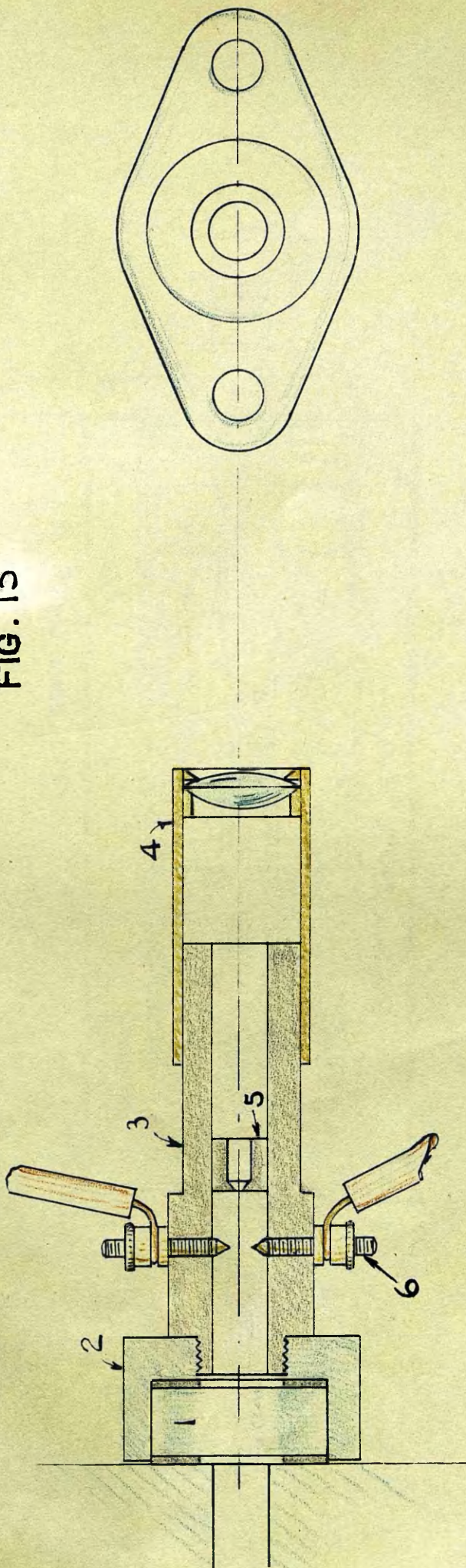
FIG. 12

the setting of the apparatus. A scale was made on the ground glass screen of the camera box in the following way. The engine was set at its inner dead centre and a spark was caused to pass at the gap. A mark was made on the glass screen against the image of the spark. The fly-wheel was turned in succession to positions at 5° intervals, the spark was passed and a mark made at each. In this way a scale of crank angles was formed on the glass screen. When the engine was running the true spark point could be noted with ease. The scale is clearly seen in Fig. 10 p. 17

With battery ignition a train of several sparks appeared each cycle, when contact was made in the primary circuit. A magneto arranged in a manner described later gave one spark, and this was used in certain of the photographic tests.

(b) Window in cylinder. This is shown in Fig. 13 p. 20. The window consisted of a piece of optical glass 1 (Fig. 13) about 1.2 ins. in diameter and $\frac{7}{16}$ " thick, held in a steel gland 2 which was bound down to the cylinder casting by two studs. Washers of rubber insertion were used as packing between the glass and the gland on one side, and the glass and the cylinder on the other. Screwed into the gland was a vulcanite piece 3 as shown, and this in turn carried a brass tube 4 fitted with a lens of short focal length. Adjustment was made by sliding the tube 4 on the vulcanite body. A small aperture was formed by boring a hole in a cylindrical piece of vulcanite 5. It was not expected at first that the igniting spark inside the engine would be sufficiently luminous to make a clear record on the films, and, with a view to obtaining this if necessary, an auxiliary spark-gap was provided for by the terminals 6. For the tests described, this was not required. The aperture in the cylinder, which was used for the window was a hole of about $\frac{3}{8}$ in. diameter lying on the axis of the cylinder/

FIG. 13



WINDOW & CAMERA LENS
FOR
GAS ENGINE

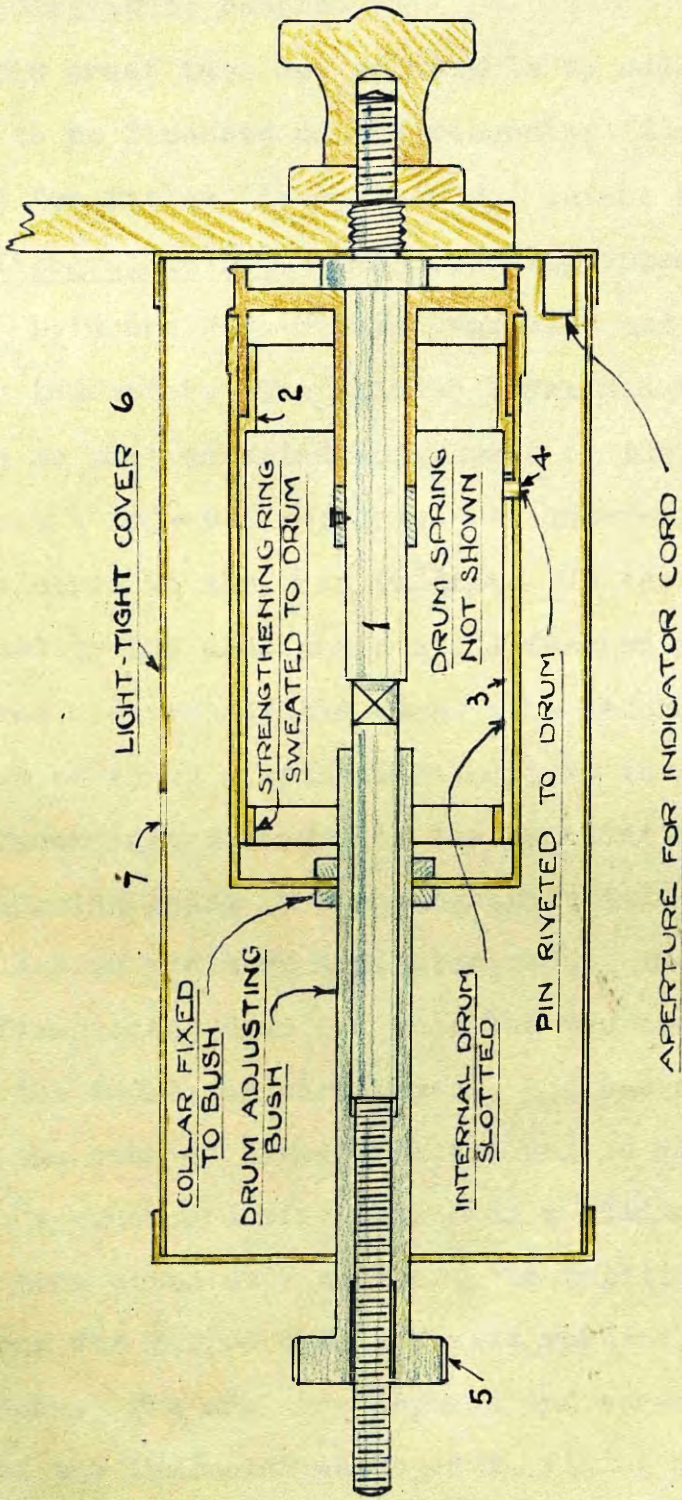


FIG. 14.

cylinder. The length of the hole was $2\frac{7}{8}$ in. The metal surrounding it was kept cool by the jacket. It may have been because of this that the window remained clean after many hours of running and that there was no deposit of carbon on the glass to interfere with the intensity of the photographic record.

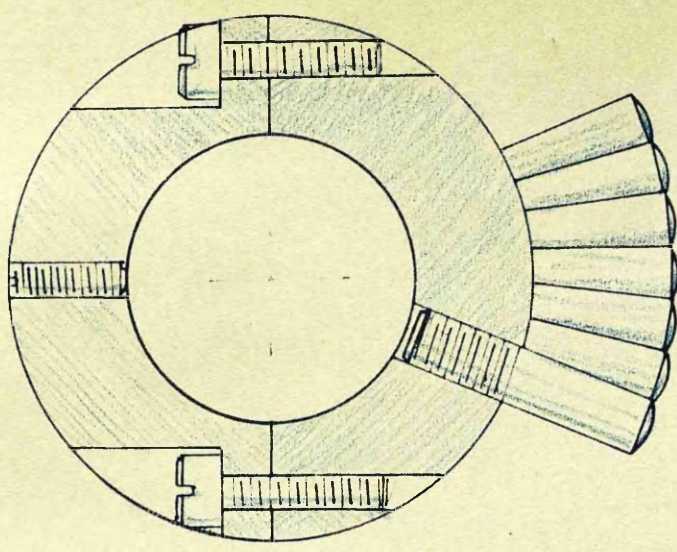
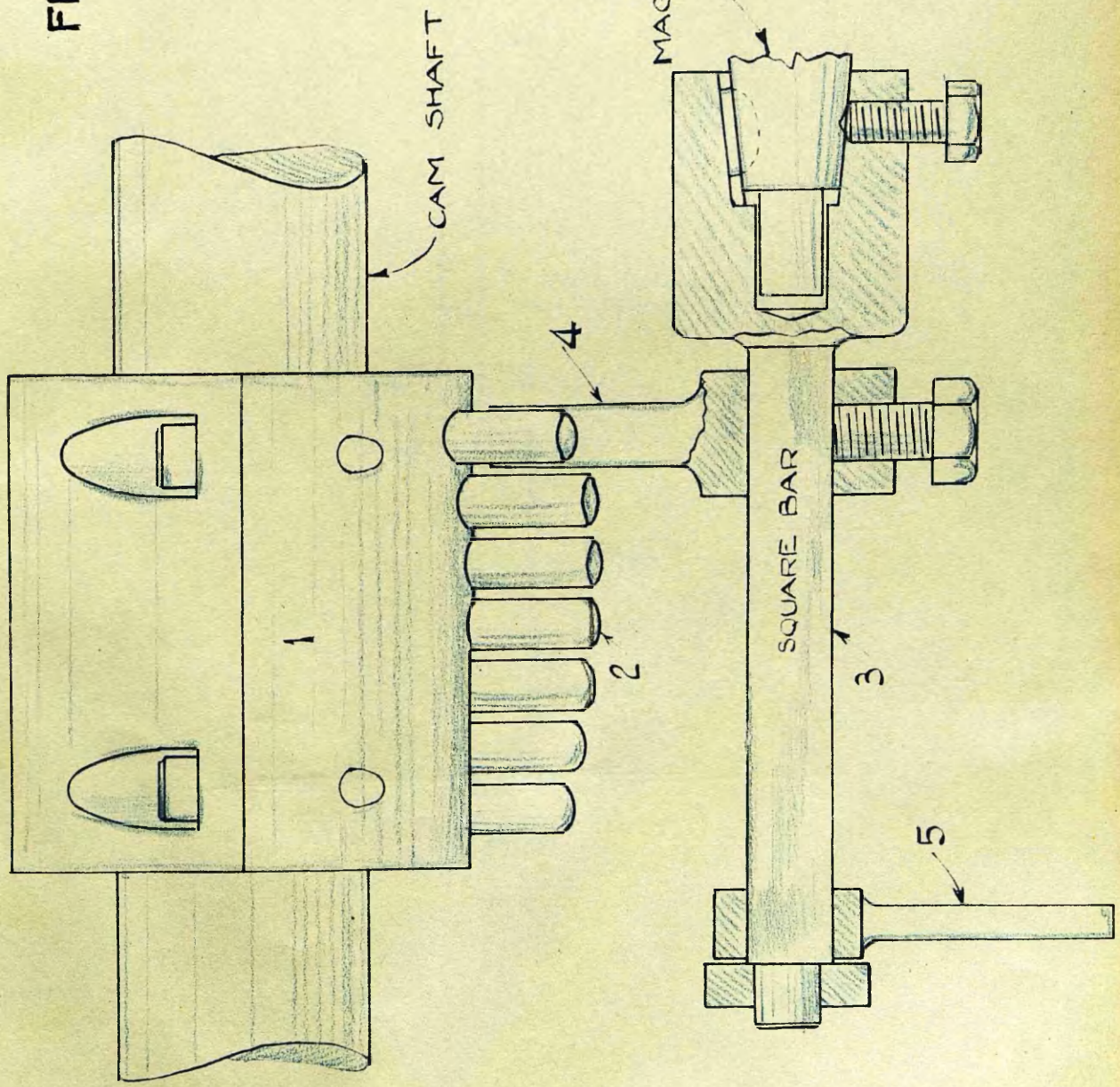
The brass tube was adjustable to allow the beam of light to be focussed on the recording film as it moved to and fro inside its cylindrical camera box.

(c) Photographic Drum. The recording apparatus shown in Fig. 11 p. 18 and Fig. 14 p. 21 was made out of parts of a Crosby indicator. The spindle 1 was made of considerable length so that an axial adjustment of the drum over a range of about 2 ins. was possible. An internal drum 2 was fitted and soldered to the drum pulley. It was slotted at 3 parallel to the axis and a small feather 4 in the recording drum was made to fit the slot. The recording drum was thus capable of being displaced axially by turning the milled head 5, without interfering with the oscillation transmitted from the reducing gear. The photographic film was carried on the drum like an ordinary indicator card. The whole was enclosed in a fixed outer drum 6. This had two apertures, one through which the indicator cord passed, and one as at 7 through which the beam of light from the engine was directed on the film. A cardboard ring which was a sliding fit on the outer drum acted as a shutter. In position on the engine the drum was fitted with its axis vertical and the milled head down. The ordinary tapered and screwed fitting on the body of the indicator was used in fixing the apparatus to a bracket on the engine. Once a satisfactory adjustment had been made for focus, etc. an arm was rigidly fixed to the cylinder to act as a stop for registering the apparatus in position when it was necessary to replace it after the removal from the engine. After some initial adjustments the arrangement worked most satisfactorily.

(d)/

(d) Magneto Ignition. It was considered desirable to have a single igniting spark per cycle, capable of being advanced or retarded through considerable angles. Another device had therefore to be made from available apparatus to meet these requirements. The engine ran at little over 200 revs/min and at this comparatively low speed the arrangement shown in Fig. 12 p.18 and Fig. 15 p.24 proved very satisfactory. A split sleeve of steel 1, fitted to the cam shaft, carried seven radial pins 2 distributed angularly over 45° , and spaced at $\frac{3}{8}$ in. from each other axially along the sleeve. A magneto taken from a 4-cylinder petrol engine was fitted below this on a bracket, with its driving spindle parallel to the cam shaft. Held securely on the magneto spindle by means of a tapered boss, feather and set-screw was a squared bar 3 carrying an arm 4 which, when the cam shaft rotated, was carried round through a limited angle by one of the radial pins and then released. By the action of a spring in tension behind and attached to the arm 5 the magneto spindle rapidly returned until this arm hit a stop. The return motion of the magneto spindle was arrested by the stop just after the armature had passed a pole. Thus when the appropriate lead was attached to the spark plug a single spark was the result. The point at which the spark took place was adjustable by moving the arm along the bar so as to engage with any desired pin. Finer adjustment was made by moving the ordinary lever on the magneto which operates the ring carrying the steel shoes. When preliminary difficulties due to shorting at the spark-plug and the auxiliary gaps were overcome, the magneto so arranged worked very well within the working limitations of so simple a device. In this connection it must be pointed out that the time between the instant of the release of the arm 4 and the instant when the spark occurs is practically constant. If the engine speed is not constant the angular position of the spark is therefore variable.

FIG. 15



MAGNETO DRIVE FOR GAS ENGINE

SCALE: FULL SIZE.

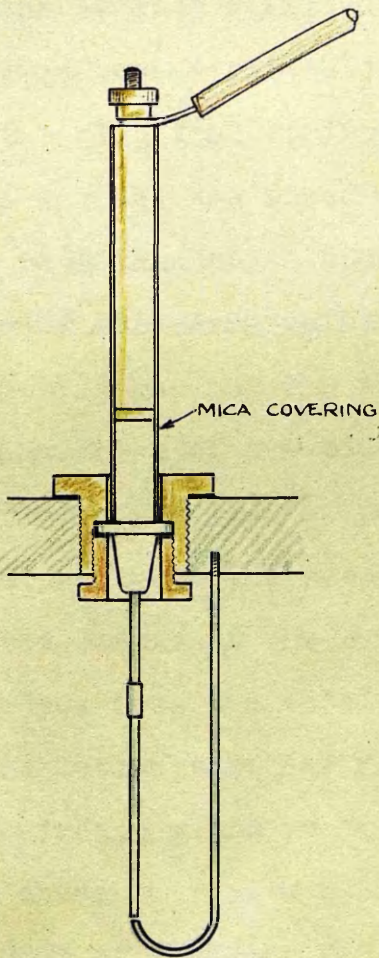
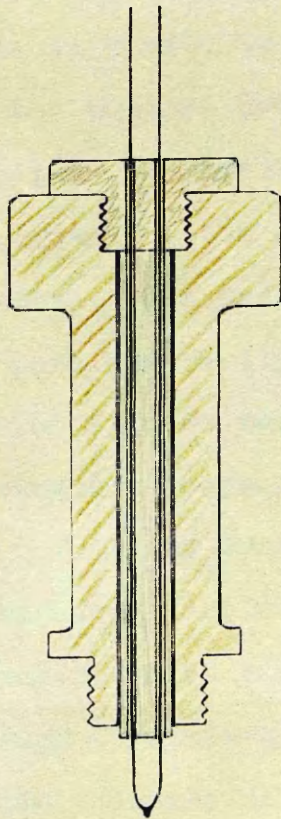
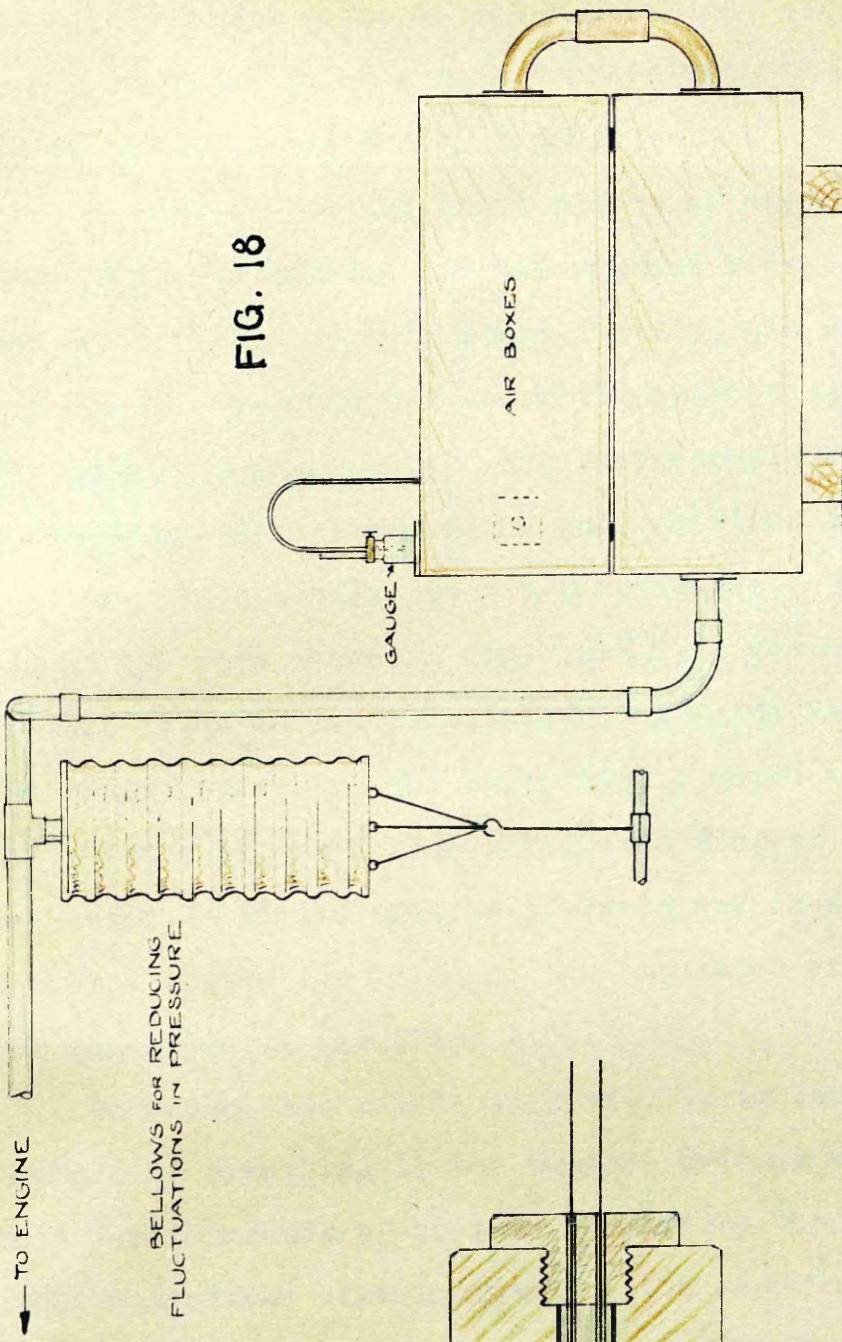


FIG. 16

A simple expedient adopted in the tests overcame this difficulty. The engine was so loaded that a missed cycle occurred in not fewer than 25 cycles. The speed was so uniform that it became possible - apart from missed cycles - to confine the variation of the spark-point to a fraction of a degree of crank angle. A variation of half a degree was easily detected on the ground glass screen of the spark indicator.

(e) Spark Plug. Access to the inside of the engine cylinder could be had through the flanged cover on the top of the cylinder. The engine indicator and the spark plug were carried on the cover. The sparking circuit was a source of considerable difficulty before continuous running of the engine became possible. The magneto, when tried by holding the plug lead at the appropriate distance from a part of the engine, was found to be capable of giving a spark up to $\frac{3}{8}$ in. long. Under running conditions however, it was found necessary to have the total gap-length (adding the plug gap and the auxiliary gaps) less than $\frac{1}{8}$ in. The insulation of the plug gave considerable trouble owing partly to the kind of position it occupied on the engine, and partly to the need for letting the plug-points down into the centre of the combustion space. The removal of sharp edges from the metal parts of the plug and the use of mica insulation together with the device of tightening up the binding gland on the plug from the inside of the cover - as shown in Fig. 16 p.25 - helped to overcome the difficulties of shorting and leakage.

At first sight it might seem that the light poles at the plug would set up pre-ignition due to their overheating. This in practice did not occur except once or twice at long intervals when the air/gas ratio was particularly small, or when it was so great as to set up the prolonged burning characteristics of weak mixtures. This freedom from pre-ignition/



pre-ignition was agreeably surprising, and shows that the fairly light poles of the spark plugs cooled quickly enough to be at quite a safe temperature when the fresh charge was entering the cylinder.

In addition to the above pieces of apparatus which were specially devised for the present tests, two more may be mentioned at this stage, namely, the exhaust thermocouple and the air measuring apparatus.

The Exhaust Thermocouple. The thermocouple was one of Platinum and Platinum-Rhodium and was fixed in the exhaust pipe as near the valve as was practicable. The fixture was of the form shown in Fig. 17, p. 27. The wires ran through holes in the porcelain rod 1 which was carried in the brass holder 2. The slate disc 3 which was fixed to the outside of the holder acted as a stop to the porcelain insulator. Liquid plaster-of-Paris was used to cement the wire inside the holes of the insulator and to cement the porcelain to the brass body.

To render the couple as sensitive to temperature changes as possible, it was thinned down at the junction to a few thousandths of an inch, following the practice of certain American experimenters.⁽¹⁾ The recording instrument was a portable potentiometer. The calibration curve used with the instrument was obtained partly from actual calibration and partly from figures supplied by the Cambridge Scientific Instrument Company.

Air Measuring Apparatus. This was arranged to make use of the method of the calibrated throttle-plate. Mr. R.O. King has published a description of air boxes and figures for the flow of air through throttle-plates, which he used for measuring the air consumption of petrol engines.⁽²⁾

For/

(1) Rosecrans and Felbeck: "A Thermodynamic Analysis of Gas Engine Tests". Bulletin 150, Engineering Experiment Station, University of Illinois.

(2) "Engineering", April 13 and 20, 1923.

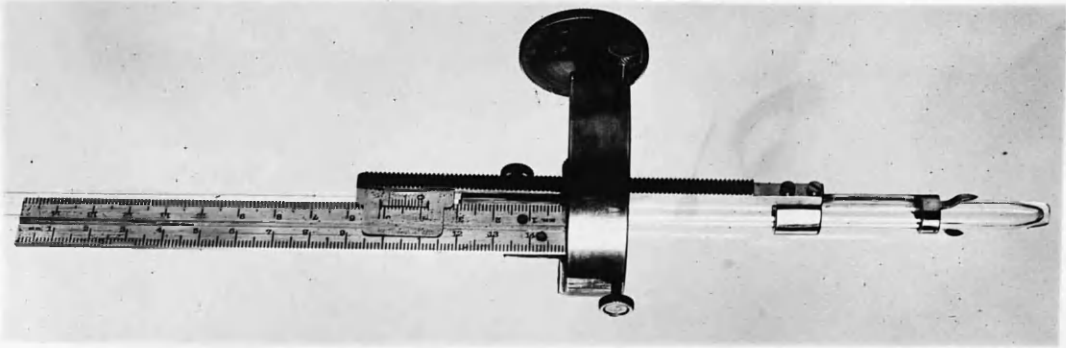


FIG. 20

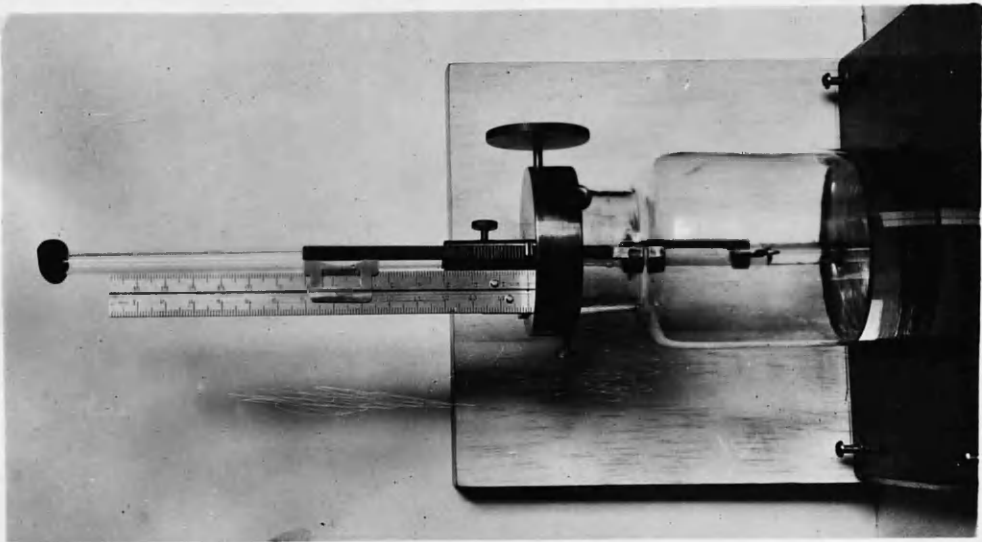


FIG. 19

For slow speed single cylinder engines the apparatus requires modification and the adaptation^{or} arranged and used by Professor Goudie consists of two air-boxes in series, each 2 ft x 2 ft x 5 ft. In the suction pipe there is a T-connection to leather bellows (see Fig. 18 p. 27) the lower end of which is loaded by means of strong india rubber thongs. The leather bellows serve to reduce to a very great extent the pressure fluctuations in the box. The oil gauge used on the air boxes (see Figs. 19, 20, p. 29) was devised for the present tests as an improvement on the gauge described by R. O. King from the point of view of convenience in reading. A bore of 2 mm. in the gauge tube such as he used is found to induce a considerable capillary effect in the oil column so that there is a large zero error. The fluctuation in the ordinary working is such as to render the capillarity a variable quantity. The introduction of a tube of $\frac{1}{4}$ " bore eliminated the zero error, but owing to the large independent fluctuations of the oil in the tubes, it was found necessary to reduce the bore at the immersed end to about 1 mm. The motion of the index-points was controlled by a rack and pinion and was readable on the scale. The zero was read with the points just touching the oil surface, while the reading of the head of oil was made with the points lying in the same plane as the bottom of the meniscus.

Method of calculating the Air/Gas ratio. If the idle cycles are frequent the mean air box reading may be taken as representing an average rate of consumption covering idle and working cycles. Let $A \text{ ft.}^3$ be the average air consumption of the engine per minute at 15°C and 760 mm. and let $g \text{ ft.}^3$ be the gas used per cycle reduced to the same/

same temperature and pressure. Let n be the number of working cycles per minute and m the number of idle cycles. The air used per working cycle is, say a ft.³. The air drawn in per idle cycle is approximately $a+g$. Hence the air per minute is $na + m(a+g)$,
 i.e. $A = (m+n)a + mg$ or $a = \frac{A-mg}{m+n}$

$$\text{The air/gas ratio} = \frac{A}{g(m+n)} - \frac{m}{m+n}$$

But $m+n = \frac{R}{2}$ where $R = \text{revs/min.}$

$$\text{The air/gas ratio } \frac{a}{g} = 2\left(\frac{A}{Rg} - \frac{m}{R}\right)$$

When the missed cycles are very infrequent the reading on the air box, if taken in the interval between the idle cycles, represents the rate of air flow when every cycle is a working cycle. Hence the air/gas ratio $\frac{a}{g} = \frac{2A}{Rg}$.

Engine Indicator. The indicator used was of the Mahak type and was tested continually for friction and slackness at the pins. It proved very satisfactory for use in these tests.

-----oOo-----

SECTION III.

Photographic Records of Explosions.

Reference to Fig.21 p.33 will show the kind of record obtained photographically under the best conditions and its relationship to the displaced indicator diagram.

The short dash of light is typical of the magneto spark. There is a considerable interval between the passing of the spark and the burst of incandescence which follows. It is well known that there is no appreciable rise in pressure due to combustion for some time after ignition takes place. This is well illustrated by the indicator diagram. But there is similarly a pause before the luminosity of the burning period becomes noticeable. As the point of maximum pressure is approached, the incandescence of the gases becomes intense and the instant of maximum intensity of incandescence seems to fall close to that of maximum pressure. In the example furnished by Fig.21, the spark took place at 13° before dead centre, but the maximum pressure and the maximum intensity of luminosity occur considerably after the dead centre has been passed.

This record of the nature of the relationship between the pressure and volume and the luminosity of the explosive charge in a gas engine is new, and its value lies not so much in what it proves as in the problems which it helps to emphasise.

If luminosity were regarded as evidence of "burning" then the process of burning would seem to persist for a considerable part of the expansion stroke. It is considered that it can be satisfactorily demonstrated along the lines of experiments to be described later that the luminous condition/

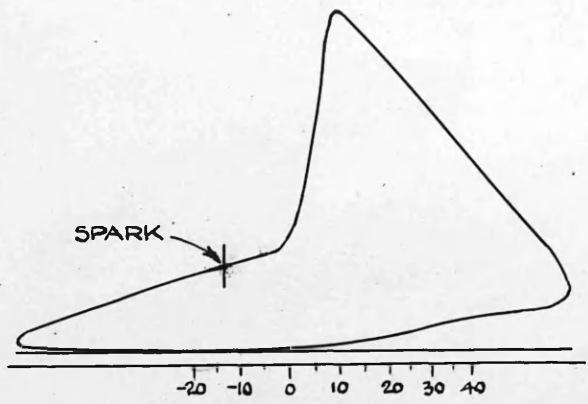


FIG. 21

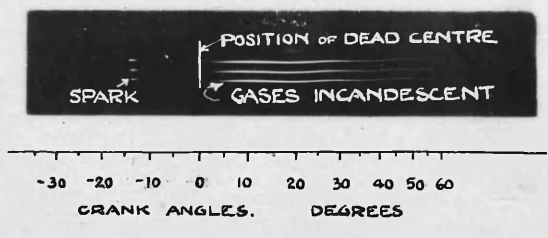
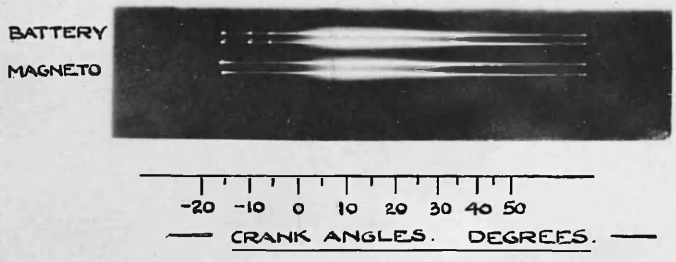


FIG. 22



condition is independent of the presence of any simultaneous chemical activity such as is implied in the term "burning".

The time of attaining any particular intensity of luminosity, or the maximum pressure, after the passing of the spark may be expected to vary with such factors as the quality of the combustible mixture and its density at the instant the spark takes place. It might be considered, therefore, that the variation of the jacket temperature and of the angle of advance of the spark would yield interesting information about the conditions governing combustion speed. Specific tests of this kind were made.

Effects of variation in strength and kind of spark.

Before these tests are described a word will be said about the spark ignition. The strength of the spark, provided it is sufficient to fire the mixture, seems to have no appreciable effect on the speed of inflammation. A few tests have been made by Bone, Fraser and Witt⁽¹⁾ on mixtures of CH_4 and O_2 , with sparks of different intensity; but no alteration in the speed of combustion could be observed.

The apparatus which has herein been described provided a means of testing this point as applied to the gas engine.

Under absolutely constant running conditions the ignition system was alternately switched to the magneto and to the coil. Indicator diagrams were taken and simultaneously an exposure was made on the photographic film for each change in the ignition. The records of combustion and the indicator diagrams were found to be the same with both types of spark.

The magneto spark has a variable intensity depending on the position of the ordinary adjusting ring which carries the steel shoes. The battery and coil arrangement is operated by/

(1) "Flame and combustion", Bone and Townend p.156 et seq.

by a contact stud carried on a vulcanite cam by the cam-shaft. As the stud passes under a brush, contact takes place in the primary circuit. Several discharges take place during the time of contact. These can be traced in Figs. 22 and 32, pp. 33 & 49

In Fig. 22 if the position of the first discharge of the battery and the beginning of the corresponding luminous period be compared with the magneto spark and its consequent line of luminosity, it will be clear that combustion is set up by the first battery discharge. Time intervals measured on the record of luminosity or on the indicator diagram from the first battery discharge are the same for the same working conditions as those measured from the single magneto spark.

Each separate discharge either from the battery or the magneto, however, is itself composed of a train of sparks taking place in rapid succession. ⁽¹⁾ With a low capacity in the secondary of a coil or magneto the number of sparks per discharge is large, and with specially low secondary capacity the discharge consists of a "preliminary spark followed by a continuous but pulsating and decaying arc." ⁽²⁾ Careful examination of the photograph Fig. 22 will illustrate the nature of a spark with low secondary Capacity. The magneto discharge appears as a point of light merging into a short dash of light of decreasing intensity. A comparison of the photograph of the explosion set up by the magneto spark with that of the explosion set up by the more concentrated first/

(1) Taylor-Jones "Theory of the Induction Coil".

(2) Taylor Jones "Spark Ignition" Phil. Mag. Dec. 1928.

first discharge of the coil tends to show that the initial spark of the magneto discharge is the igniting agent. This corroborates the statement of Patterson and Campbell,⁽¹⁾ that ignition depends on the energy of the first oscillation of a discharge and not on the total energy of the whole discharge.

Fig.22 was obtained from the explosion of a rich mixture with the use of a very sensitive film, an aperture of about $\frac{1}{32}$ in. and with eight superimposed explosions. The halation on the combustion lines illustrates the variation in intensity of the light.

The photographic records of the luminous period made in the earlier tests (A, B and C)⁽²⁾ were taken on a comparatively slow film (about 300 H and D) and have therefore a different appearance from the later records (as in Figs.22,32 etc.) taken under improved photographic conditions.

Observations.

As a rule the required observations consisted of gas-meter readings, revolutions, explosions, spark angle, jacket temperature and air-box readings. The writer had the assistance of one other observer and the readings were planned in the following way. One observer took the meter reading. After thirty secs. he took the spark angle reading and thirty secs. later he noted the air-box reading. In the same sequence the other observer was meanwhile reading the revolution counter, the explosion counter and the jacket temperature. The combustion records and indicator diagrams were then taken off, and, after a chosen interval of time the sequence of test/

(1) Proc.Phys.Soc. 1919. p.177.

(2) See page 37 et seq.

test readings was repeated. When the engine was running steadily under load it was found that the whole of the readings for a test could be made in 6 minutes with remarkable consistency as between the readings for tests made under the same conditions. Care was taken, however, to have the engine running for a considerable time under steady conditions before the observations were commenced.

The record of the luminous period was made by exposing the moving film in each test for a chosen number of explosions, generally six. The film used at first was ordinary Kodak spool film with a speed, it is supposed, of about 300 H and D. Later it was thought necessary to get a speedier film for certain tests, and Imperial special cut film was then used having a speed of about 600 H and D. Measurements of the luminous period etc. were made directly on the negative.

In the earlier tests it was found that owing to the comparatively slow film used, the conditions had to be chosen which caused the luminosity to be as pronounced as possible. The rich mixture which was used caused the explosions to be very vigorous and this led to much vibration on the pressure record obtained from the indicator.

Combustion Tests.

The first tests were planned in the following order:-

- A. Varying Jacket Temperature.
- B. Varying Air/Gas Ratio
- C. Varying Spark Angle.

The results obtained from A and B were chiefly of a negative nature and shall only require to be dealt/

dealt with briefly. But C proved to be of very great interest and, it is believed, of importance in affording grounds for discussion relative to heat losses and "after-burning".

Combustion Tests. Series A. Varying Jacket
Temperature.

In these tests the speed, mixture strength, point of ignition and general running conditions were kept throughout as nearly constant as possible, excepting the jacket temperature which was varied from test to test. The series consisted of five tests with jacket temperatures varying from 68.5°F to 145.7°F. The incandescent period showed no sensible effect due to difference in jacket temperature. The photograph Fig 23_{p.39} indicates the nature of the records of the luminous period for this test. In table II are to be found the observations and values of the air/gas ratio. This quantity increased from test A1 to test A5 by about 1.7% and this may account for the slightly increased interval between the spark and the commencement of incandescence.

Table II

Test	Air/ Min at 15°C & 760mm A ft ³	Gas/ Cycle at 15°C & 760mm g ft ³	Revs/ Min R	Idle Cycles per Min m	Air/ Gas	Jacket Temp. °F	Spark Angle degs.	Gase- ous Vol. used/ cycle ft ³	Vol. Efficy.
A1.	24.28	0.0408	204.4	3.6	5.794	68.5	-10 $\frac{1}{4}$	0.277	0.830
A2.	23.99	0.0407	202.4	2.4	5.800	93.5	-11	0.277	0.830
A3.	24.06	0.0408	203.2	4.0	5.804	109.5	-10 $\frac{1}{2}$	0.276	0.826
A4.	23.85	0.0401	202.8	1.2	5.858	128.0	-10 $\frac{1}{2}$	0.274	0.820
A5.	23.75	0.0392	204.4	0	5.930	145.7	-10	0.271	0.811

Cylinder Diameter 7"; Stroke 15".

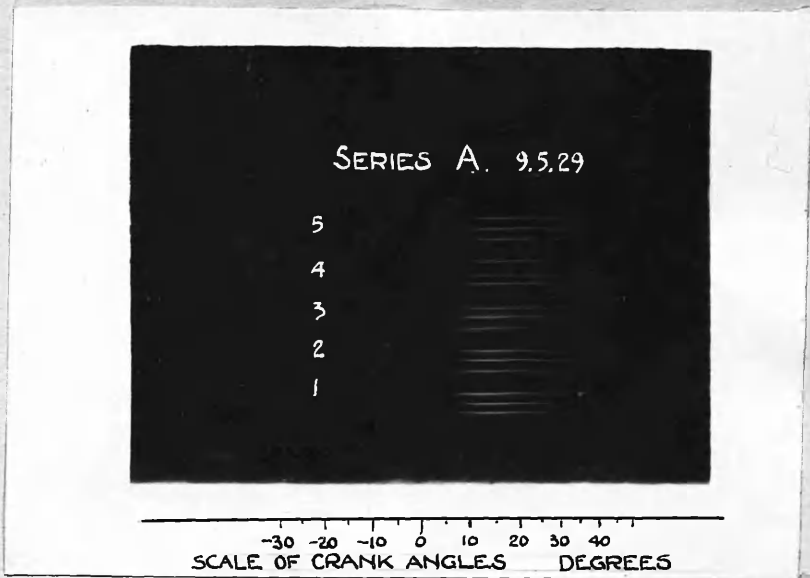


FIG. 23

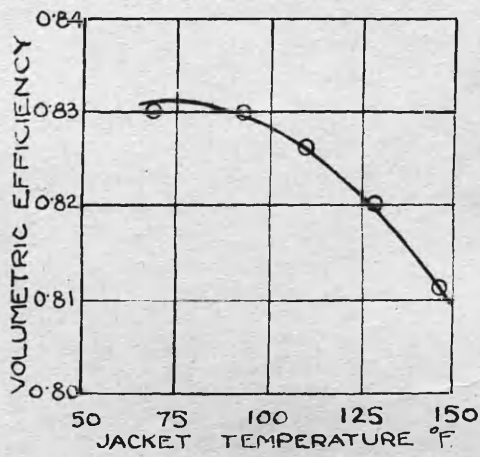


FIG. 24

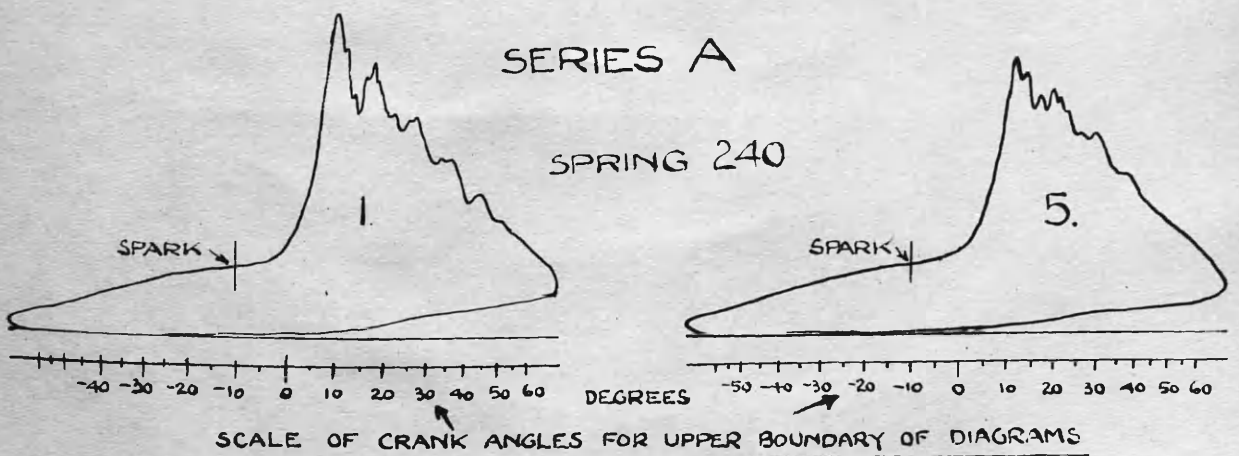


FIG. 25

The effect of increased jacket temperature on the volumetric efficiency (referred to 15°C and 760mm.) is shown in the last column of Table II. These figures yield the curve Fig.24, p39. The total effect of the change in jacket temperature from 68.5°F to 145.7°F upon the volumetric efficiency, it is interesting to note, is only about 2%.

In making the exposures for the photographic record, care was taken to include neither an idle cycle nor the working cycle immediately following an idle cycle. The working cycle following immediately upon an idle cycle has a less luminous explosion than the normal.

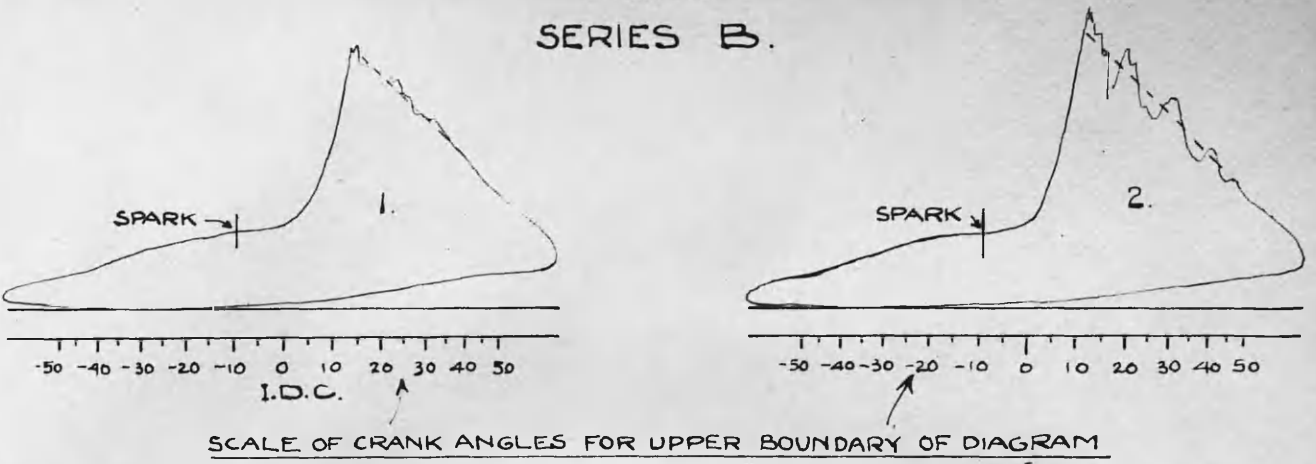
Typical indicator cards selected from tests A1 and A5 are given in Fig.25, p39. It will be seen that they are very much alike.

Combustion Tests. Series B. Varying Mixture
Strength.

With the ordinary films used in these combustion tests the exploded charge does not become sufficiently luminous to yield a satisfactory photographic record unless the mixture is a fairly rich one. The range of variation of mixture strength suitable for the present purpose is therefore very restricted. Nevertheless, as the photograph Fig.27, p41 shows, the intensity and duration of the luminosity both increase (as might be expected) with decrease in the air/gas ratio. Another noticeable effect is the shortening of the gap between the spark and the beginning of the line as the mixture strength increases.

The indicator diagrams Fig.26, p41 are ~~approximate~~ copies of those obtained in this test. The original diagrams ~~however~~ exhibit very marked vibration at the pencil in the explosion stage. This vibration becomes the more violent -
in/

FIG. 26
SERIES B.



SCALE OF CRANK ANGLES FOR UPPER BOUNDARY OF DIAGRAM

SPRING No. 240

CONSTANT SPARK ANGLE.

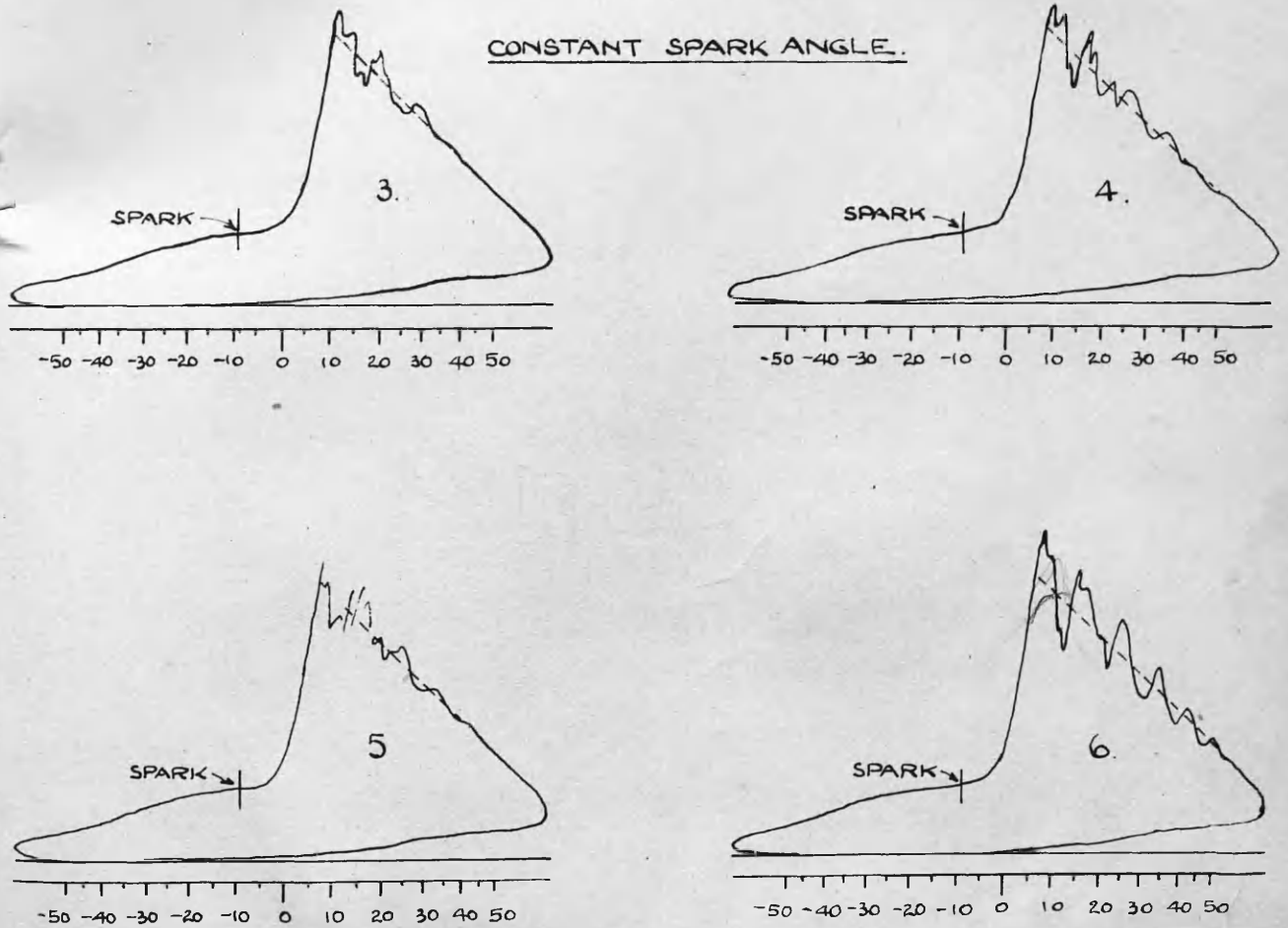


FIG. 27

in keeping with common experience - as the mixture strength increases. But a close examination of the diagrams yields the following results. The maximum pressures in cases 3,4,5, and 6 are practically the same. (The maximum pressure is obtained approximately by striking a mean line through the vibration waves in the diagram until it meets the line of rising pressure). Choosing an arbitrary ordinate - in this case at 0.25 in. from the end of the diagram - and measuring the pressure on the expansion line it is found that very nearly the same value is obtained in the cases 3,4,5, and 6. The compositions of the post-combustion mixtures in these three cases are practically the same and therefore their internal energies at .25 in. from the end of the diagram are practically the same. The spark point is the same in all cases and the four diagrams are very similar in shape. Hence the work done by the charge between the ignition point and the chosen ordinate is very nearly the same in all cases. Now the heat generated in burning the richer mixture is greater than that generated in burning the weaker. Where does the extra heat go? The longer incandescent period indicates a longer period of intense radiation and of high temperature. As shown later it is probable that the extra heat is largely radiated away. This point will be discussed more fully in a later section of this report. The maximum pressures and the pressures at 0.25 in. from the end of the diagram are given in Table IV for the series B, while Table III includes the record of the test observations.

Table III.

Test	Air/ Min at 15°C & 760mm A ft. ³	Gas/ Cycle at 15°C & 760mm g ft. ³	Revs/ Min R	Idle Cycles per min m	Air/ Gas	Jacket Temp. °F	Spark Angle Degrees
B1.	25.25	0.0380	208.4	5.0	6.34	103.5	-9
B2.	24.65	0.0391	208.0	1.8	6.04	105.2	-9
B3.	24.55	0.0407	209.2	5.4	5.90	104.0	-9
B4.	24.50	0.0418	210.0	5.0	5.54	104.2	-9
B5.	24.10	0.0424	208.0	3.2	5.44	105.2	-9
B6.	24.10	0.0422	207.2	4.0	5.48	103.7	-9

Table IV.

Test	Maximum Pressure lb/ in ²	Pressure at 0.25" from end of diagram
B1.	348	147
B2.	362	150
B3.	379	152
B4.	379	152
B5.	382	152
B6.	379	152

Combustible Tests. Series C. Varying Spark Point.

These tests yielded well defined results. The spark point was varied from an angle of 29° before, to an angle of 1° after the inner dead centre position of the crank. All the other running conditions were kept nearly constant.

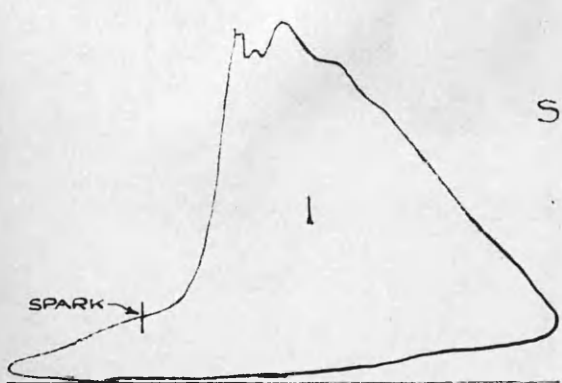
In all, five tests were made. The photographic records consisted of three exposures for a test, each exposure lasting for six engine cycles. Certain measurements were made on the negative, but to indicate the nature of the record the photograph Fig. 28, 44 is given. Table V contains the observations and results of the tests. In Fig. 29, 44 are given the indicator cards in the displaced form. As in Series B the original cards exhibited/

FIG.28



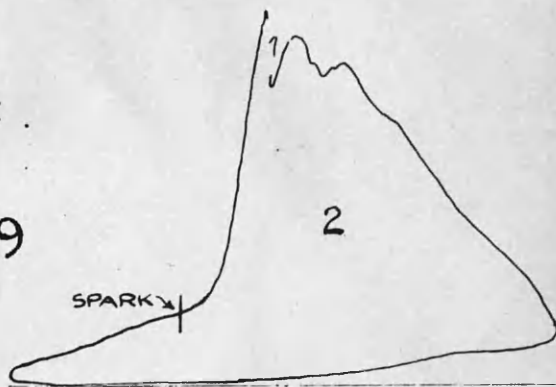
SCALE OF CRANK ANGLES. DEGREES.

-50 -40 -30 -20 -10 0 10 20 30 40 50



SERIES C.

FIG.29



-50 -40 -30 -20 -10 0 10 20 30 40 50

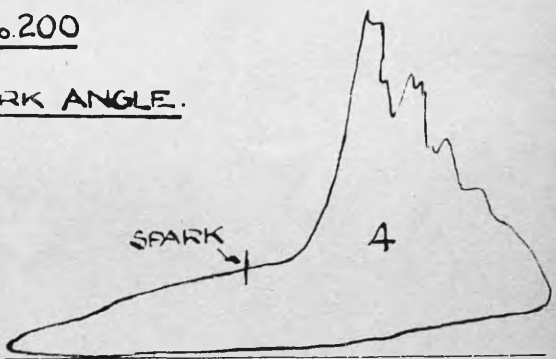
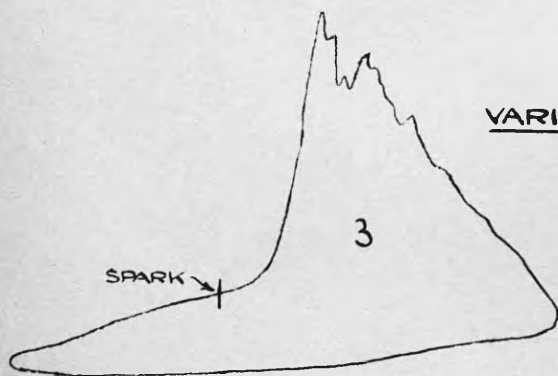
I.C.C.

-50 -40 -30 -20 -10 0 10 20 30 40 50

SCALE OF CRANK ANGLES FOR UPPER BOUNDARY OF DIAGRAM.

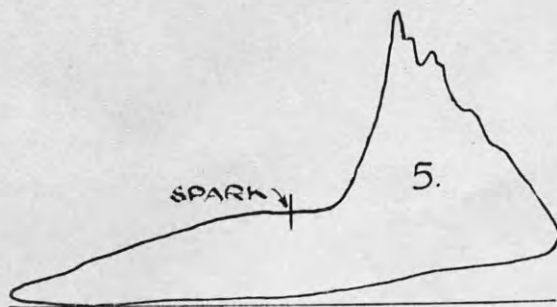
SPRING No.200

VARIABLE SPARK ANGLE.



-50 -40 -30 -20 -10 0 10 20 30 40 50

-50 -40 -30 -20 -10 0 10 20 30 40 50



-50 -40 -30 -20 -10 0 10 20 30 40 50

Table V

Test	Air/ Min at 15°C & 760mm A ft. ³	Gas/ Cycle at 15°C & 760mm g ft. ³	Revs/ Min R	Idle cycles per min m	Air/ Gas	Jacket Temp. °F	Spark Angle Degrees
C1.	22.92	0.0410	205.6	2.2	5.422	103.5	-29
C2.	22.73	0.0405	206.4	4.6	5.376	100.2	-22
C3.	22.92	0.0410	204.4	2.6	5.444	101.5	-13 $\frac{1}{2}$
C4.	23.45	0.0416	207.6	4.0	5.398	101.5	-7 $\frac{1}{2}$
C5.	23.75	0.0419	209.6	4.2	5.370	102.0	+1

exhibited very violent vibration at the pencil, because of the rather rich mixture used for the sake of getting luminosity. But the approximate maximum pressure was measured in each case by striking a mean curve through the vibration waves. The point in which this curve cuts the rising pressure curve was regarded as the point of maximum pressure. Values thus obtained, together with values for the pressures at 0.25 in. from the end of the diagram are given in Table VI. In cases 1,2 and 3 the maximum pressures, it will be noticed, are practically equal. The pressures at the arbitrary ordinate, however, steadily increase from the case C1 in which the angle of advance of the spark is 29°, to the case C5 in which the spark angle is +1°. The chosen ordinate corresponds to a piston displacement of 0.267 stroke.

Table VI.

Test	Maximum Pressure Lb/ in ²	Pressure at 0.25" from end of diagram lb/in ²
C1.	374	143
C2.	370	146
C3.	373	154
C4.	351	156
C5.	322	161

Referring/

Referring to the record of the combustion Fig. 28, the first thing to note is that the time lag between the spark and the beginning of the photographic line has a small range of variation. By choosing a point of a certain intensity at the beginning of each line and noting the angle between the spark and this point, we get what we might call an angle of ignition lag. (The values of this angle were found to vary in an apparently irregular manner between $16\frac{1}{2}^{\circ}$ and $19\frac{1}{2}^{\circ}$. Perhaps the explanation for this is to be found on a closer examination of the results.) Similarly a point of equal intensity chosen at the end of the line gives us a means of getting a relative figure for the persistence of the luminosity. The angle during which luminosity persists varies regularly with the position of the spark point. The curve on Fig. 30, 52 shows how, as the spark point is advanced, the total crank angle (or total time) during which actinic light persists becomes greater. The values of the angle as measured are given in Table VII.

In this table are also to be found values for the pressure P, the volume V and the product of PV corresponding to the point on the expansion line at which the luminescence, as recorded by the camera, disappears.

Results of Series C and their probable significance.
Variation of Combustion Speed with Density.

Reference to the diagrams in Fig. 29, throws light on the apparently irregular nature of the variation in the angle of ignition lag given in Table VII. In cases C1 and C2 the maximum pressure occurs before the dead centre is reached. In C3 and C4, however, the dead centre falls within the inflammation period. In C5 the whole inflammation period lies in the forward stroke. It therefore seems that the average density of the charge during explosion/

Table VII.

TEST	Spark Point Degrees	Line Begins Degrees	Line ends Degrees	Ignition Leg Degrees	Angle of Luminosity Degrees	Pressure at end of Line lb/in ²	Fraction of Diagram at end of line	Fraction of true stroke	Volume at end of Line V. Ft. ³	Temp. Factor PV $\frac{1 \text{ lb Ft}^3}{\text{in}^3}$
C1	-29	-11	+43	18	54	190	0.843	0.160	0.1445	27.7
C2	-22	-4	+46 $\frac{1}{2}$	18	50 $\frac{1}{2}$	172	0.872	0.201	0.1582	27.2
C3	-13 $\frac{1}{2}$	+3	+44	16 $\frac{1}{2}$	41	195	0.855	0.178	0.1505	29.3
C4	-7 $\frac{1}{2}$	+9	+40 $\frac{1}{2}$	16 $\frac{1}{2}$	31 $\frac{1}{2}$	209	0.830	0.150	0.1412	29.5
C5	+1	+20 $\frac{1}{2}$	+48	19 $\frac{1}{2}$	27 $\frac{1}{2}$	181	0.882	0.215	0.1629	29.5

explosion effects the explosive speed. The greater the density the less the time lag. The variation in the average density during explosion for the whole series of tests is only a matter of 10 per cent.

A further point arises from the fact that while the average volume of the charge during explosion in test C1 is about 0.103 ft^3 , the average volume in C5 is about 0.95 ft^3 and yet the latter shows the longest ignition lag of the series. It seems therefore that the speed of explosion in C1 is higher because the density is increasing as the explosion proceeds, while in C5 the density is rapidly decreasing while the explosion proceeds. Higher speed of explosion no doubt results from higher density towards the end of the explosion period.

Variation of Temperature at end of Luminous Period.

In Table VII the column of values of PV applying to the point where the actinic light ceases, is included for the following reason. Towards the end of the luminous period it may be assumed that the charge is approximating to a condition of thermal equilibrium. It is reasonable, therefore, to test the temperature at this point by means of the characteristic law $PV = WRT$ or $T = K \times PV$ where k is a constant.

The reading of the points on the diagrams which represent equal intensities of luminosity can only be a roughly approximate process. The results obtained, therefore, for PV as tabulated in Table VII do not prove that the intensity of luminosity is not a function of temperature only. The values of pressure contained in Table VI referring to the arbitrary ordinate show clearly that the expansion lines of the diagrams taken with an advanced spark lie below those with a less advanced spark/

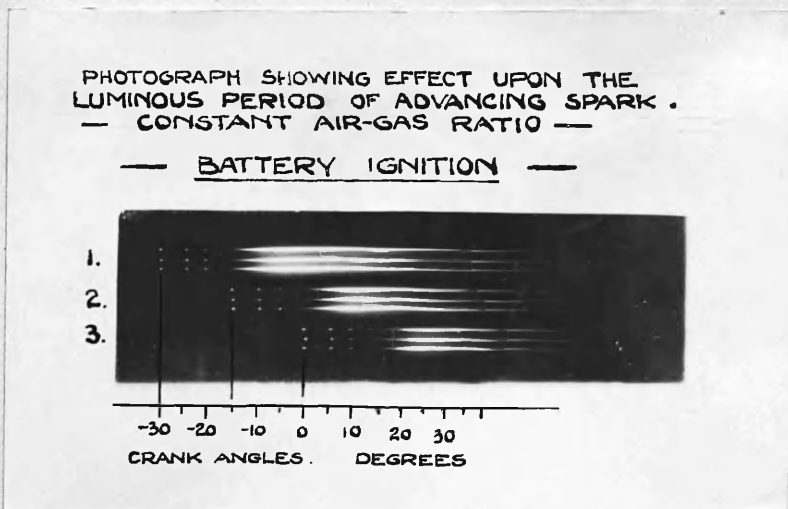
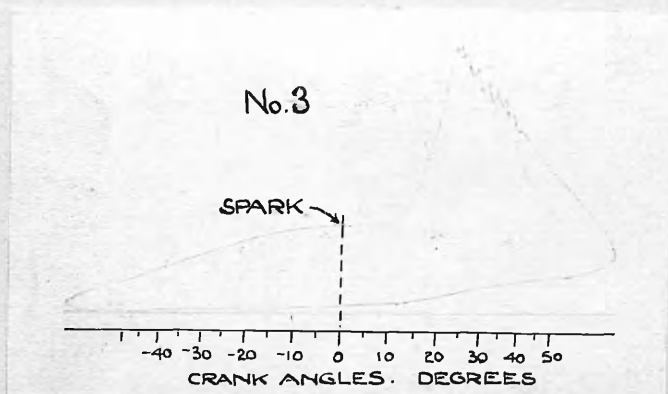
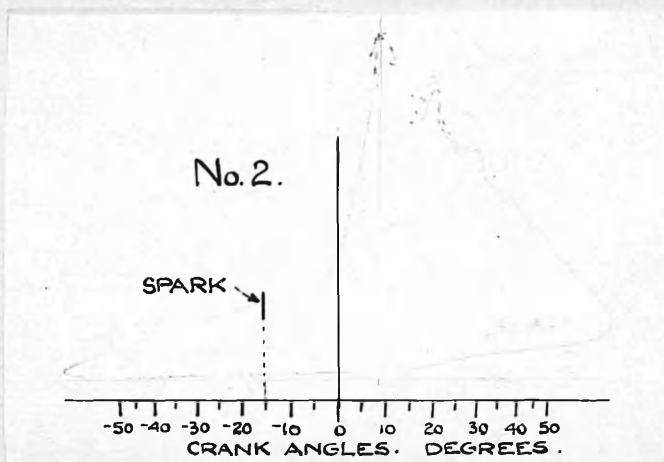
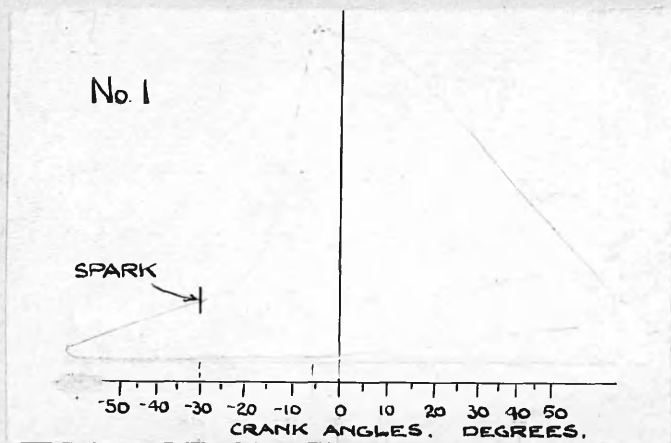


FIG. 32

spark - over the whole range.

A photographic test made at a later date to verify the conclusions come to in connection with Series C. is illustrated by Fig. 32, p. 49. With constant air-gas ratio a series of exposures was made at various angles of advance of the spark, a specially rapid film being used. The longer incandescent period due to advancing the spark is very clearly illustrated, and the cessation of the incandescence is seen to take place earlier in the expansion stroke as the spark is advanced. The actual indicator diagrams corresponding to the tests are given.

Exhaust Temperature and Variable Spark Point-

A decrease in the internal energy of the gaseous products after the prolonged incandescent period experienced with early ignition, is indicated by a few temperature measurements at exhaust, made with different points of ignition. The clear result obtained was that the temperature of exhaust falls steadily with the advancement of the spark - and this in spite of the smaller quantity of work obtained from the charge. The figures in Table VIII and the curve in Fig. 52 demonstrate the nature of the variation. This indicates that early ignition gives rise to (a) a hotter jacket, and (b) a cooler exhaust.

The exhaust temperatures were measured by the thermocouple of Platinum and Platinum-Rhodium fixed in the exhaust pipe as near the valve as was practicable. (see p. 28) The readings were made on a portable potentiometer. When the engine was running steadily with very few missed cycles, contact was made continuously by hand in the galvanometer circuit of the potentiometer while adjustment was made. The potentiometer reading increased/

Table VIII

Spark Angle Degrees	Exhaust Temp. °C
-41	531
-31 $\frac{1}{4}$	535
-21 $\frac{1}{2}$	546
-12 $\frac{1}{4}$	559
- 4	568
+ 3	575

Table IX.

TESTS	CO ₂	O ₂	N ₂	CO	H ₂	CH ₄	Heavy Hydro- Carbons.
A & B	4.1	0.3	6.3	18.4	49.2	19.7	2.0
C	4.5	0.6	6.0	16.1	48.6	21.9	2.3

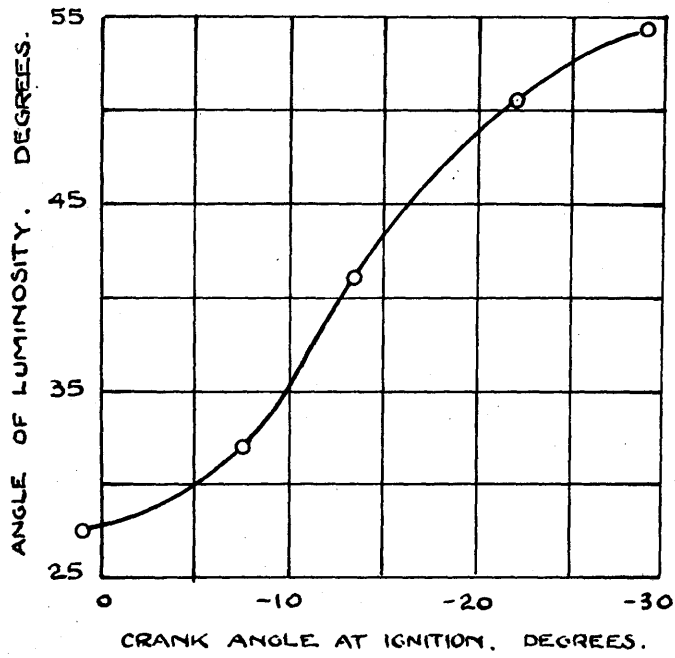


FIG. 30

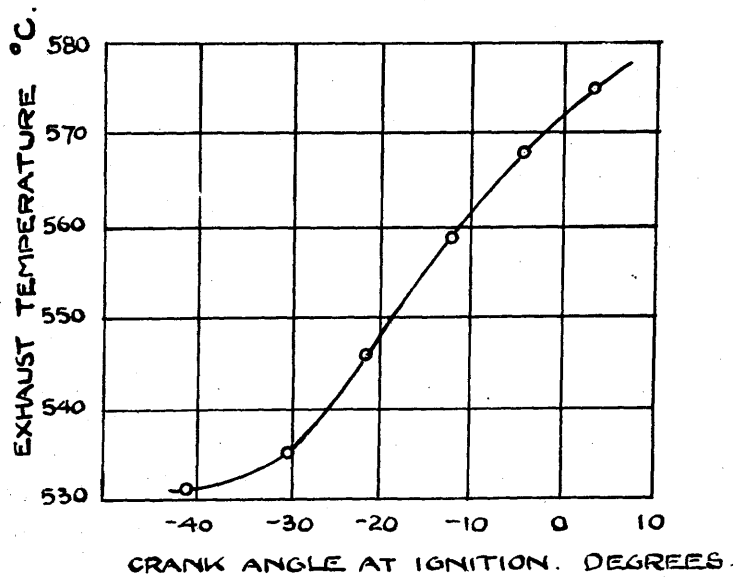


FIG. 31

increased steadily until a maximum was reached. This maximum was noted as the reading for the normal exhaust temperature. Difference between the relative figures obtained are readable to within 1 degree while the accuracy of the absolute temperature value is reckoned to be within 10 degrees. The magnitude of the effect of the metal surfaces in close proximity to the thermocouple is, however, unknown.

Quality of Gas. The compositions of the gas used in the tests A. B. and C. are to be found in Table IX. These were supplied by Mr. McLusky, manager of the Gas Department of Glasgow Corporation.

Discussion of Tests A, B and C.

It has been general among those who have studied the combustion process by optical or visual means to regard the luminosity as a sign of the chemical activity which is implied in the term "burning". Thus Bone, for example, speaks of the "final period of intense luminosity during which presumably the main combustion occurred"⁽¹⁾. Ellis and Wheeler, too, in describing some photographs of explosions⁽²⁾ in a glass sphere which showed that the core of the gaseous charge exhibits a revival of luminescence as the burning process goes on, state that this phenomenon "is due to the completion of combustion, under increased pressure, of molecules of combustible gas that escaped being burnt whilst the flame was travelling", and they conclude that this means that "after-burning" takes place.

The writer is of opinion that there is no evidence to show that the luminous condition is more than a temperature effect which may persist after the chemical activity which gives rise to it has subsided. It is patent that chemical activity must exist during the period of very weak luminosity which lies just after the passing of the spark and during which the greater part of the rise in pressure takes place. Yet it is only when the temperature becomes very high that the combustion is accompanied by the radiation of light to a marked extent.

If/

(1) "Flame and Combustion in Gases". p.158.
 (2) Journal of the Chemical Society. Feb.1927.

If the luminous condition was necessarily a mark of chemical activity then burning would appear (in Series C.) to be more prolonged with an advanced spark - and high average density - than when the spark was retarded. This does not appear to be reasonable. It is true that the luminous condition persists further down the expansion stroke in the case of the retarded spark than in the case of the advanced spark (see Fig.32 p.49); but it also is true that after the prolonged period of intense radiation accompanying the latter condition, the internal energy of the charge is less at any given point in the expansion line than when the spark is retarded. This is demonstrated by the readings of exhaust temperature (Table VIII) and by the pressure readings at 0.25" from the end of the diagram, given in Table VI. It will be still further demonstrated in the account of the later tests of Series D.

There is no evidence in these tests of the protracted chemical activity which is implied in the term "after-burning". The writer is of the opinion that both thermal and chemical equilibrium may be assumed with confidence to exist after an interval of time from the point of maximum intensity of radiation, equal to the time which elapses between the spark and the point of maximum intensity. This time varies in the tests according to the angle of advance of the spark and the air/gas ratio. It ranges from 18° to 30° of crank angle or from about 0.015 to 0.0236 second.

(1)

It was Hopkinson's conviction in working with normal mixtures that combustion was quite complete by the time/

time the flame front reached the walls of the explosion chamber, i.e. by the time maximum pressure was reached. This was at variance with Clerk's conception which is described as follows in his own words:⁽¹⁾

"The explosion is complete when maximum pressure is attained. It does not follow from this that the combustion is complete; that is another matter. The explosion arises from the rapid spreading of the flame throughout the whole mass of the mixture. More or less rapid inflammation means more or less explosive effect, but not complete combustion. The complete burning of the gases present may not occur until long after complete inflammation".

In the present tests there seems to be nothing which can be regarded as proving Hopkinson wrong or Clerk right. Clerk's conception was largely based on the results of his classic experiment on the re-compression and re-expansion of the gases in the engine Cylinder.⁽²⁾ A later section of this report deals with a repetition of this experiment the results of which do not seem to support all of Clerk's conclusions.

(1) "The Gas, Petrol and Oil Engine". Vol.I. p.128, 1910.
(2) Proc. Roy. Soc. Vol.77A. 1906. p.500.

SECTION IV

Effects of Varying Spark-Advance on the Indicator Diagram; and Measurement of Rate of Heat Loss.

Combustion Tests, Series D.

The results of Series C drew special attention to the thermodynamic effects of altering the angle of advance of the spark. Owing to the rather rich mixture which had to be used in these tests (in order to induce marked luminosity and so obtain a sufficiently clear photograph with the slow film used) the indicator records were all subject to much vibration. It was therefore considered desirable to use a larger air/gas ratio to obviate the vibration; but in order to get good photographic records with this weaker mixture a film with a speed of about 600 H and D was used.

The new tests were arranged in the manner previously described, the exhaust temperature being included among the observations. The indicator diagrams obtained are illustrated in Fig. 33 p.58 while the photographic record of the explosions is given in Fig. 34 p.58. Table X p.59 contains the observations and chief data relating to the tests.

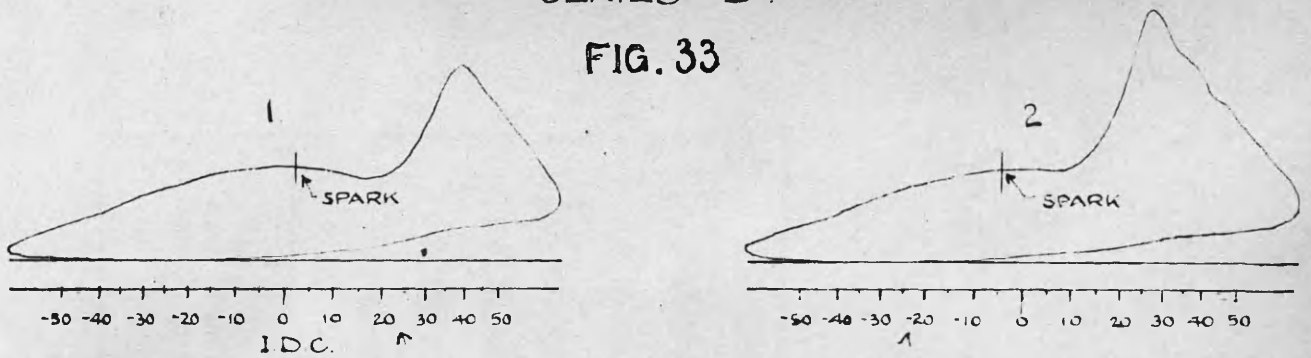
For mechanical reasons it was necessary to use the battery and coil ignition in tests 5 and 6; but as has been seen (p.35) this in no way affects the records of combustion.

It is rather difficult to control the air/gas ratio so as to keep it quite constant throughout a series of tests. The values show a slight increase in the ratio from No.1 to No.6, but they are sufficiently close to illustrate again the properties of the luminous period. This is especially true because the increasing ratio would tend to nullify rather than to increase the effects demonstrated by the photograph.

Luminosity/

SERIES D.

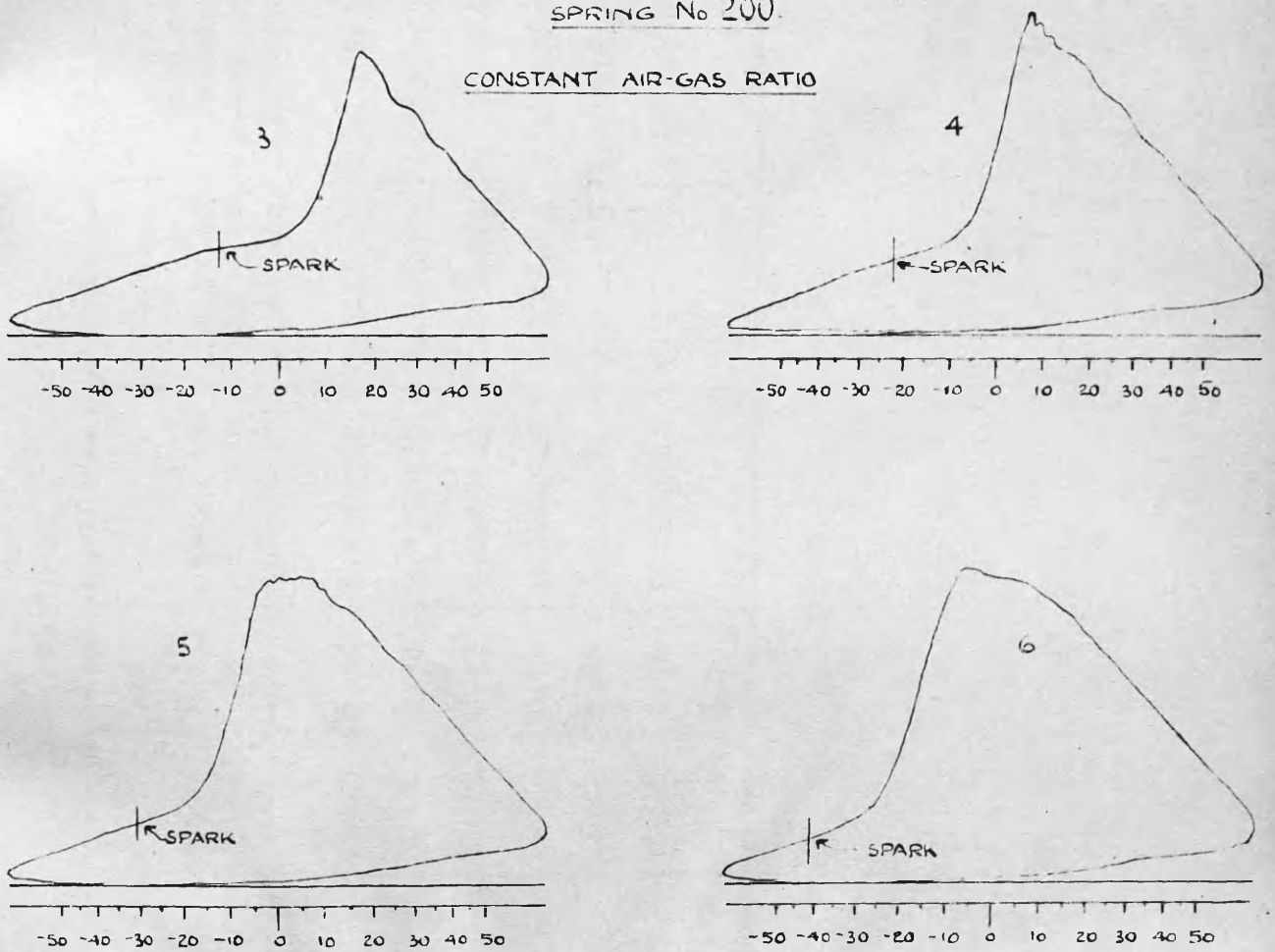
FIG. 33



SCALE OF CRANK ANGLES FOR UPPER BOUNDARY OF DIAGRAM

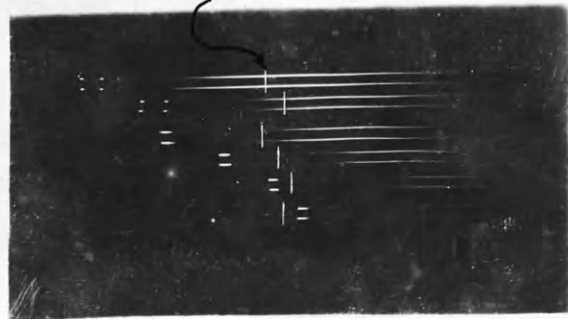
SPRING No 200.

CONSTANT AIR-GAS RATIO

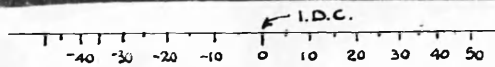


SERIES D.

VERTICAL LINES GIVE POSITION OF DEAD CENTRE



- No. 6
- 5
- 4
- 3
- 2
- 1



SCALE OF CRANK ANGLES — DEGREES

FIG. 34

Table X

Test	Crank Angle at Spark	Air/Min at 15°C & 760mm & A ft. ³	Gas/Cycle at 15°C & 760mm & g. ft. ³	Revs/Min. R.	Air/Gas Ratio $\frac{2A}{Rg}$	Mols. of fuel gas per cycle.	Mols. of air per cycle.	Mols. of clearance gases per cycle.	Total gaseous charge per cycle. Mols.
D1.	+ 3°	24.90	0.0355	210.8	6.66	0.0000930	0.0006243	0.00008007	0.0007974
D2.	- 4½°	24.88	0.0355	209.6	6.70	0.0000930	0.0006271	0.00008007	0.0008002
D3.	- 12½°	24.87	0.0352	210.4	6.73	0.0000922	0.0006247	0.00008007	0.0007970
D4.	- 21½°	24.62	0.0351	208.4	6.70	0.0000920	0.0006244	0.00008007	0.0007965
D5.	- 31½°	24.51	0.0353	210.1	6.66	0.0000925	0.0006166	0.00008007	0.0007892
D6.	- 41°	24.35	0.0345	208.8	6.76	0.0000904	0.0006164	0.00008007	0.0007890
				Mean	6.70			Mean	0.0007950

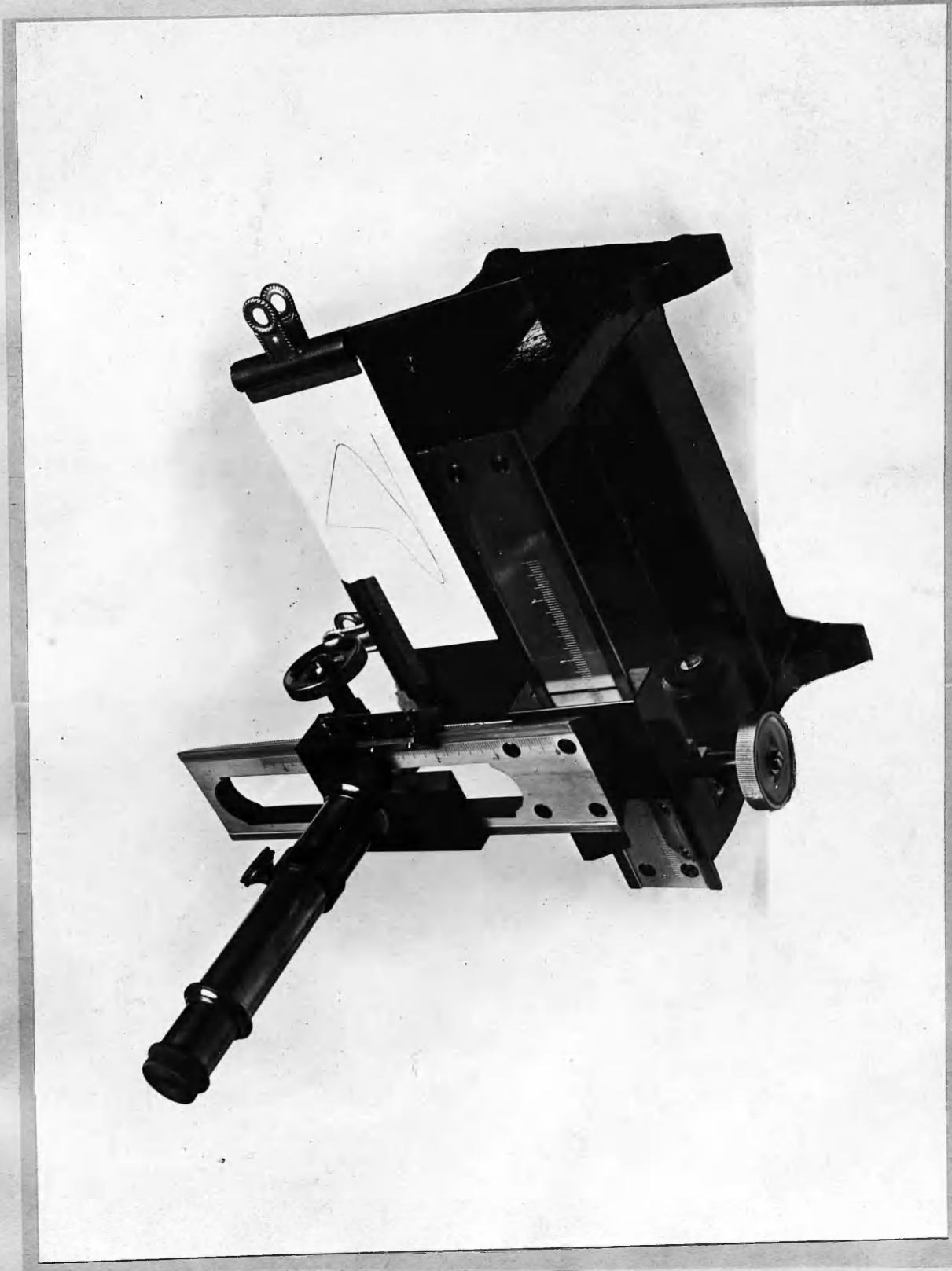


FIG. 35

Luminosity and Pressure.

In the record of explosions (Fig.34 p.58) the photographic drum drive was subject to a change of adjustment between tests. To render the tests easily comparable, the position of crank dead-centre is marked on the photograph for each case. A careful comparison of the photographic records and the indicator cards did not reveal any clear difference between the points of maximum intensity, and maximum pressure. The intensity of the luminosity increases, however, from No.1 to No.6 as can also be observed in the records of Series C.

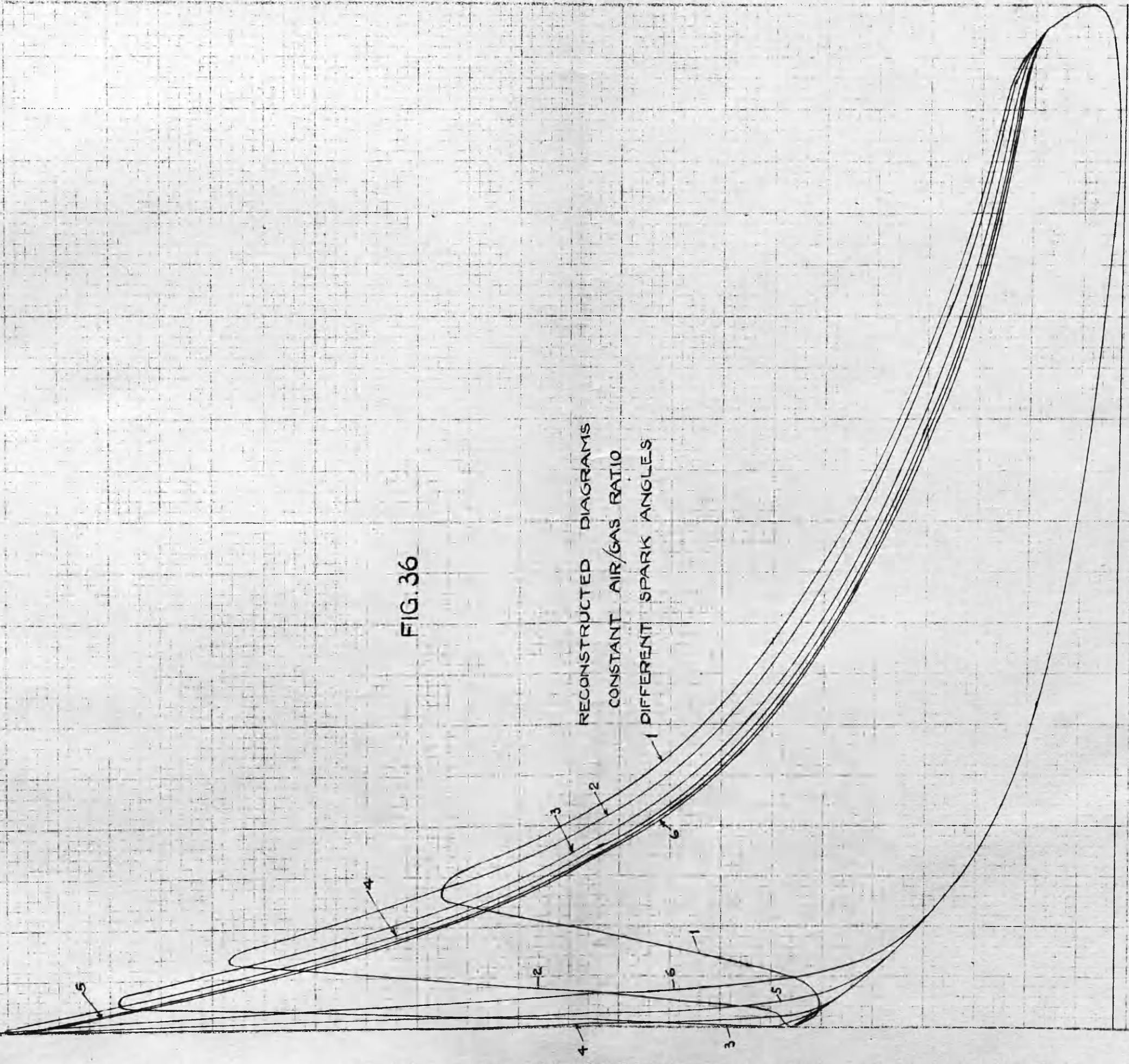
The Indicator Diagrams.

The reduced vibration experienced with the weaker mixture used in these tests made it possible for the diagrams to be measured up and transformed to the ordinary base of piston displacement. The microscope arranged by the writer for this purpose is shown in Fig.35, p.60. It has two traversing racks at right angles and reads by means of Vernier scales to 0.002 in. in each direction. It may be urged here that whatever inaccuracy in its indications of absolute measurements may be charged against the mechanical indicator, information of very great value can be obtained in the comparative study of diagrams obtained under different conditions, when the diagrams are measured up with the aid of a microscope of the kind referred to.

The diagrams were transformed with the use of Table I p. 11. The result is shown in Fig.36, p.62. The diagrams of tests Nos.3,4,5 and 6 exhibit nearly parallel expansion lines and from this it may be inferred that during expansion there is no marked disturbance due to any uneven combustion. This, together with the appearance of the photographic combustion lines for these tests, tends to show that the gases in/

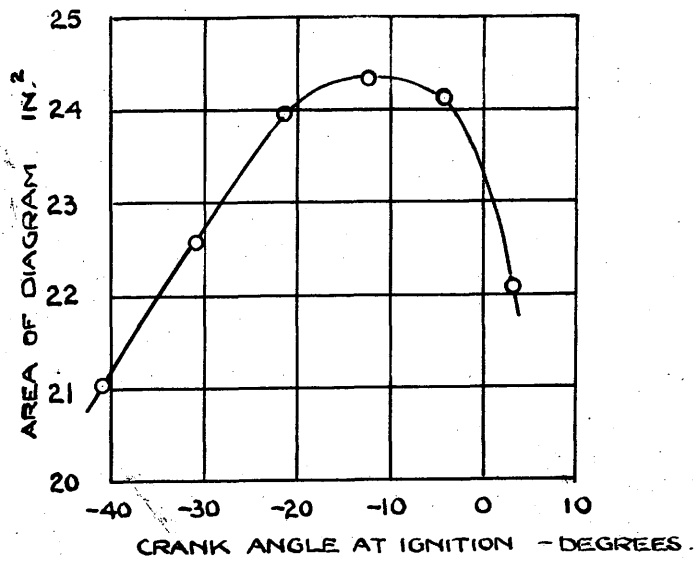
FIG. 36

RECONSTRUCTED DIAGRAMS
CONSTANT AIR/GAS RATIO
DIFFERENT SPARK ANGLES



TEST	CRANK ANGLE AT SPARK DEGREES	AREA OF DIAGRAM AS PLOTTED IN ²
D1	+3	22.05
D2	-4¼	24.10
D3	-12¼	24.31
D4	-21½	23.94
D5	-31¼	22.55
D6	-41	21.04

FIG.37



in all these tests are in a similar state of equilibrium at any given volume on the expansion curves.

Optimum Spark Angle. When the areas of the positive loops of the indicator diagrams are plotted on a base of spark-angles the maximum value corresponds with what is now known as the "optimum spark setting". The curve is given in Fig. 37 p. 62 and shows that the best spark setting for the given conditions of speed and air/gas ratio is about -12° .

Temperature. To examine more closely than was done in the previous tests the relationship between the temperature and the luminosity, curves of "mean temperature" were plotted on a base of crank angles for all the tests of Series D. The curves are shown in Fig. 38 p. 64 together with the curves of pressure.

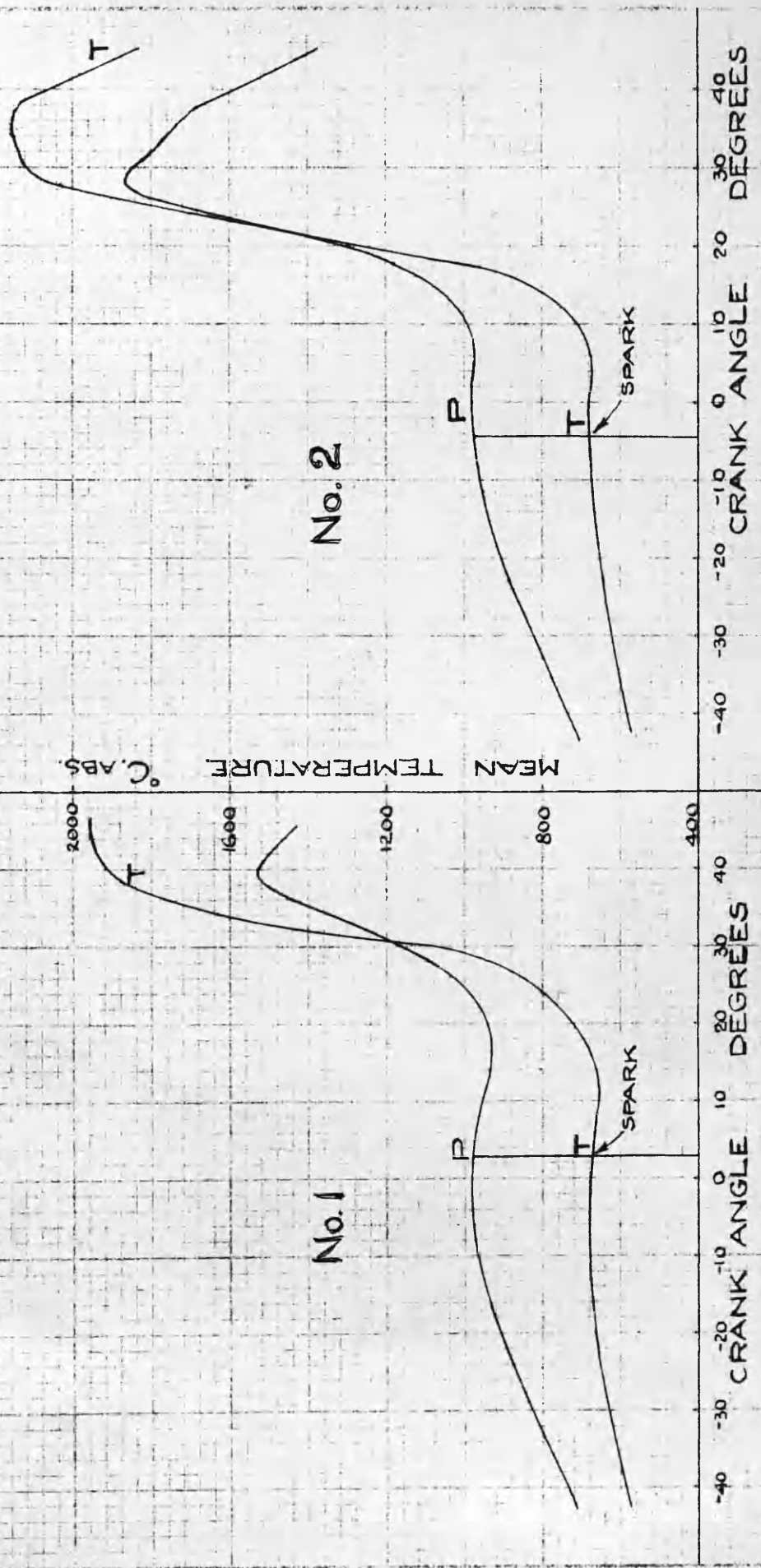
The "mean temperature" according to the practice followed by Professor W.T. David and others, is the temperature reckoned from the pressure curve. In the experiments with a closed vessel such as David performed, the mean temperature was directly deducible from the pressure; but in the gas/engine the changing volume is to be taken into account. The method of calculating the temperature is described on p. 86 of the Appendix. This method does not take account of the change in the number of molecules due to combustion. If a correction for this change is made, the figures obtained are about $3\frac{1}{2}$ per cent higher than the temperatures shown by the curves for the period following combustion. For the combustion period itself the correction is indeterminate.

Speed of Combustion. The time interval elapsing between the spark and the maximum pressure has been called by some observers the "time of combustion". It has been thought desirable/

FIG. 38

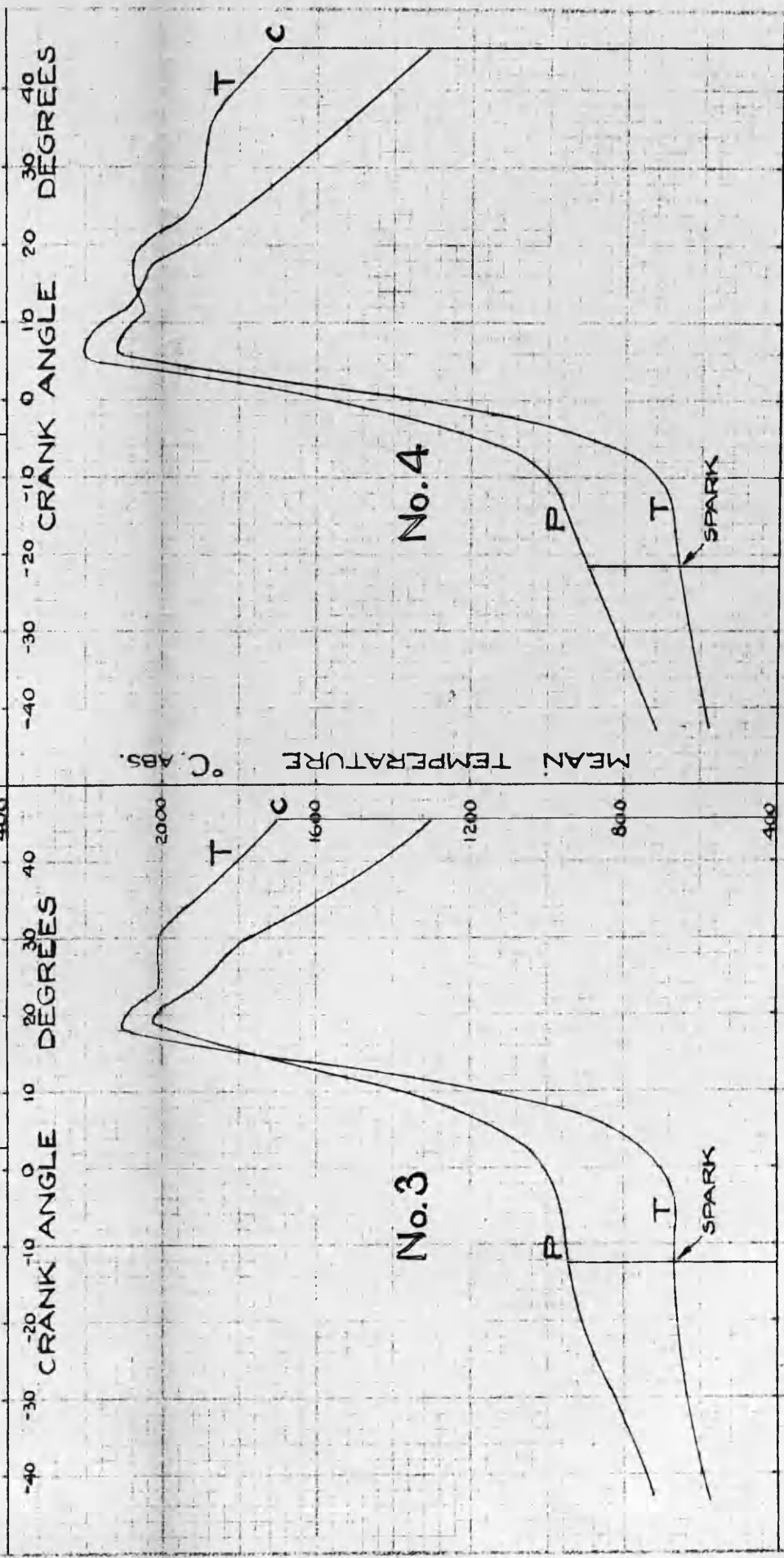
before 10 64

SERIES D



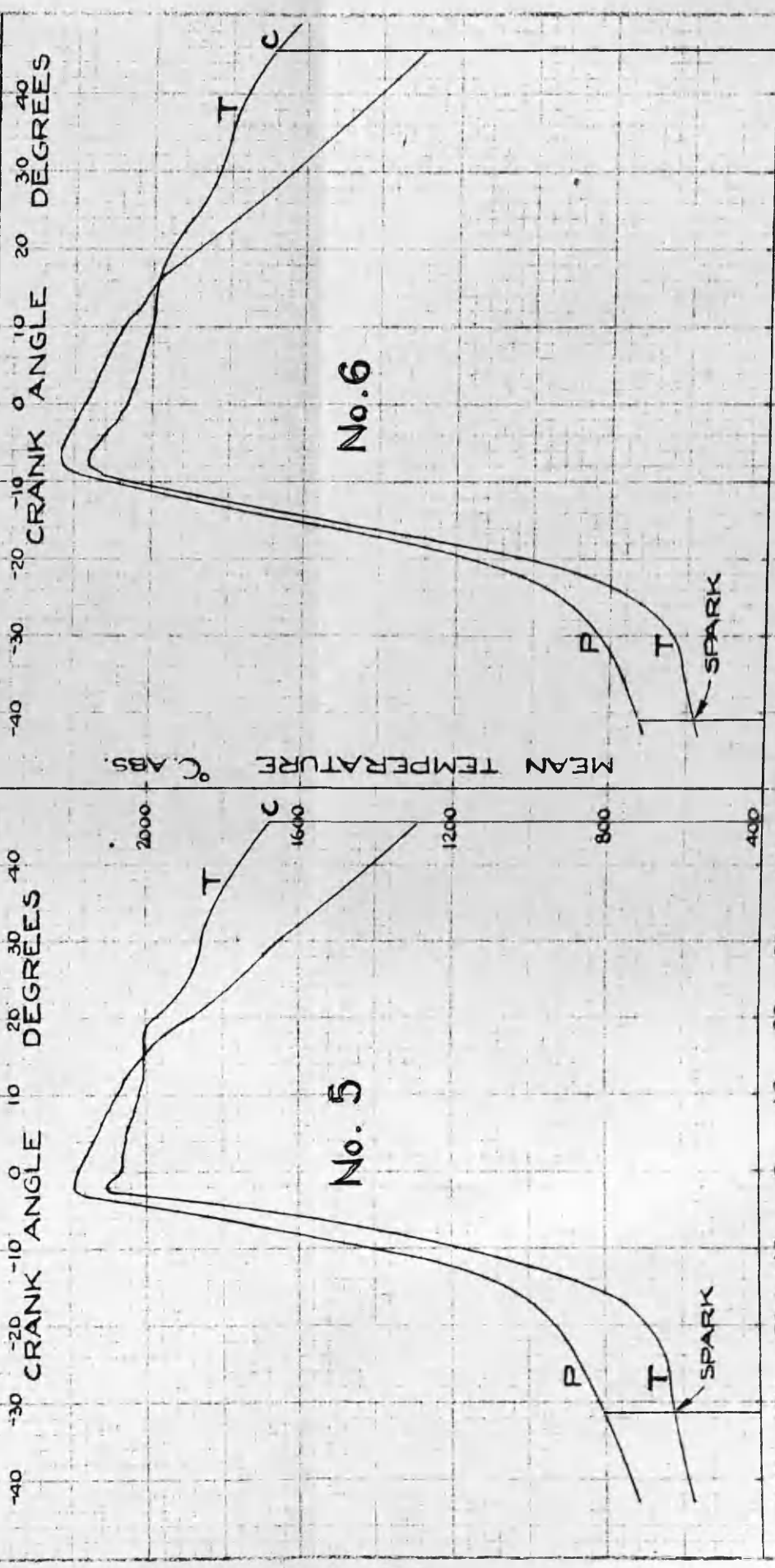
No. 1

No. 2



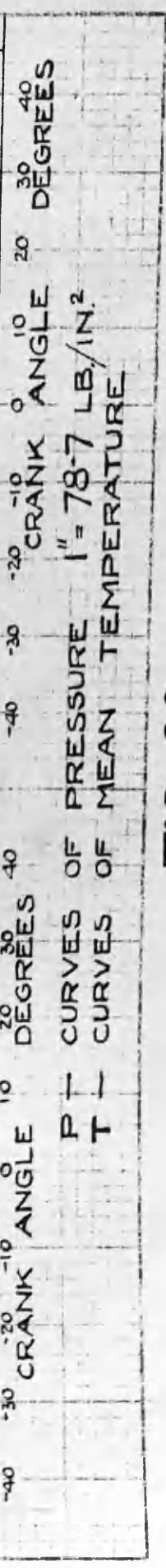
No. 3

No. 4



No. 5

No. 6



P — CURVES OF PRESSURE $1'' = 78.7 \text{ LB./IN.}^2$
 T — CURVES OF MEAN TEMPERATURE

FIG. 38

desirable to collect into one table the times of combustion for all the tests. This is done in Table XI.

Table XI

A		B		C		D	
Air/ Gas = 5.837 Spark at $-10\frac{1}{2}^{\circ}$		Spark at -9°		Air/ Gas = 5.402		Air/ Gas = 6.70	
Jacket Temp. °F	Time of Combust. sec.	Air/ Gas	Time of Combust. sec.	Spark Angle	Time of combust. sec.	Spark Angle	Time of Combust. sec.
68.5	0.0159	6.34	0.0172	-29	0.0154	-41	0.0263
93.5	0.0168	6.04	0.0164	-22	0.0145	-31 $\frac{1}{4}$	0.0232
109.5	0.0152	5.90	0.0156	-13 $\frac{1}{2}$	0.0148	-21 $\frac{1}{2}$	0.0220
128.0	0.0168	5.54	0.0155	-7 $\frac{1}{2}$	0.0189	-12 $\frac{1}{4}$	0.0224
145.7	0.0171	5.44	0.0156	+1	0.0191	-4 $\frac{1}{4}$	0.0249
		5.48	0.0157			+3	0.0261

An examination of the figures referring to Series D in conjunction with the indicator diagrams in Fig. 33 p. 58 seems to lead to certain conclusions. The speediest combustion takes place in test No. 4. In this particular test the dead-centre falls near the middle of the combustion period, i.e. the gaseous density has its maximum value half way through that period. In tests Nos. 5 and 6 the maximum pressure is reached before the point of maximum density, and in Nos. 1, 2 and 3 it is reached a considerable time after the point of maximum density has been passed. It would appear, therefore, that the speed of the combustion wave depends on the average density of the charge during the burning process.

The table in general seems to show that a marked speeding up of combustion accompanies a decrease in the air/gas ratio, a result supported by common observation.

In these tests the combustion time ranges from 0.0156 sec. to 0.0263 sec. depending on working conditions. The writer has recently seen a reference to work on combustion in the petrol engine cylinder by Professor Watson (1) in which the combustion times were found to vary from 0.01 to 0.018 sec. It is perhaps surprising that the combustion times/

times should not differ more widely as between the gas engine and the petrol engine. With our knowledge of the form of the indicator card for the gas engine running at 200 revs/min. it can be fully understood why the general form of the diagram of a petrol engine running at over 1000 revs/min. indicates little "constant volume burning".

A measure of the rate of heat loss at maximum temperature.

Referring to the curves of mean temperature in Fig.38 (opposite p.64) it will be noticed that the maximum temperature is much the same in the tests 3,4,5 and 6, and that the temperature is maintained at a high value, approximating to the maximum, for a period which depends on the angle of advance of the spark.

If it be assumed that the loss of heat up to the point of maximum temperature is the same in all cases then an examination of the diagrams will afford a means of obtaining the rate of heat-loss in the region of the high temperature. There is strong justification for this assumption. From the instant the spark takes place until the flame-wave almost reaches the walls, the temperature of the gases in contact with the walls does not rise to a great extent. The loss by conduction, therefore, is moderate. Loss by radiation becomes specially marked only when the flame is approaching the walls, i.e. when the point of maximum pressure is nearly reached. The loss by radiation and conduction in the first part of the combustion stage, therefore, may be reasonably assumed to be the same in all the four tests 3,4,5 and 6.

Let/

Let the two curves ABC and A' B' C' (Fig.39) represent the changes in the mean temperature in two tests with

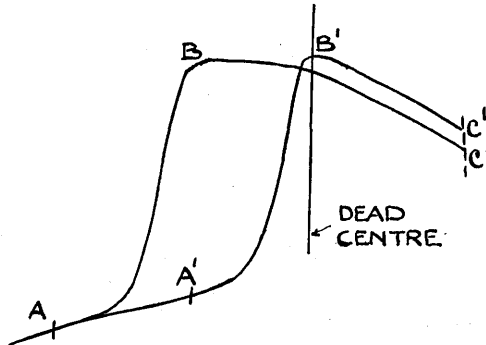


FIG.39

the same air/gas ratio, but in one of which the spark is at A and in the other at A'. The mean temperature from B to C is nearly the same as the mean temperature from B' to C', and the extra heat lost in ABC may be regarded as the loss due to the difference BB' in the interval during which the high temperature is maintained.

If Partington and Shilling's ⁽¹⁾ equations are applied to the pre-combustion mixture at A and A' and to the post-combustion mixture at C and C', and if the work areas between A and C, and between A' and C' are found, an application of the energy equation will yield a value for the difference in the heat lost — assuming the heat of combustion of the charge to be the same in both cases.

Taking the curves for tests 3,4,5 and 6 in Fig.38 and choosing the point C in each case as shown we obtain the values given in table XII.

Table XII

Test	I_A C.H.U.	I_c C.H.U.	Work done between A & C C.H.U.
D3	2.85	9.77	1.405
D4	2.81	9.77	1.33
D5	2.66	9.625	1.12
D6	2.45	9.625	0.81

Table XIII gives the value of the difference in heat-loss between chosen tests.

The figure obtained using tests 4 and 6 would appear to be too high. The values are far from consistent owing to the fact that we are here dealing with small differences

(1) "The Specific Heat of Gases."

of rather large quantities.

This method of estimating rate of heat-loss in the combustion stage is put forward tentatively, as a method possible when the indicating apparatus is of a specially high standard.

Table XIII

Taking Tests	Difference in Heat lost C.H.U.	Difference in duration of high temperature period. Degrees of Crank Angle	Rate of Heat loss. C.H.U./degree.
D3 and D6	0.35	25	0.014
D4 and D6	0.305	16	0.019
D5 and D6	0.10	6	0.016
Mean Rate:			0.017

The heat of combustion of the charge is very nearly 16 C.H.U. and therefore the rate of heat-loss obtained, namely 0.017 C.H.U. per degree of crank-angle, indicates that, within an angle of 10 degrees in the region of the dead-centre, the charge loses about 1 per cent of its heat of combustion. This is perhaps less than one might expect.

In order to compare this rate of heat-loss with that obtained by another method, Fig.40 p.68 was prepared. The curve shows the rate of heat-loss on a temperature base, replotted from figures obtained by the Clerk "zig-zag diagram" method and graphed in Fig.54 (opposite p.85). The point obtained from the considerations above described as applied to Series D is found to lie below the extended curve obtained by the Clerk method.

It is to be noted, however, that the Clerk method cannot take in the expansion line, and its application gives the values for the lines of recompression and re-expansion - for which the temperatures are very much lower than that of the combustion stage. Here the average temperature for the high-temperature period is 1940°C.abs.

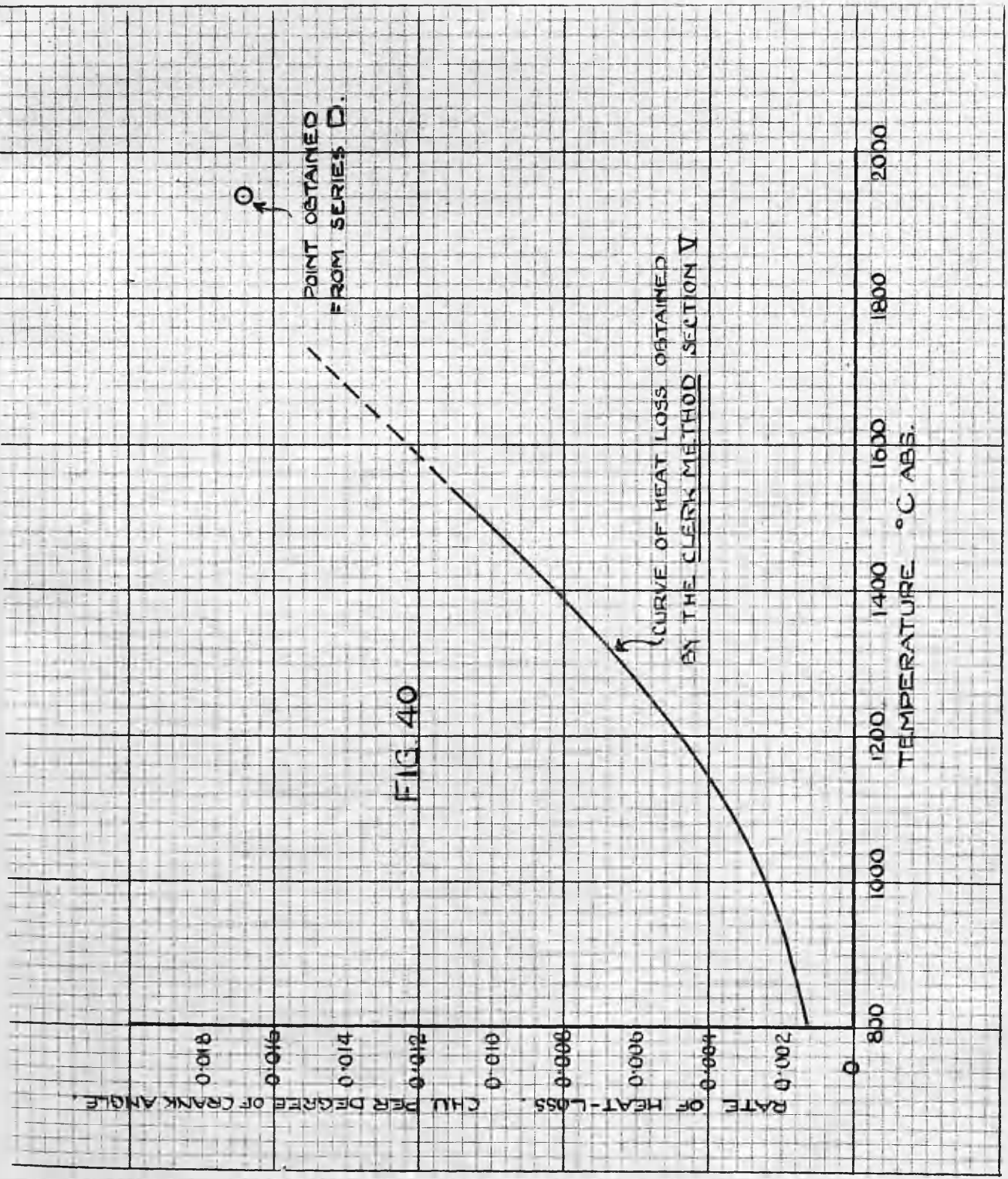


FIG. 40

SECTION V.AN EXAMINATION OF CLERK'S "ZIG-ZAG DIAGRAM"METHOD FOR DETERMINING RATE OFHEAT LOSS AND FOR FINDINGSPECIFIC HEATS OFGASES.

Clerk's classic experiment on the successive compression and expansion of the products of combustion in the cylinder of a gas engine was described in 1906 in the Proceeding of the Royal Society (Vol.77A). Since that time there is on record, apart from repetitions by Clerk himself, only the work of Hopkinson on the compression and expansion of air as representing an application of the same method.

It is difficult fully to appreciate the points of the method without actually applying it from beginning to end.

To verify some of Clerk's conclusions the present test was carried out. Use was made of a set of special cam rollers designed by Professor Goudie. Each was so arranged that by removing a distance piece on the roller pin a spring instantly forced the roller along the pin and out of action. The arrangement can be seen clearly in the photograph Fig.12, p.18

An ordinary mechanical indicator (Maihakmake) was used for the pressure records. Previous experience had shown that cord-stretch effects tended to distort the Clerk diagram so that the ends of the successive double lines did not show up as cleanly acute. To overcome this, the Clerk diagram was recorded on the displaced scale. This was later transformed to the true diagram on a large scale by using Table I and taking the pressure readings on the displaced card by means of a microscope.

Before the test, the valves were ground in, and leakages at the indicator connections and the spark-plug repaired. In spite of this it was fully understood that, since the cylinder liner and piston in use were far from new, leakage past the piston would be not inconsiderable. It was also noted that although/

although the indicator was in good condition considerable leakage took place past the indicator piston. Whatever results were to be obtained, therefore, it was noted that leakage would represent a source of sensible error.

Clerk's Method. Before the exhaust could take place in the course of a normal working cycle, the cam rollers were released so that neither the exhaust valve nor the admission valve could open during the subsequent revolutions of the engine. The process, when recorded on an ordinary indicator, yielded a diagram like that shown in Fig. 41, p. 71

Brief Sketch of the Analytical Process. Adopting so far as possible Clerk's symbols, let the work done on the gas during compression AB be W , and by the gas during expansion BC, W_1 . Let S be the average thermal capacity at constant volume of the gas in the cylinder (expressed in ft.-lb.) between A and B at which points the temperatures are respectively t_0 and t_1 .

$$S = \frac{W - \text{Heat lost during compression AB}}{t_1 - t_0} \quad \text{--- (1)}$$

Let the heat lost be written down as $Sx\theta$ where θ is a range of temperature, then $S = \frac{W - S\theta}{t_1 - t_0}$

$$\text{or } S = \frac{W}{t_1 - t_0 + \theta} \quad \text{--- (2)}$$

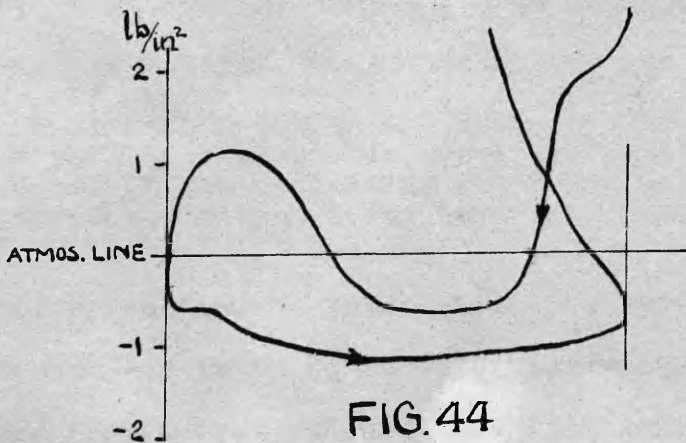
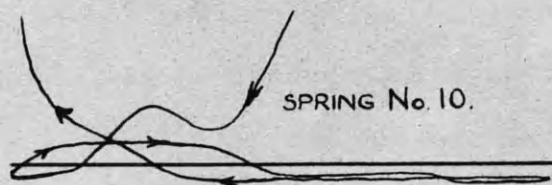
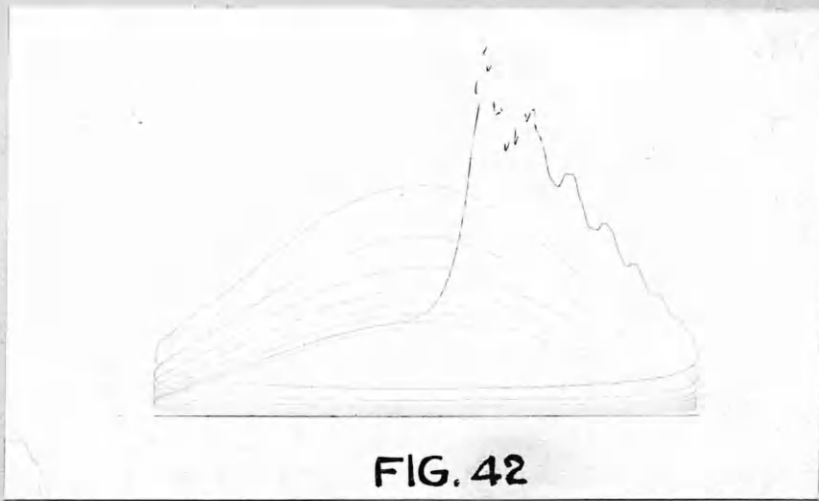
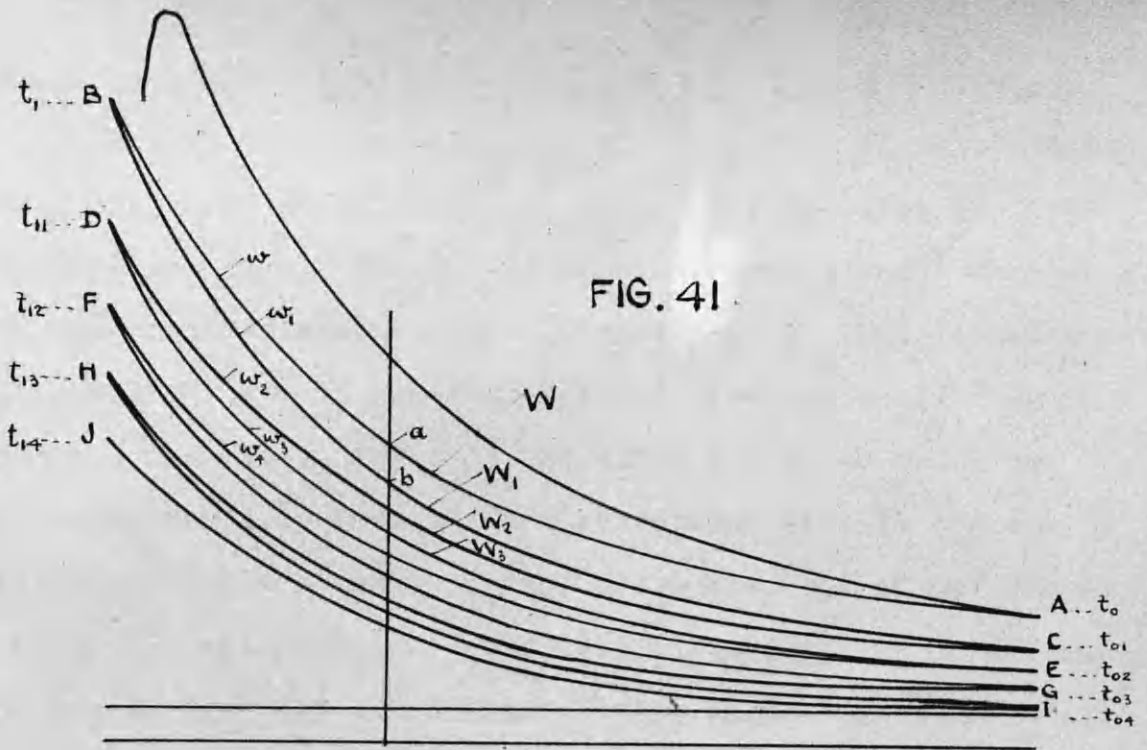
The quantity θ is approximately determinable from consideration of the double strokes such as ABC. If S_1 is the average thermal capacity of the charge between the temperature t_0 at A and the temperature t_{01} at C

$$S_1 = \frac{\text{Heat lost in ABC} - (W - W_1)}{t_0 - t_{01}}$$

Let the heat lost during ABC be written $S_1 g$

$$\text{Then } S = \frac{W - W_1}{g - (t_0 - t_{01})}$$

$$\text{or } g = t_0 - t_{01} + \frac{W - W_1}{S_1} \quad \text{--- (3)}$$



As a first approximation assume $W - W_1 = 0$ i.e. $g = t_0 - t_{01}$.

Plot such values as t_0 and t_{01} on a base of revolutions. From the curve so obtained get values for the drop in temperature in the first half of each revolution. This drop in temperature is approximately equal to θ . Substituting this value for θ in equation (2) get a value for S . By putting this value for S_1 in equation (3) a new value is obtained for g . Successive applications of this process to all such double strokes as ABC, yield a series of new values for g from which the curve of drop in temperature on a base of revolutions can be modified. New values for θ are obtained from the first halves of the revolutions on this modified curve and by substituting these in equations such as (2) new values are obtained for S . This is found to be a sufficient approximation in view of the limitations of the method.

Similarly for the high pressure end of the diagram the two typical equations

$$S = \frac{W_1}{t_1 - t_{01} - \theta} \quad \text{and}$$

$$g = t_1 - t_{01} - \frac{W_1 - W_2}{S_1} \quad \text{are applied to the expansion}$$

lines and such double strokes as BCD.

Expedients Adopted. Clerk stated that when the values of g were plotted on a base of mean temperature in the double strokes, a curve was obtained such that half the ordinate at the mean temperature value for any single stroke gave the value of θ for that stroke. He defined "mean temperature" as follows:

"Mean temperature during any expansion or compression stroke or part of a stroke is taken in relation to time, the obliquity of the connecting rod being neglected and the motion of the piston being taken as simple harmonic motion."

With the interpretation of this definition herein adopted, the above statement was found to be very nearly true.

For the reason that calculations made by the above methods are/

are liable to very considerable disturbance due to possible indicator errors so small as 0.1 mm., Clerk adopted another procedure in obtaining his final results. He drew on his diagram a vertical line at $\frac{3}{10}$ ths of the stroke from the inner end and confined his observations to the segments lying on the high pressure side of the line. Referring to the partial compression lines by $1c, 2c,$ etc. and to the partial expansion lines by $1e, 2e,$ etc. we have, during $1c$ and $1e$, an observed fall of temperature of $t_a - t_b$ (see Fig 41, p. 71) The true temperature fall value $g' = t_a - t_b + \frac{w - w_1}{S}$, where w and w_1 are the work values.

The value given to S in applying this expression is that obtained from the calculations on the full line. The values such as g' thus obtained are plotted on a base of mean temperature for the combined partial compression and partial expansion strokes. Following the general procedure described above, values for θ' were found by taking half the ordinate corresponding to the mean temperature for $\frac{3}{10}$ ths of the single stroke, where

$$S = \frac{w}{t_i - t_a + \theta'} \quad \text{on compression lines and}$$

$$S = \frac{w_1}{t_i - t_b - \theta'} \quad \text{on expansion lines.}$$

The Form of the Diagram. Before proceeding to a detailed description of the present test ~~it is~~ it is desirable to consider briefly the thermodynamic factors determining the form of the diagram.

Giving the symbols their usual significance, the First Law of Thermodynamics is expressible by

$$dQ = C_v \cdot dT + \frac{pdv}{J}.$$

Postulating $p v = W R T$ and $W = 1$ we have

$$\begin{aligned} dT &= \frac{\partial T}{\partial v} \cdot dv + \frac{\partial T}{\partial p} \cdot dp. \\ &= \frac{p}{R} dv + \frac{v}{R} dp. \end{aligned}$$

$$\begin{aligned} \therefore dQ &= C_v \left(\frac{p}{R} dv + \frac{v}{R} dp \right) + \frac{pdv}{J} \\ &= \frac{C_v}{R} + \frac{1}{J} pdv + \frac{C_v}{R} \cdot vdp \end{aligned}$$

$$\text{But } C_p - C_v = \frac{R}{J} \qquad \frac{1}{J} = \frac{C_p - C_v}{R}$$

$$dQ = \left(\frac{C_v}{R} + \frac{C_p - C_v}{R} \right) pdv + \frac{C_v}{R} \cdot vdp.$$

$$\text{or } \frac{dQ}{dt} = \frac{C_p}{R} \cdot p \cdot \frac{dv}{dt} + \frac{C_v}{R} \cdot v \cdot \frac{dp}{dt} \quad \text{where } t \text{ is time.}$$

At the dead centres $\frac{dQ}{dt}$ is finite, but $\frac{dv}{dt} = 0$.

Therefore the converging pairs of lines have common tangents at the points A, B, C etc. The out-of-phase diagram, however, will have zero gradient at the points corresponding to the dead centre positions as reference to page 11 will show.

Description of Test. The engine was run steadily on lead for a considerable time. Readings were taken at the beginning and end of a chosen interval of time in a manner similar to that adopted in the previously described tests. In the interval an exhaust temperature reading was noted and a light spring diagram obtained. Immediately the second set of readings was taken, the cam rollers were released and an indicator diagram was obtained. The diagram is shown in Fig. 42,^{p.71} which consists of an actual card.

It should be noted here that Clerk ran his engine light for this purpose and used a cold jacket. In the present test the engine ran on load throughout the period of the test and the taking of the diagram, and a temperature of 112°F was registered at the jacket.

The Diagrams. The displaced diagram was first converted to the ordinary P-V scale. This was done by mounting it under a microscope which could be traversed in two directions at right angles, the displacements of the microscope being noted on/

TABLE XIV

TRUE DISPLACEMENT	0.5	0.292	0.211	0.153	0.108	0.073	0.046	0.026	0.012	0	0.011	0.027	0.050	0.080	0.120	0.173	0.242	0.341	0.591
UPPER CURVES	8.16	8.57	8.85	9.14	9.46	9.75	10.04	10.27	10.43	10.57	10.34	10.11	9.84	9.51	9.20	8.87	8.54	8.25	7.84
	7.88	8.20	8.44	8.70	8.95	9.19	9.39	9.57	9.72	9.85	9.68	9.50	9.28	9.05	8.77	8.50	8.26	8.04	7.70
	7.74	8.035	8.22	8.42	8.63	8.84	9.03	9.19	9.32	9.43	9.29	9.12	8.95	8.74	8.52	8.30	8.09	7.91	7.62
	7.64	7.89	8.07	8.25	8.44	8.62	8.78	8.92	9.03	9.13	9.02	8.87	8.72	8.54	8.34	8.14	7.95	7.81	7.55
	7.58	7.81	7.96	8.12	8.28	8.46	8.61	8.74	8.84	8.93	8.82	8.70	8.56	8.38	8.21	8.05	7.89	7.74	7.50
	7.52	7.74	7.88	8.04	8.19	8.36	8.48	8.59	8.69	8.78	8.67	8.57	8.44	8.29	8.11	7.96	7.81	7.69	7.45
DIAGRAM DISPLACEMENT	0	0.05	0.1	0.15	0.2	0.25	0.3	0.35	0.4	0.5	0.6	0.65	0.7	0.75	0.8	0.85	0.9	0.95	1.0
LOWER CURVES		7.87	7.80	7.78	7.75	7.77	7.73		7.72		7.72			7.74	7.76	7.79	7.82	7.88	
		7.67	7.63	7.59	7.58	7.58	7.56		7.57		7.57			7.58	7.59	7.61	7.63	7.67	
		7.58	7.53	7.50	7.49	7.50	7.48		7.49		7.49			7.49	7.50	7.52	7.53	7.57	
		7.49	7.47	7.44	7.43	7.44	7.43		7.43		7.44			7.45	7.45	7.46	7.48	7.50	
		7.45	7.42	7.40	7.39	7.40	7.40		7.40		7.40			7.40	7.41	7.42	7.43	7.46	
TRUE DISPLACEMENT	0.5	0.719	0.776	0.830	0.871	0.905	0.932		0.971		1.0			0.975	0.954	0.924	0.879	0.808	0.591

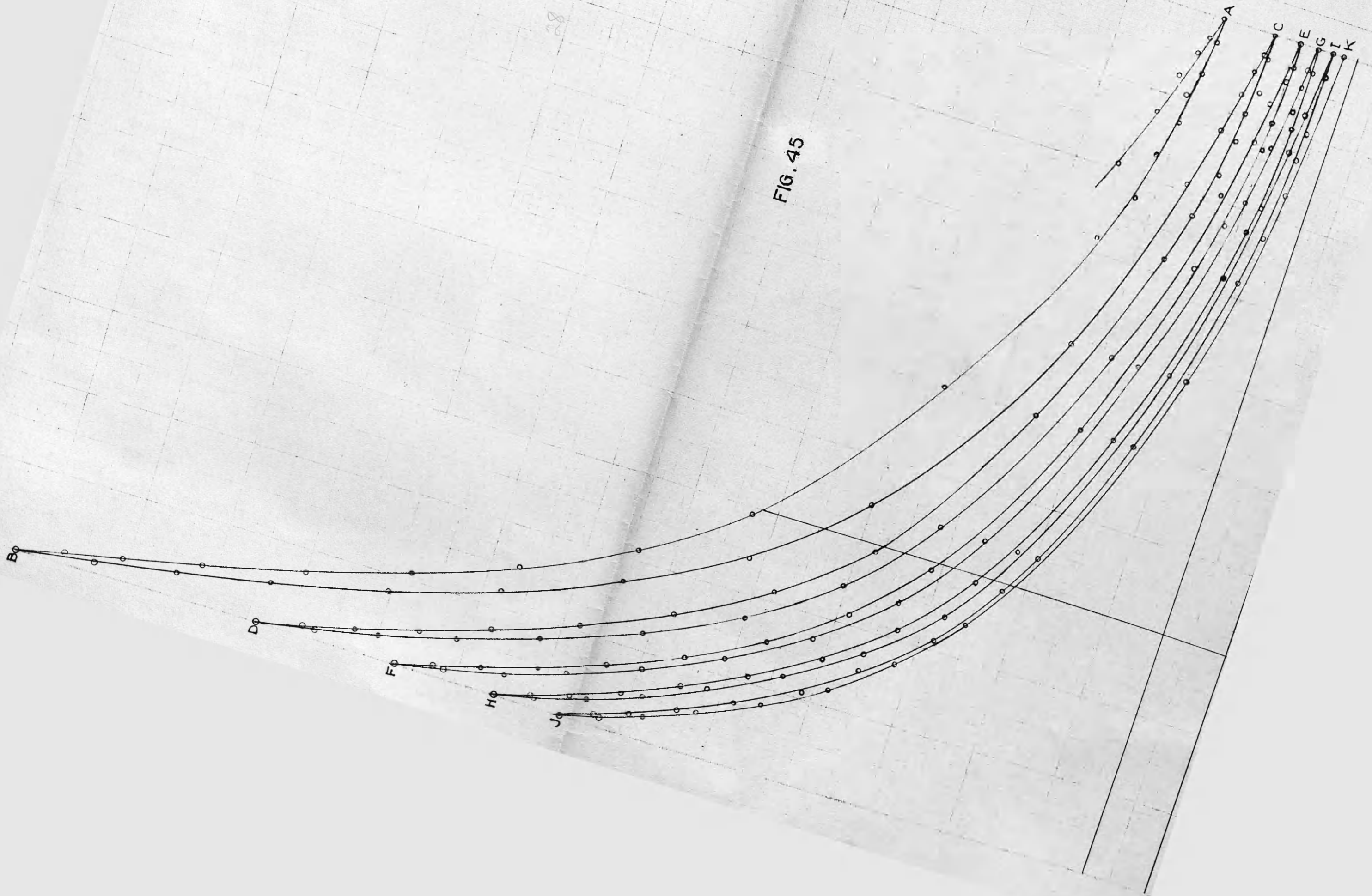
READING ON ATMOSPHERIC LINE 7.33 cm.
 (ALL READINGS IN CMS.)

FIG.45

before p.76

28

FIG. 45



on Vernier scales. The atmospheric line was arranged to lie parallel to one of the directions of traverse of the microscope. At regular intervals along this line sets of readings were made in the other direction of traverse on the various convolutions of the curve. The result is given in Table XIV together with the corresponding fractional displacements on the true curve.

The light spring diagram is shown in Fig. 43^{p.71}, on the displaced scale. Its true scale form is shown in Fig. 44^{p.71}. The displaced diagram has an advantage again in this case. It is generally the conditions at the end of suction or the end of exhaust which are required from a light spring card. By opening up the end scales, the displaced diagram shows with accuracy the pressures at those points.

The diagram Fig. 45 was built up from the values in Table XIV. It has the characteristic form of the diagram originally described by Clerk.

AB, CD, EF etc. are compression curves. BC, DE, FG, etc. are expansion curves.

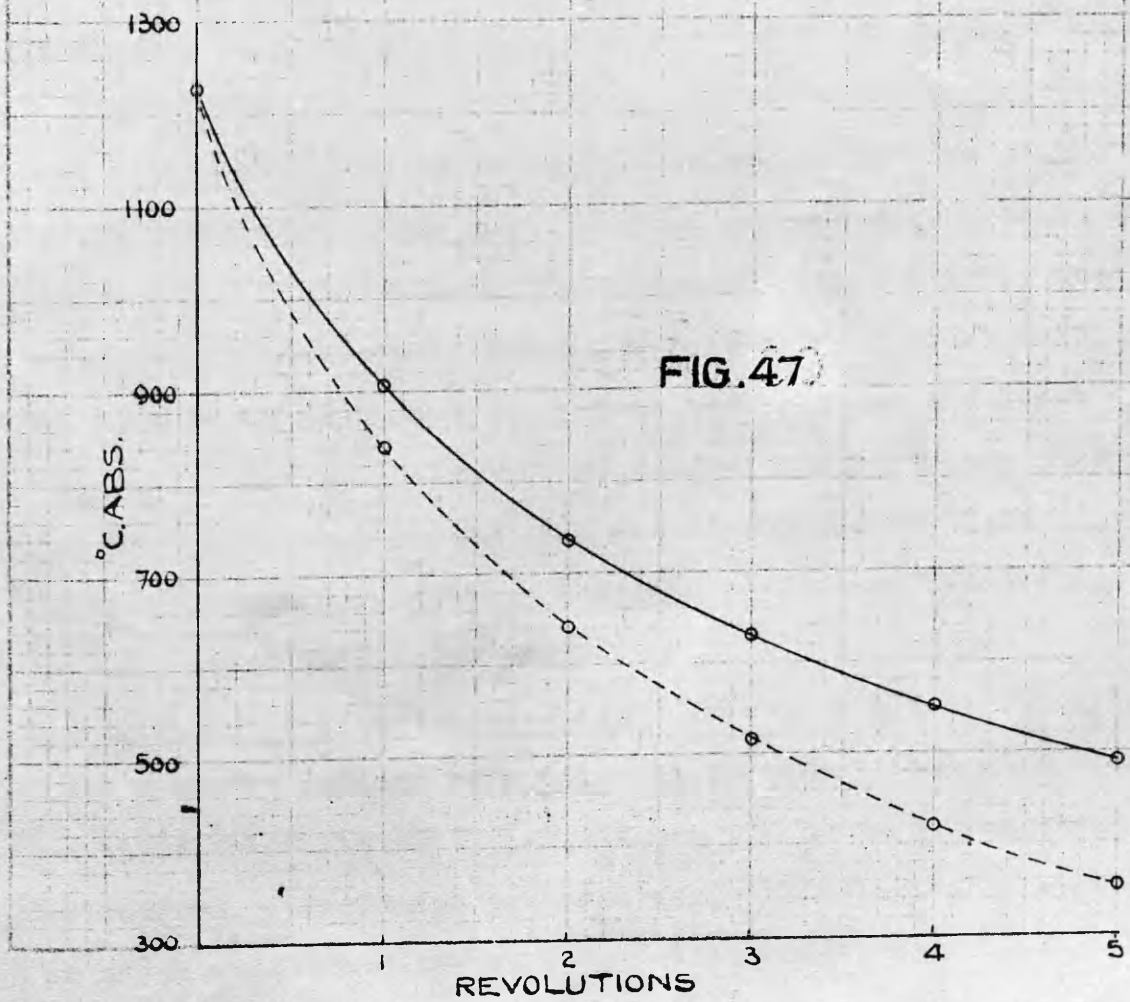
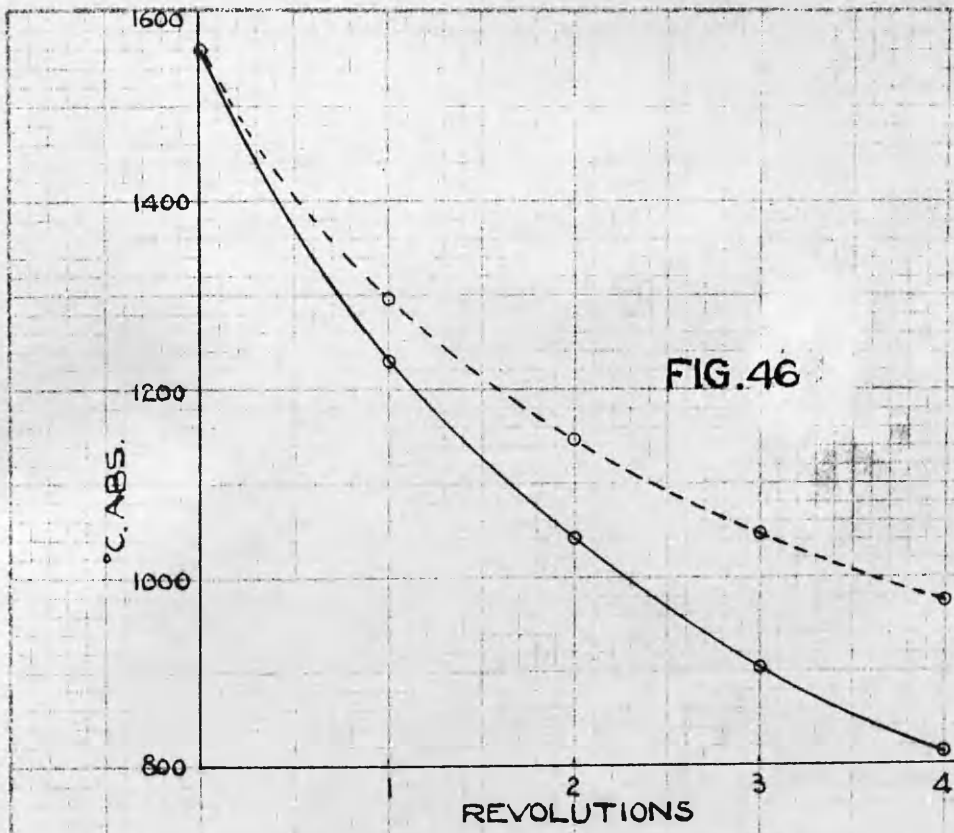
All the calculations were based on this diagram. Areas were measured by means of an Amsler planimeter.

Summary of Work Done in the Present Test.

The mass of the gaseous charge in the cylinder was found (see Appendix)^{p.86} and hence the temperatures at the principal points on the curves. The temperatures at the ends of the diagram were plotted in Figs. 46 and 47, Fig. 46 referring to the high pressure end and Fig. 47 to the low pressure end. The dotted curves are the modifications obtained when the methods described on pp. 71-72 are applied.

The final values of the specific heat expressed in ft.-lb. per ft.³ at S.T.P (to follow Clerk's practice) range from 28.2 to 25.8 as obtained on the expansion lines, and from 28.25 to 25.6 as obtained on the compression lines.

These results are all high as compared with the figures now generally adopted. But this was also Clerk's experience in/



in his original work.

Before he applied the expedient of plotting "true temperature falls" on a base of mean temperature, Clerk states that in calculating the mean temperature he made an allowance for the slowing down of the engine during the test. This he based on tachometer readings.

Slowing Down Test. The rate at which the speed drops just after the cam rollers are released is, however, not easy to obtain from snap readings. To find definitely the nature of the change in speed in the present test an apparatus illustrated in the photograph Fig.48 was set up. It consisted of a drum alongside which a slide rest carried a tuning fork, the vibration of which was maintained electrically. The end of one prong of the fork carried a brass style which could be made to bear on an indicator paper wrapped round the drum. By operating a cone clutch the drum was made to rotate with the crank shaft. The vibrations of the fork were recorded about a helical line round the drum. An examination of the waves in the record of vibrations yielded a clear indication of the change in speed. The curve of time per revolution is given in Fig.49, reference to which will show that in the first five revolutions the drop in speed was only 3.5%. Clerk mentions 5% in this connection. Regarding the time for the first revolution after release of the cam rollers as 1, the times for the subsequent revolutions were 1.008, 1.016, 1.025, 1.035, 1.045 respectively. These were the correction factors applied in estimating mean temperature.

Calculation of Mean Temperature. Pressures and the corresponding volumes were noted at various piston displacements on the diagram Fig.45. From these the temperatures were calculated. These temperatures were then plotted on a base of crank angles and the curves in Fig.50 were thus formed. The tabulated values are to be found in Table XV. The mean temperature in any stroke was obtained by measuring the area under/



FIG.48.

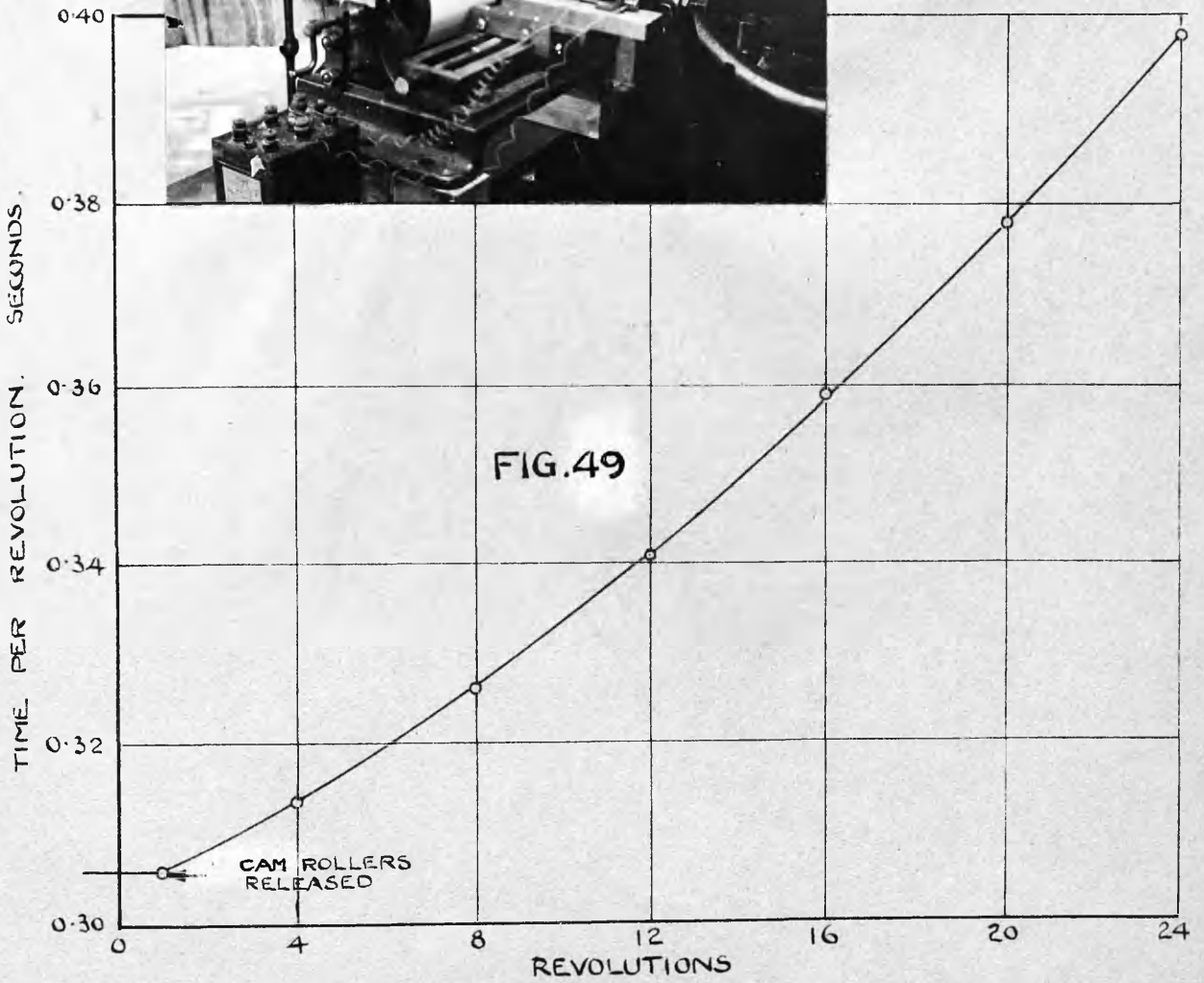


TABLE XV

FRACTION OF STROKE	0	0.05	0.1	0.3	0.5	0.7	0.9	1.0
VOLUME FT. ³	0.09114	0.1078	0.1245	0.1913	0.2581	0.3250	0.3918	0.4252
CRANK ANGLE	0°	24°	34°	61°	85°	108°	140°	180°
TEMPERATURES °C ABS.	1560	1537	1486	1343	1298	1191	1181	1227
	1231	1447	1363	1161	1056	980	931	908
		1150	1090	931	865	781	750	
	1041	998	952	830	775	716	706	633
		958	917	788	736	667	642	
	904	870	833	708	646	594	588	550
836		802	674	617	565	549		
813	775	738	627	568	516	515	492	
	748	707	610	542	480	476		

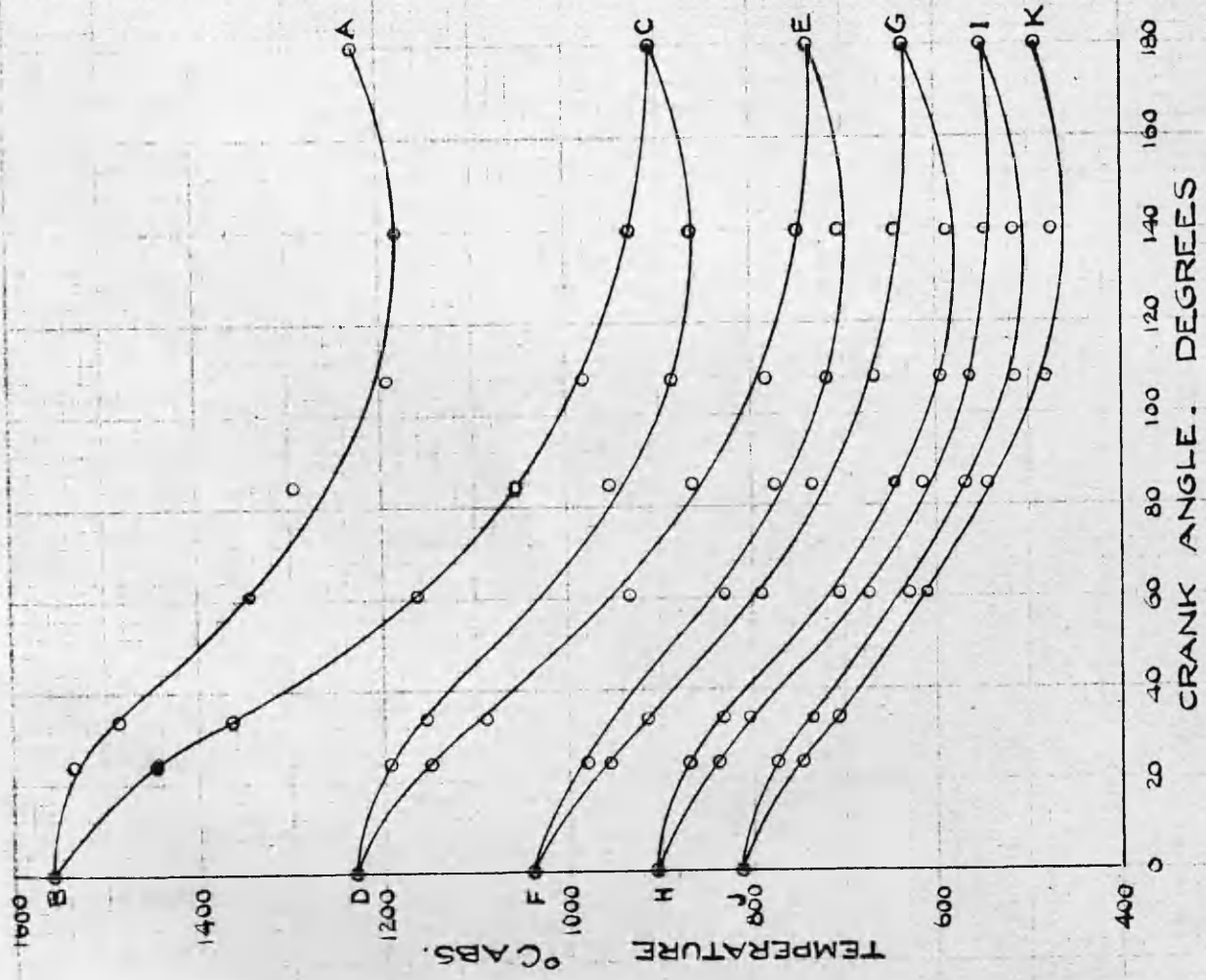


FIG. 50

CRANK ANGLE. DEGREES

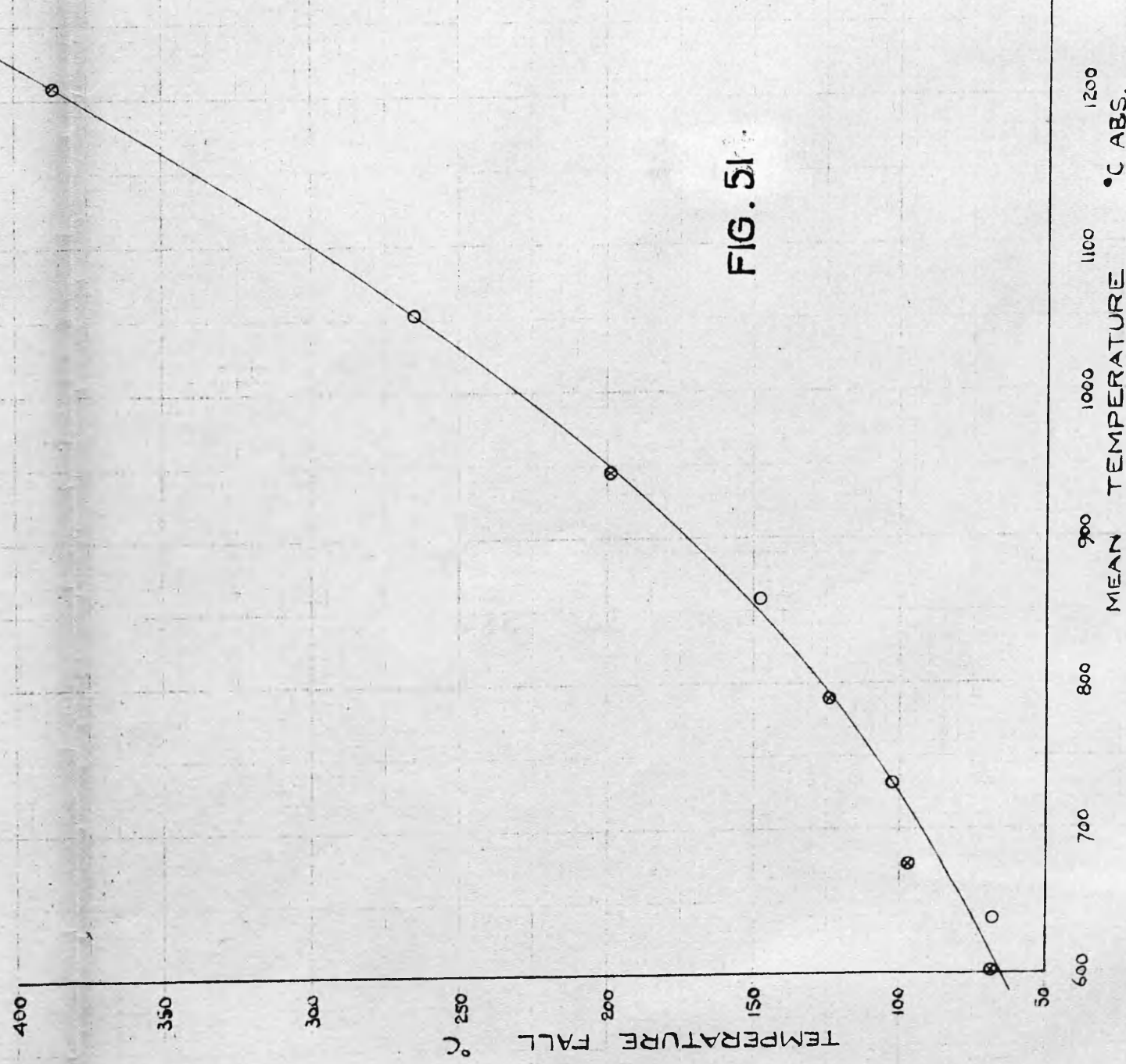


FIG. 51

MEAN TEMPERATURE °C ABS.

under the temperature curve for that stroke and dividing by the base length. A similar procedure was followed later for the partial strokes. The time correction factors were applied to the mean values so obtained.

This is a part of the work not dealt with in detail by Clerk in his paper read before the Royal Society; but it is assumed that his procedure was substantially the same as herein described. In finding the mean temperatures he neglected the obliquity of the connecting rod, but in the present test the true crank angles were used.

Clerk refers to a small error in the indicator at the low pressure end as considerably affecting the results. It was perhaps when he proceeded to find the temperatures along the curves that he found this out. Reference to Table XV or to Fig. 50 will show that during each compression stroke for a part of the half revolution the temperature is apparently lower than that at the beginning of compression. An error of 0.1 mm in the indicator diagram can account for this. The error in obtaining the mean temperature for the whole stroke, or for a double stroke, is not perhaps of very great moment; and when the calculations are confined to the high temperature end of the diagram it is not likely that the error is important.

Some reference to this will be made later.

The "true temperature falls" for the full double-strokes are plotted on a base of mean temperature in Fig. 51. The values of θ as obtained by the method of approximations will be found to agree closely with the values derived from this curve in the manner previously described. This is a valuable corroboration of the validity of Clerk's expedient of securing the "true temperature falls" from such a curve.

A similar curve is given in Fig. 52^{p. 81} for the partial double strokes. From this curve were obtained the finally-adopted values of the specific heat. These are found to be smaller/

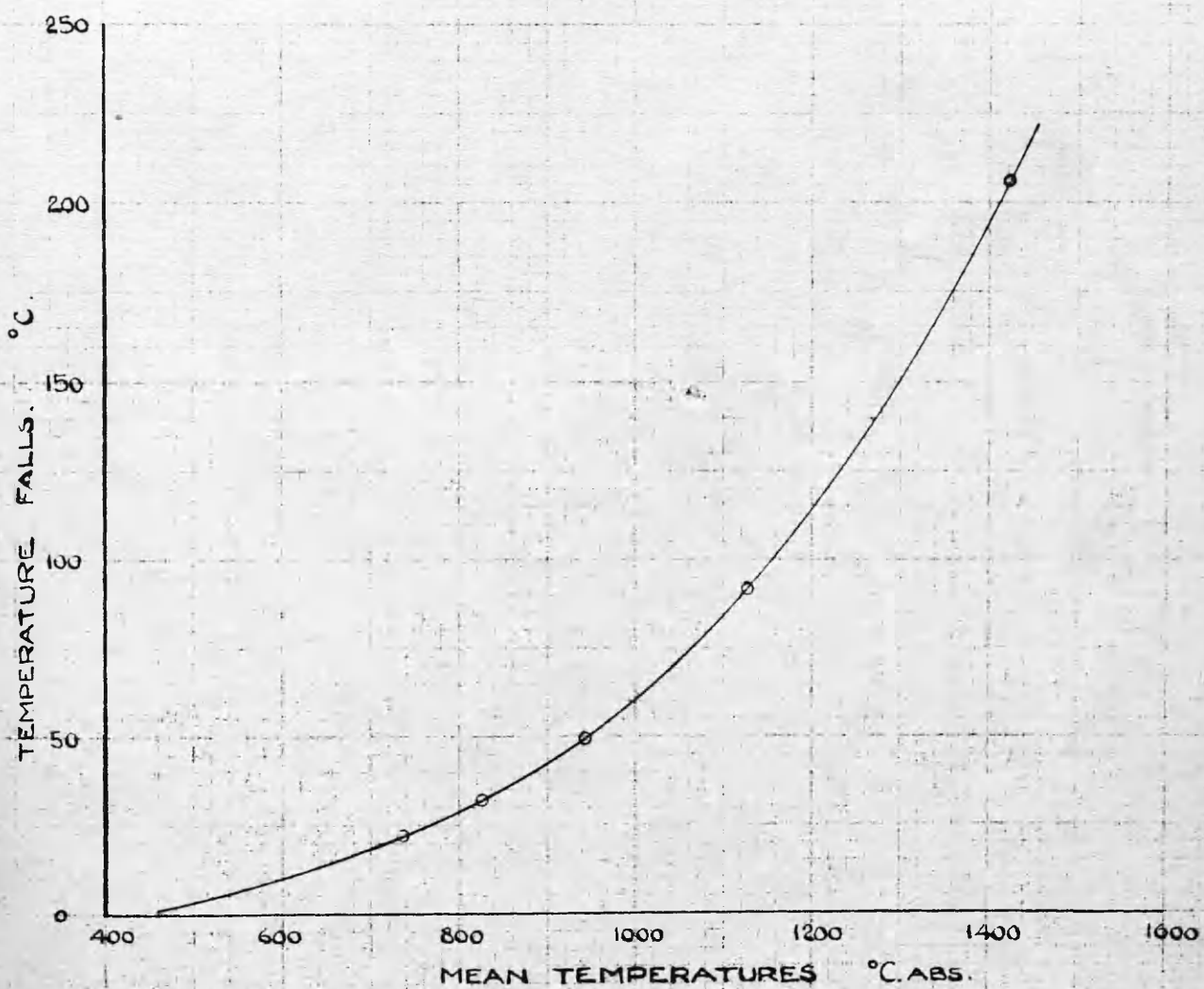


FIG. 52

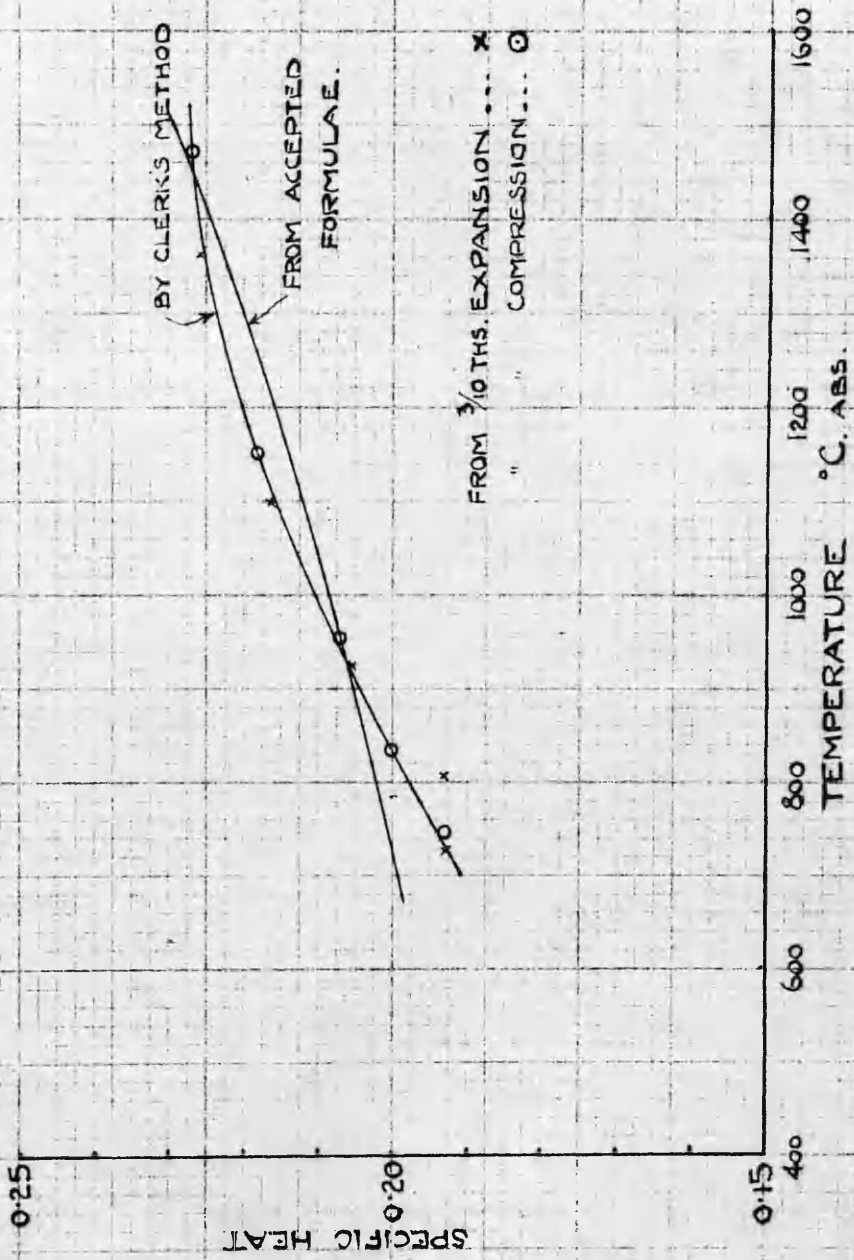


FIG. 53

smaller than the values obtained from the full strokes. This was also Clerk's experience.

When the final specific heat values found in this test were converted to thermal units per lb. and plotted on a base of temperature, they gave a curve concave downwards (Fig. 53, p. 82). This was the type of curve given by Clerk's original experiment.

It is difficult to show conclusively why this should be characteristic of the method, for although leakage is known to take place, its amount is unknown; and the effects of leakage in general are so complex that its influence on the shape of the curve is not easily predicted. The temperatures are calculated on the assumption that the mass remains constant. The true temperature values should on the whole be greater than those used. This by itself would tend to make the calculated values of the thermal capacity too great; but, because of leakage, the work values, w , w_1 , etc. are smaller than they would be without leakage. This by itself would make the calculated values of the thermal capacity too small. These two influences practically annul each other. But the thermal capacities on the lower range apply to a smaller mass (due to leakage) than the thermal capacities on the higher range. A correction for such loss in mass would reduce the downward concavity of the curve and bring it into closer correspondence with the generally accepted form which is also given in Fig. 53, p. 82.

This curve was obtained by applying the equations for the specific heat of the constituents given by Partington and Shilling. (See the corrected constants used by Professor W.J. Goudie in "Energy Charts for the Calculation of Standard Efficiencies of Internal Combustion Engines", Proc. of Eng. and Shipbuilders in Scotland, 1929).

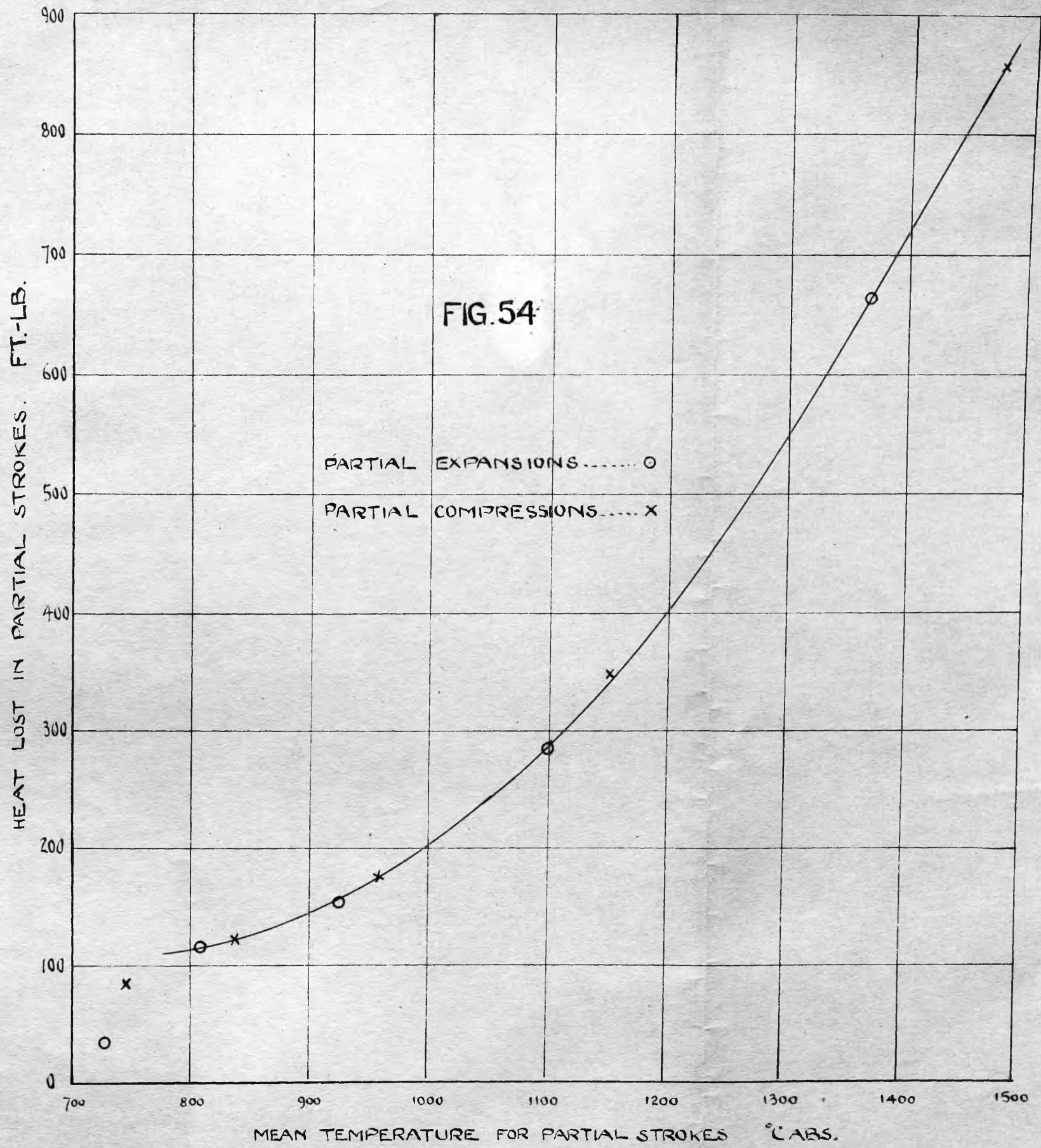
The reason for the high values of the specific heat obtained from the full strokes no doubt lies in the usual defects of a mechanical indicator. Because of friction, the observed temperature/

temperature on the diagram at the inner end of the stroke tends to be low, and at the outer end high. It is possible that the total error in the difference in temperature between the ends of a curve for the full stroke amounts to something of the order of 40° , by far the greater part of which error is attributable to the outer - or low temperature - end. The use of the high temperature end only is a very sound expedient.

Some Comments on Clerk's Conclusions. Clerk believed that combustion was still proceeding even during the first re-expansion BC (Fig. 41, p. 71). In support of this view he directed attention to the fact that the specific heat calculated from the first three-tenths of the stroke BC was smaller than that calculated from the whole stroke. A reference to the figures given in the appendix pp. 87-9) shows that this applies to every expansion line down the range, and since it cannot be seriously contended that combustion is proceeding so far, the argument seems to fall through. It is sufficiently clear that the errors inseparable from the low temperature end of the diagram can alone quite account for the discrepancy.

Hopkinson performed some experiments on the compression and expansion of air and the consequent changes in temperature. He concluded that heat was actually being gained by the gas during part of the expansion stroke. Clerk followed this up with a series of tests on air and found that "the gas does not on the whole gain heat during the first half of the expansion stroke as was found by Hopkinson. But the experiments do show that for some reason the heat loss is divided very unequally between the compression and expansion strokes."

These experiments on air were carried out at comparatively low temperature. The work at the high temperatures in the tests on the gaseous products in a gas engine cylinder is not likely to show these effects to a very marked degree. Certainly, in the test herein described the values obtained from/



from the expansion and compression lines are in so full agreement that there is no clear evidence of this uneven distribution of heat loss. To verify this, the points in Fig.54 were obtained from the separate partial compression and partial expansion strokes and were found to lie on a continuous curve except at the low temperature end where the values are necessarily unreliable.

The above-mentioned work of Clerk and Hopkinson is summarised in the Second Report of the British Association Gaseous Explosions Committee.

**
*

APPENDIX. (TO SECTION V)

Readings and Calculations in the Test of the Clerk Method.

Engine Dimensions. Cylinder diameter = 7 ins; stroke, 15 ins.

Stroke displacement volume = 0.3341 ft^3

Clearance volume . . . = 0.09114 ft^3

Observations, Etc.

Jacket temperature = 44.4°C ; Spark point = -12° ; Revs/min. = 203.2.

Air drawn in per minute = 24.06 ft^3 at 15°C and 760 mm.

Gas used per cycle = 0.0406 ft^3 at 15°C and 760 mm.

The volume of the lb-molecule of gas at 15°C and 760 mm = 378.4 ft^3 .

Mols of air per cycle = $\frac{24.06 \times 2}{203.2} \times \frac{1}{378.4} = 0.00062582$.

Mols of fuel gas per cycle = $\frac{0.0406}{378.4} = 0.0001073$.

Temperature of exhaust gases = 562°C by potentiometer.

Pressure of exhaust gases at end of stroke = 14 lbs/in^2 abs. from the displaced light-spring diagram.

(The displaced light-spring diagram shows definitely that at the end of the exhaust stroke the gases are under a partial vacuum. This is no doubt due to the effect of the exhaust calorimeter consisting of a long pipe through which the gases pass at high velocity. Towards the end of the stroke where the piston speed drops to zero the gases in the pipe are still moving with high velocity and are thus setting up a partial vacuum in the cylinder.)

The method used in obtaining the total mass of gas in the cylinder during the test is that described by Rosecrans and Felbeck in "A Thermodynamic Analysis of Gas Engine Tests" (University of Illinois Engineering Experiment Station. Bulletin No.150).

Volume of 1 mol at 562°C and 14 lb/in^2 = $\frac{562 + 273}{288} \times \frac{14.7}{14.0} \times 378.4$
 $= 1152 \text{ ft}^3$.

Mols of exhaust gas in clearance space = $\frac{0.0914}{1152} = \underline{\underline{0.0000791}}$

The composition of the charge within the cylinder is therefore

fuel gas	0.0001073
air	0.0006258
exhaust gas	0.0000791
Total	0.0008122

The temperature at any point in the cycle may be found by applying $PV = \bar{M}\bar{R}T$ where M is the number of mols and \bar{R} is the universal gas constant. The value of \bar{R} adopted here is 2797 ft.lb./°C x mol.

The curves of Fig.45 are plotted from Table XIV to a scale of 4" = 1 cm. along the pressure axis. The spring number of the original diagram is 200.

1 cm on the original diagram represents $\frac{200}{2.54}$ lb/in².

4 ins. on the new diagram represents $\frac{200}{2.54}$ lb/in².

or 1 in. = 19.68 lb/in².

The distance of the zero pressure line below the atmospheric line = $\frac{30.26 \times 0.491}{19.68} = 0.755$ in. where 30.26 ins. is the barometer reading.

On Fig.45 1 in.² = $19.68 \times \frac{0.3341}{10} \times 144 = 94.68$ ft.lb.

Areas:	$W = 49.77 \text{ in}^2 = 4712.2 \text{ ft.lb.}$	$\therefore W_1 = 4108.6 \text{ ft.lb.}$
$W - W_1 = 6.375 \text{ in}^2 = 603.6 \text{ ft.lb.}$	$W_2 = 3548.6 \text{ ft.lb.}$	
$W_1 - W_2 = 5.915 \text{ in}^2 = 560.0 \text{ ft.lb.}$	$W_3 = 3291.1 \text{ ft.lb.}$	
$W_2 - W_3 = 2.72 \text{ in}^2 = 257.5 \text{ ft.lb.}$	$W_4 = 2934.2 \text{ ft.lb.}$	
$W_3 - W_4 = 3.77 \text{ in}^2 = 356.9 \text{ ft.lb.}$	$W_5 = 2788.9 \text{ ft.lb.}$	
$W_4 - W_5 = 1.535 \text{ in}^2 = 145.3 \text{ ft.lb.}$	$W_6 = 2498.2 \text{ ft.lb.}$	
$W_5 - W_6 = 3.07 \text{ in}^2 = 290.7 \text{ ft.lb.}$	$W_7 = 2390.3 \text{ ft.lb.}$	
$W_6 - W_7 = 1.14 \text{ in}^2 = 107.9 \text{ ft.lb.}$	$W_8 = 2214.2 \text{ ft.lb.}$	
$W_7 - W_8 = 1.86 \text{ in}^2 = 176.1 \text{ ft.lb.}$	$W_9 = 2136.1 \text{ ft.lb.}$	
$W_8 - W_9 = 0.825 \text{ in}^2 = 78.1 \text{ ft.lb.}$		

The temperatures along the curves given in Table XV are obtained by a successive application of $T = \frac{PV}{MR}$.

Examination of Full Expansion Lines.

From Fig.46 the first approximations are,

$$\theta_1 = 185; \theta_2 = 102; \theta_3 = 71; \theta_4 = 51.$$

$$S = \frac{W_1}{t_1 - t_{o1} - 185} = \frac{4108.6}{467} = 8.80 \text{ ft.lb.}$$

$$S_1 = \frac{W_3}{t_{11} - t_{o2} - 102} = \frac{3291.1}{390} = 8.44 \text{ ft.lb.}$$

$S_2/$

$$S_2 = \frac{W_5}{t_{12} - t_{03} - 87} = \frac{2788.9}{337} = 8.29 \text{ ft.lb.}$$

$$S_3 = \frac{W_7}{t_{13} - t_{04} - 51} = \frac{2390.3}{303} = 7.56 \text{ ft.lb.}$$

$$\frac{W_1 - W_2}{S} = \frac{560}{8.80} = 63.7; \quad \frac{W_3 - W_4}{S_1} = \frac{356.9}{8.44} = 42.3.$$

$$\frac{W_5 - W_6}{S_2} = \frac{290.7}{8.92} = 35.1; \quad \frac{W_7 - W_8}{S_3} = \frac{176.1}{7.56} = 23.3.$$

Temperature falls on double strokes become:

$$g = 1560 - 1231 - 64 = 265.$$

$$g_1 = 1231 - 1041 - 42 = 148.$$

$$g_2 = 1041 - 904 - 35 = 102.$$

$$g_3 = 904 - 813 - 23 = 68.$$

These are used to form the modified curve in Fig.46, p.77

New temperature falls on expansion lines from modified curve are 152, 83, 55, 36.

For second approximation

$$S = \frac{W_1}{t_1 - t_{01} - 152} = \frac{4108.6}{500} = 8.22 \text{ ft.lb.} = 28.2 \text{ ft.lb./ft.}^3$$

$$S_1 = \frac{W_3}{t_{11} - t_{02} - 83} = \frac{3291.1}{409} = 8.04 \text{ ft.lb.} = 27.6 \text{ ft.lb./ft.}^3$$

$$S_2 = \frac{W_5}{t_{12} - t_{03} - 55} = \frac{2788.9}{353} = 7.91 \text{ ft.lb.} = 27.1 \text{ ft.lb./ft.}^3$$

$$S_3 = \frac{W_7}{t_{13} - t_{04} - 36} = \frac{2390.3}{318} = 7.53 \text{ ft.lb.} = 25.8 \text{ ft.lb./ft.}^3$$

Where the ft.^3 is at S.T.P. and the volume of the lb.mol is taken as 359 ft.^3 at 0°C and 760 mm .

Examination of Full Compression Lines.

From Fig.47 the first approximations are

$$\theta'_1 = 195; \quad \theta'_2 = 96; \quad \theta'_3 = 59; \quad \theta'_4 = 44.$$

$$S' = \frac{W}{t_1 - t_0 + 195} = \frac{4712.2}{528} = 8.93 \text{ ft.lb.}$$

$$S'_1 = \frac{W_2}{t_{11} - t_{01} + 96} = \frac{3548.6}{419} = 8.48 \text{ ft.lb.}$$

$$S'_2 = \frac{W_4}{t_{12} - t_{02} + 59} = \frac{2934.2}{361} = 8.13 \text{ ft.lb.}$$

$$S'_3 = \frac{W_6}{t_{13} - t_{03} + 44} = \frac{2498.2}{315} = 7.93 \text{ ft.lb.}$$

$$\frac{W - W_1}{S'} = \frac{603.6}{8.93} = 67.6; \quad \frac{W_2 - W_3}{S'_1} = \frac{257.5}{8.48} = 30.4.$$

$$\frac{W_4 - W_5}{S'_2} = \frac{145.3}{8.13} = 17.9; \quad \frac{W_6 - W_7}{S'_3} = \frac{107.9}{7.93} = 13.6.$$

$$\frac{W_8 - W_9}{S'_4}$$

$$\frac{W_8 - W_9}{S_4} = \frac{78 \cdot 1}{7 \cdot 80} = 10 \cdot 0.$$

Temperature falls on double strokes become

$$\begin{aligned} g_1' &= 1227 - 908 + 67 \cdot 6 = 387. \\ g_2' &= 908 - 739 + 30 \cdot 4 = 199. \\ g_3' &= 739 - 633 + 17 \cdot 9 = 124. \\ g_4' &= 633 - 550 + 13 \cdot 6 = 97. \\ g_5' &= 550 - 492 + 10 = 68. \end{aligned}$$

These are used to form the modified curve in Fig. 47, p. 77

The new temperature falls on compression lines from the modified curve are respectively 240, 110, 66, 49, 34.

For second approximation

$$S_1' = \frac{W}{t_1 - t_0 + 240} = \frac{4712 \cdot 2}{573} = 8 \cdot 22 \text{ ft.lb.} = 28 \cdot 25 \text{ ft.lb./ft.}^3$$

$$S_2' = \frac{W_2}{t_{11} - t_{01} + 110} = \frac{3548 \cdot 6}{433} = 8 \cdot 19 \text{ ft.lb.} = 28 \cdot 1 \text{ ft.lb./ft.}^3$$

$$S_3' = \frac{W_4}{t_{12} - t_{02} + 66} = \frac{2934 \cdot 2}{368} = 7 \cdot 98 \text{ ft.lb.} = 27 \cdot 4 \text{ ft.lb./ft.}^3$$

$$S_4' = \frac{W_6}{t_{13} - t_{03} + 49} = \frac{2498 \cdot 2}{320} = 7 \cdot 80 \text{ ft.lb.} = 26 \cdot 8 \text{ ft.lb./ft.}^3$$

$$S_5' = \frac{W_8}{t_{14} - t_{04} + 34} = \frac{2214 \cdot 2}{297} = 7 \cdot 46 \text{ ft.lb.} = 25 \cdot 6 \text{ ft.lb./ft.}^3$$

where the ft.³ is measured at S.T.P.

Mean Temperatures:

These are obtained from Fig. 50, (opposite p. 80)

(a) Mean temperatures on full strokes.

Curve	Area under curve in. ²	Mean height ins.	Mean Temp °C.abs.	Mean Temp. corrected for speed °C.abs.	Averages for double strokes	
					°C.abs	°C.abs.
AB	20.30	4.51	1302	1302	1209	1052
BC	16.04	3.565	1113	1117		
CD	13.14	2.920	984	987	945	858
DE	11.17	2.480	896	904		
EF	9.12	2.028	806	813	790	731
FG	8.05	1.789	758	767		
GH	6.46	1.435	687	695	677	638
HI	5.61	1.247	649	660		
IJ	4.64	1.030	606	616	601	
JK	3.90	0.866	573	586		

Allowance is made for the fact that the ordinates are measured from 400°C abs.

(b) Mean/

(b) Mean temperatures on partial strokes.

Curve	Area under curve in ²	Mean height ins	Mean Temp °C.abs	Mean Temp. corrected for speed °C.abs	Average for double segments °C.abs.
1c	8.19	5.370	1474	1474	1421
1e	7.38	4.839	1368	1368	
2c	5.685	3.728	1146	1151	1125
2e	5.30	3.475	1095	1100	
3c	4.20	2.754	951	959	942
3e	3.955	2.593	919	926	
4c	3.26	2.138	828	838	823
4e	3.05	2.000	800	809	
5c	2.555	1.675	735	748	738
5e	2.42	1.587	717	729	

Work areas:

$$\begin{array}{llll}
 \omega - \omega_1 = 2.035 \text{ in}^2 = 192.7 \text{ ft.lb.} & \omega = 2430.9 \text{ ftlb.} & \omega_5 = 1513 \text{ ftlb.} & \\
 \omega_2 - \omega_3 = 1.03 \text{ in}^2 = 97.5 \text{ ft.lb.} & \omega_1 = 2238 \text{ ftlb.} & \omega_6 = 1366.7 \text{ ftlb.} & \\
 \omega_4 - \omega_5 = 0.615 \text{ in}^2 = 58.2 \text{ ft.lb.} & \omega_2 = 1887.9 \text{ ftlb.} & \omega_7 = 1325 \text{ ftlb.} & \\
 \omega_6 - \omega_7 = 0.50 \text{ in}^2 = 47.34 \text{ ft.lb.} & \omega_3 = 1790 \text{ ft.lb.} & \omega_8 = 1217.1 \text{ ft.lb.} & \\
 \omega_8 - \omega_9 = 0.30 \text{ in}^2 = 28.4 \text{ ft.lb.} & \omega_4 = 1576.4 \text{ ft.lb.} & \omega_9 = 1189 \text{ ft.lb.} &
 \end{array}$$

When faired up by drawing a curve these values (become (i.e. $\omega - \omega_1$, etc.))_Λ respectively 193, 98, 63, 42, and 28.

Observed temperature falls:

$$\begin{array}{ll}
 1c \text{ and } 1e, & 1343 - 1161 = 182. \\
 2c \text{ and } 2e, & 1010 - 931 = 79. \\
 3c \text{ and } 3e, & 830 - 788 = 42. \\
 4c \text{ and } 4e, & 708 - 673 = 34. \\
 5c \text{ and } 5e, & 627 - 612 = 15.
 \end{array}$$

When faired up by drawing a curve these values become respectively 182, 79, 42, 26, 18.

True temperature falls on the double partial strokes are

$$\begin{array}{ll}
 g_n = 182 + \frac{193}{8.23} = 205.4 \\
 g_{n_1} = 79 + \frac{98}{8.19} = 91.0 \\
 g_{n_2} = 42 + \frac{63}{7.98} = 49.9 \\
 g_{n_3} = 26 + \frac{42}{7.8} = 31.4 \\
 g_{n_4} = 18 + \frac{28}{7.46} = 21.8
 \end{array}$$

These are plotted against mean temperature to form Fig. 52, p. 81

From Fig. 52 the values of temperature-falls on the single parts are found. These are as follows:

$$\begin{array}{ll}
 1e, & 89.5 \\
 2e, & 42 \\
 3e, & 23.5 \\
 4e, & 15 \\
 5e, & 10.5 \\
 1c, & 117 \\
 2c, & 49.5 \\
 3c, & 26 \\
 4c, & 17 \\
 5c, & 11.5
 \end{array}$$

Final Values of Specific Heat.

$$S_{1e} = \frac{w_1}{1560-1161-89.5} = \frac{2238}{309.5} = 7.23 \text{ ft.lb.} = 24.8 \text{ ft.lb./ft}^3 = 0.2256 \text{ CHU/lb. x } ^\circ\text{C.}$$

$$S_{2e} = \frac{w_2}{1231-931-42} = \frac{1790}{258} = 6.94 \text{ ft.lb.} = 23.8 \text{ ft.lb./ft}^3 = 0.2166 \text{ CHU/lb. x } ^\circ\text{C.}$$

$$S_{3e} = \frac{w_5}{1041-788-23.5} = \frac{1513}{230.5} = 6.58 \text{ ft.lb.} = 22.5 \text{ ft.lb./ft}^3 = 0.2053 \text{ CHU/lb. x } ^\circ\text{C.}$$

$$S_{4e} = \frac{w_7}{904-674-15} = \frac{1325}{215} = 6.17 \text{ ft.lb.} = 21.2 \text{ ft.lb./ft}^3 = 0.1926 \text{ CHU/lb. x } ^\circ\text{C.}$$

$$S_{5e} = \frac{w_9}{813-610-10.5} = \frac{1189}{192.5} = 6.17 \text{ ft.lb.} = 21.2 \text{ ft.lb./ft}^3 = 0.1926 \text{ CHU/lb. x } ^\circ\text{C.}$$

$$S_{1c} = \frac{w}{1560-1343+117} = \frac{2430.9}{334} = 7.28 \text{ ft.lb.} = 25.0 \text{ ft.lb./ft}^3 = 0.2272 \text{ CHU/lb. x } ^\circ\text{C.}$$

$$S_{2c} = \frac{w_2}{1231-1010+49.5} = \frac{1887.9}{270.5} = 6.98 \text{ ft.lb.} = 23.9 \text{ ft.lb./ft}^3 = 0.2178 \text{ CHU/lb. x } ^\circ\text{C.}$$

$$S_{3c} = \frac{w_4}{1041-830+26} = \frac{1576.4}{237} = 6.65 \text{ ft.lb.} = 22.8 \text{ ft.lb./ft}^3 = 0.2075 \text{ CHU/lb. x } ^\circ\text{C.}$$

$$S_{4c} = \frac{w_6}{904-708+17} = \frac{1366.7}{213} = 6.42 \text{ ft.lb.} = 22.0 \text{ ft.lb./ft}^3 = 0.2004 \text{ CHU/lb. x } ^\circ\text{C.}$$

$$S_{5c} = \frac{w_8}{813-627+11.5} = \frac{1217.1}{197.5} = 6.17 \text{ ft.lb.} = 21.2 \text{ ft.lb./ft}^3 = 0.1926 \text{ CHU/lb. x } ^\circ\text{C.}$$

Volumetric Composition of the Fuel Gas is

CO₂, 3.9%; C₂H₆, 2.2%; O₂, 0.5%; CO, 18.2%; CH₄, 20.2%;

H₂, 49.1%; N₂, 5.9%

Volumetric Composition of Products.

0.022 C₂H₆ gives rise to 0.044 CO₂ and 0.066 H₂O, using 0.077 O₂
 0.182 CO " " " 0.182 CO₂ " 0.091 O₂
 0.202 CH₄ " " " 0.202 CO₂ and 0.404 H₂O, " 0.404 O₂
 0.491 H₂ " " " 0.491 H₂O " 0.2455 O₂

∴ 1 ft.³ of gas uses from the air 0.817 ft.³ O₂ and forms

0.428 ft.³ CO₂ and 0.961 ft.³ H₂O.

The actual air/gas ratio = 5.833.

When 1 ft.³ of gas is burned with 5.833 ft.³ dry air the composition of the products is: 0.467 CO₂ + 0.961 H₂O + 4.967 N₂ + 0.413 O₂.

i.e. by volume: 6.859% CO₂, 14.116% H₂O, 72.959% N₂, 6.066% O₂.

Assuming that this is also the composition of the exhaust gases in the clearance space, the equivalent molecular weight of the gaseous charge is:

$$0.06859 \times 44 + 0.14116 \times 18 + 0.72959 \times 28 + 0.06066 \times 32 = 28.183.$$

This/

This is made up of $3.018\text{CO}_2 + 2.541\text{H}_2\text{O} + 22.624 \text{O}_2$ and N_2 .

These figures are used for finding the curve of specific heat from the equations of Partington and Shilling (corrected by Professor Goudie). The equations are:

$$\begin{aligned} \text{for } \text{CO}_2 \quad C_v &= 5.396 + 5.057 \times 10^{-3} T - 1.02 \times 10^{-6} T^2. \\ \text{for } \text{O}_2, \text{N}_2 \text{ etc } C_v &= 4.9467 + 0.31 T^2 \times 10^{-6}. \\ \text{for } \text{H}_2\text{O} \quad C_v &= 7.249 - 2.468 \times 10^{-3} T + 2.34 \times 10^{-6} T^2. \end{aligned}$$

They apply to the lb-molecule.

By dividing the values of the specific heat of the mixture by 28.183 the specific heats in C.H.U/lb x °C are obtained. These are plotted together with the experimental values in Fig. 53, p. 82

-----oOo-----

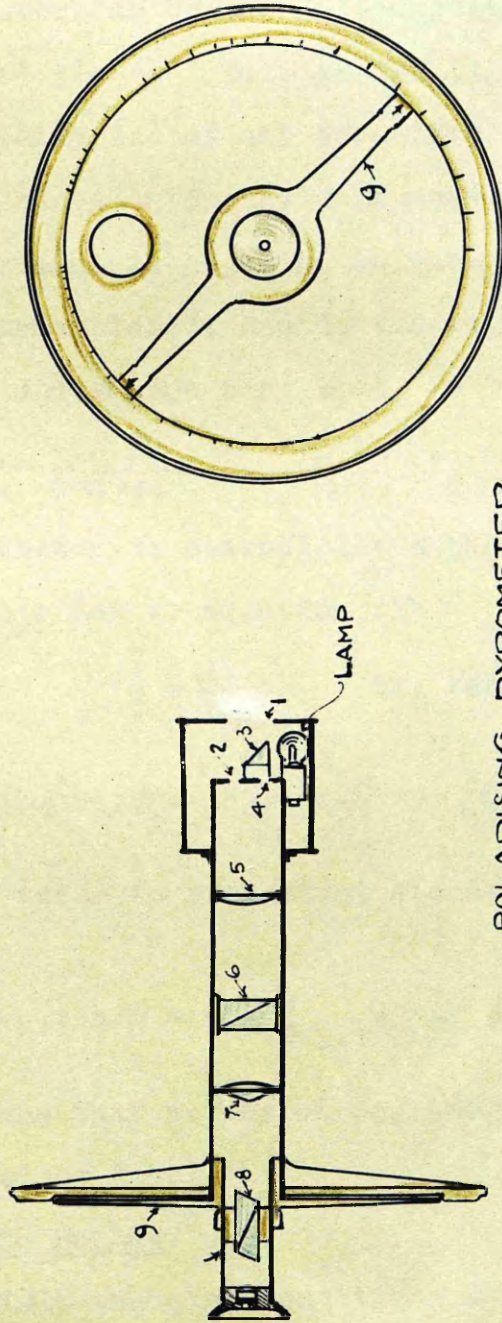
SECTION VI.

The marked luminosity of the charge during the combustion period led to an examination of the possibilities of making use of it in determining the temperature of the gases. All optical pyrometers are based on the theory of "black body" radiators and the question that arose was how nearly the luminous charge in the engine approximated at any instant to "black body" conditions. This could only be answered by trial.

A polarising pyrometer was obtained which was calibrated directly to read the temperatures of a "black body" or total radiator. A National Physical Laboratory certificate accompanied the instrument stating that it was correct "within the limits of setting in technical practice."

Polarising Pyrometer.

The polarising pyrometer is illustrated by the diagram Fig. 55, p. 94. The radiation from the hot object passes through the window 1 and then through the circular hole 2. The electric lamp illuminates the matt surface of a right-angled prism 3 and the light is directed to the circular hole 4 which is placed symmetrically with 2 about the optical axis of the system. The lens 5 renders the two beams of light parallel. They are each split into two components polarised at right angles by the Rochon prism 6. An image from each of the two sources is brought into juxtaposition by the effect of the biprism combined with the lens 7. All the other images formed by the system are screened out. The visible images appear as two semi-circular areas. The Nicol prism 8 is capable of rotation, the amount being readable at the index arms 9. If the beams from the lamp and the outside source are of equal intensity, the two halves of the visible field are equally illuminated when the/



POLARISING PYROMETER

FIG. 55

the plane of polarisation of the Nicol is at 45° to the direction of polarisation of either beam. The appearance through the eyepiece is then that of a uniformly illuminated circle with a diametral line across it.

The observations in practice are confined to a narrow band of the spectrum by the introduction into the system of a suitable red glass. This passes light which may be regarded as being all of one effective wave length λ .

If a standard intensity I is used at the electric lamp and the instrument is adjusted in turn to match this against two other intensities I_1 and I_2 the angles of rotation of the Nicol, ϕ_1 and ϕ_2 are such that

$$\frac{I_1}{I_2} = \frac{\tan^2 \phi_1}{\tan^2 \phi_2} \quad - - - - - (1)$$

The pyrometer is essentially a photometer.

Applying Wien's Law to equation (1)

$$\frac{I_1}{I_2} = e^{\frac{c_2}{\lambda} \left(\frac{1}{T_2} - \frac{1}{T_1} \right)} \quad \text{or, taking logarithms,}$$

$$2(\log \tan \phi_1 - \log \tan \phi_2) = \frac{c_2}{\lambda} \left(\frac{1}{T_2} - \frac{1}{T_1} \right)$$

If ϕ_2 and T_2 refer to a constant standard, then the equation becomes

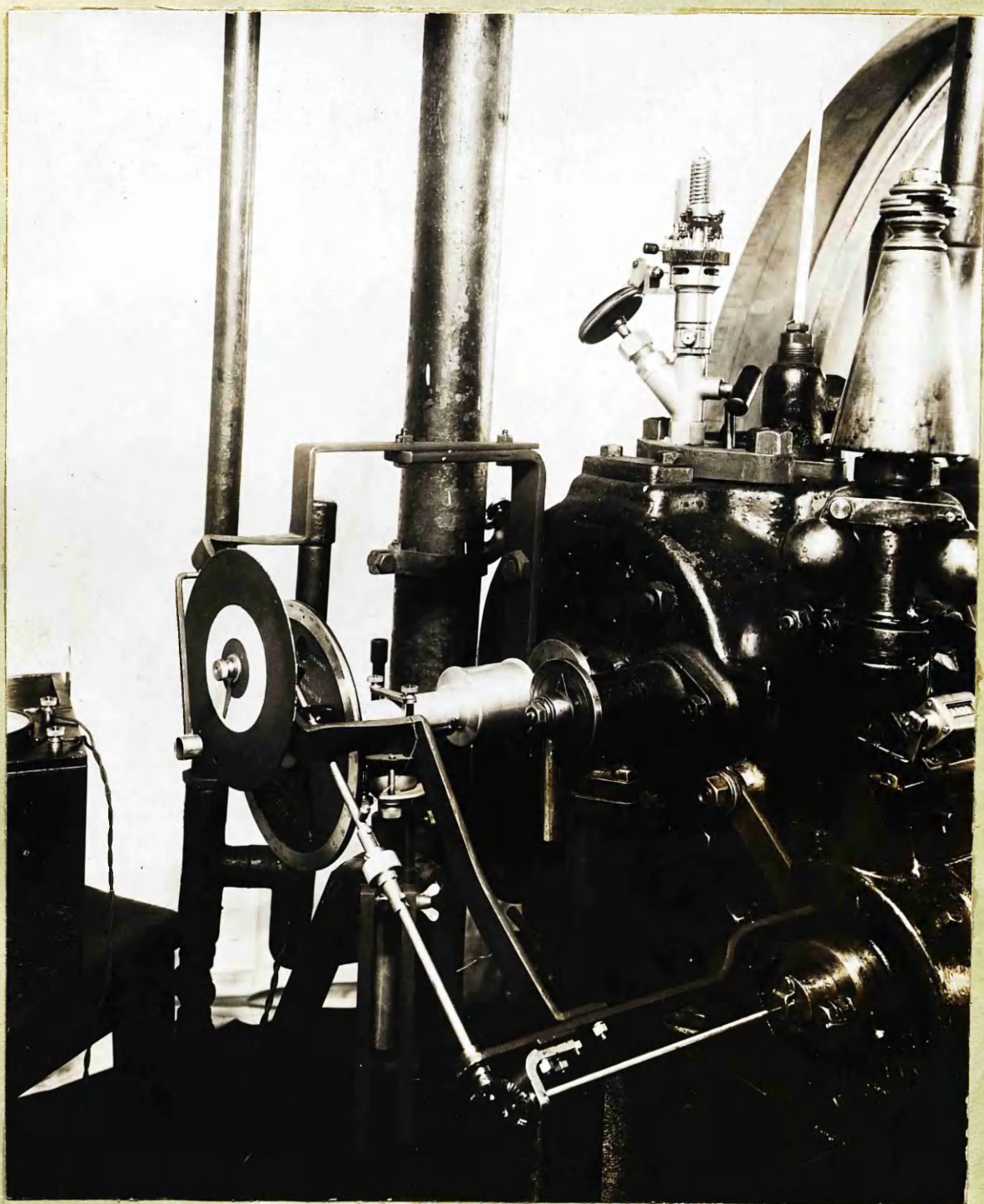
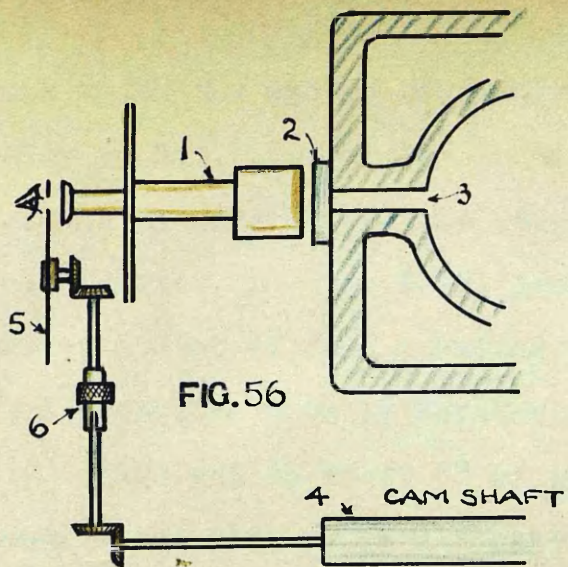
$$\log \tan \phi = a - \frac{b}{T} \quad - - - - - (2)$$

This means that values of $\log \tan \phi$ plotted against $\frac{1}{T}$ give a straight line.

Application to Engine.

The rapidly changing conditions during combustion rendered it necessary to make use of the repetitive nature of the cycle in order to examine the luminosity at any given point. But any apparatus devised for regularly intermittent observation had to treat both the standard beam from the lamp and the beam from the engine absolutely alike. Otherwise the two halves of the visible field could not be properly matched.

The/



The arrangement which the writer devised is illustrated diagrammatically in Fig.56, p.96. The pyrometer 1 is placed on the axis of the cylinder. On the cam-shaft 4 a spindle is carried which drives, through level gears, a disc 5. This disc carries a slot at such a radius as to uncover the eyepiece of the pyrometer when it rotates. The length of the slot is equivalent to about 5° of cam-shaft angle. A clutch 6 enables the disc to be disengaged while its phase angle is altered. The details of the arrangement are clearly seen in the photograph Fig.57, p.96. This apparatus yielded very consistent results, the matching being much more easily accomplished than might have been expected.

Tests.

The electric lamp of the pyrometer was standardised against an amyl acetate lamp according to the maker's instructions and according to the terms of the N.P.L. certificate. The current was noted on the ammeter which accompanies the instrument, and this was the current maintained throughout the tests.

With the engine running normally, observations of the gas-consumption etc. were made in the ordinary way. The phase angle of the disc was adjusted until the pyrometer gave its maximum temperature reading. This was found to be about 1200°C . while the indicator diagram recorded a maximum temperature of about 1900°C . It was at once evident that the instrument was not receiving a "black body" radiation.

It was not known, however, to what extent absorption by the window was affecting the readings. To test this, readings were made on a standard flame (paraffin lamp) with and without the cylinder-window intervening between the pyrometer and the flame. The difference, even when the/

the window was slightly stained with rust and moisture, . was found to be only of the order of 20°C. This was checked by measuring the absorption of the window on a Lummer-Brodhun photometer.

If T_1 and T_2 are the temperatures read off when there is no window and when there is a window between the pyrometer and a full radiator, it may be shown, by using equations (1) and (2) page 95, that

$\log_e K = C \left(\frac{1}{T_1} - \frac{1}{T_2} \right)$ where K is the absorption coefficient and C is a constant.

When the value of K obtained on the Lummer-Brodhun photometer was applied, it was again found that the effect of the absorption on the readings was of little account.

The low reading of temperature is almost entirely, it would appear, due to the fact that the gaseous charge during combustion is far from radiating like a "black body".

Since this luminous charge is not a full radiator and therefore does not conform to Wien's Law, an alternative is to assume that it conforms to some equation of the same form as Wien's. This is done in certain cases. ⁽¹⁾

It might be asked why not take a gas flame, note its temperature with some form of direct-reading instrument, and also the reading on the pyrometer, then by means of air-blast obtain higher temperatures and corresponding readings? Such a method seems the simplest for solving the problem. But it does not fit this case. The ordinary Bunsen flame is so faintly luminous as not to be seen at all through the polarising pyrometer, and this is still true when, with the air-blast on, the flame is hot enough to melt with ease an iron wire. It seems that the charge in the engine is/

(1) Mendenhall & Ingersoll. Phys.Rev. 25, p.1. 1907.

is altogether different in its characteristics from the ordinary bunsen flame. Is its luminosity due to its high ^{density} pressure or to the formation of carbon particles during combustion? Whatever may be the cause, it would seem that we cannot reproduce artificially for calibration purposes the conditions of combustion inside the cylinder.

If a law similar to Wien's is assumed then an equation such as (2) p.95 applies to the instrument. The values of ϕ and T at two points are all that are required. To obtain such values it is not unreasonable to suggest that two points may be chosen fairly late in the luminous period of combustion in the engine, where thermal equilibrium may be regarded as complete. The temperatures at these points will closely agree with the "mean temperatures" obtained from the indicator diagram. These mean temperatures with the corresponding values of ϕ will fix the desired equation, and by using it, probable values of temperature may be obtained for the early part of the combustion process. This treatment applied to some tests revealed weakness. It would appear that changes in the working conditions have a considerable influence on the quality of the radiation, and this renders a single equation obtained on the basis above described only valid (if at all) for a single set of conditions of spark advance and air/gas ratio.

Two series of tests were run, one series (J) at different angles of advance of the spark and the second series (K) at different air/gas ratios.

TableXVI gives the essential figures relating to the conditions of the tests and TableXVII gives the composition of the gas.

Table XVI

Test	Air/min at 760mm & 15°C. ft ³	Gas/cycle at 760mm. & 15°C. ft ³	Ratio $\frac{\text{Air}}{\text{Gas}}$ $\frac{2A}{Rg}$	Exhaust temp. °C	Angle of Advance of Spark Degrees.
J1	22.41	0.0421	5.26	526	-30 $\frac{1}{2}$
J2	23.54	0.0400	5.656	548	-22 $\frac{1}{2}$
J3	23.50	0.0401	5.648	549	-15 $\frac{1}{2}$
J4	23.60	0.0403	5.650	559	- 5 $\frac{1}{2}$
J5	23.41	0.0401	5.580	584	+ 4
K1	23.50	0.0401	5.648	549	-15 $\frac{1}{2}$
K2	23.97	0.0376	6.136	536	-15 $\frac{1}{2}$
K3	24.48	0.0359	6.496	520	-15 $\frac{1}{2}$
K4	24.52	0.0345	6.800	508	-15 $\frac{1}{2}$
K5	24.80	0.0328	7.236	494	-15 $\frac{1}{2}$

Jacket temperature in all cases within 2° of 110°F.

Table XVII

CO ₂	O ₂	CO	CH ₄	H ₂	N ₂	Heavy Hydro-carbons
3.6	0.3	19.1	18.4	50.8	5.6	2.2

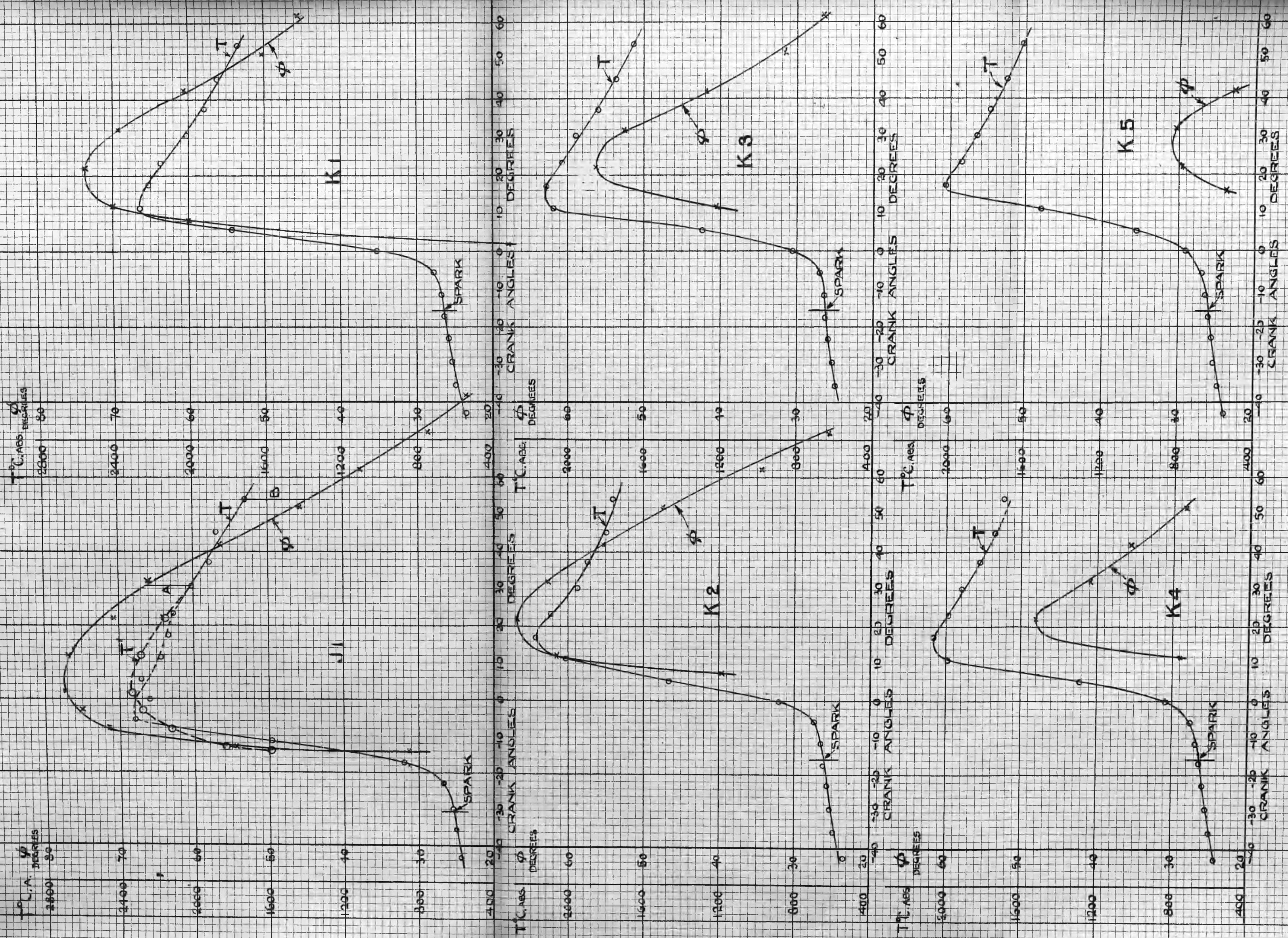
During each test observations were made by means of the pyrometer on the red radiation at different points in the cycle. The values of ϕ thus obtained give a measure of the intensity relative to that of the red radiation from the standard amyl acetate flame. The figures for this part of the work are given in Table XVIII p. 100.

Curves of "mean temperature" were obtained from the indicator diagrams for J1 and for Series K, in a manner already described in connection with Series D on p.63. These curves are to be seen in Fig. 58 (opposite p. 102). On the same base of crank angle, the values of ϕ are plotted in each case.

In the case of Test J1 points are chosen on the ordinates A and B to apply the temperature equation as described on p. 99. Extrapolating back into the region of chemical and thermal instability the curve T' is obtained.

Variations in the red radiation in relation to the pressure etc.

The point that is noticed at once is that in all these tests the maximum value of ϕ is later than the maximum "mean/



T—CURVES OF MEAN TEMPERATURE
 T'—CURVE OF TEMPERATURE ESTIMATED FROM VALUES OF ϕ
 ϕ —CURVES OF ANGLE OF ROTATION OF THE PRISM HEAD ON THE POLARISING PYROMETER
 INNER DEAD CENTRE AT 0°

FIG. 58

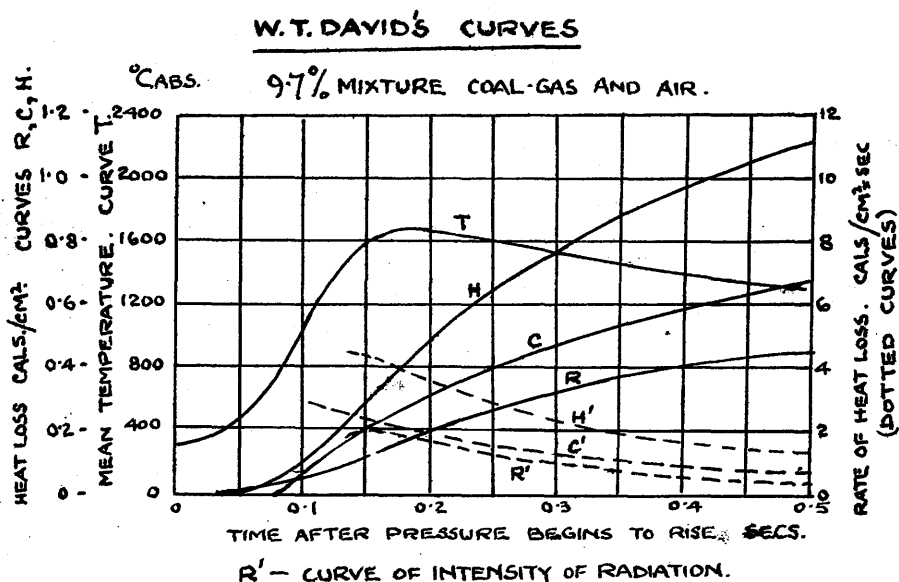
"mean temperature", which falls practically on the point of maximum pressure. The recording gear has been re-examined for back-lash correction etc. but any inaccuracy that could be found was insufficient to affect this feature of the curves.

It might with reason be assumed that the maximum intensity on any one wave-length coincides with the maximum intensity of total radiation of all wave lengths.

If this is true (and it is so for a "black body") the tests are at variance with the work of Professor W.T.David. (1)

David's curves, an example of which is given in Fig. 59 show the maximum intensity as taking place previous to maximum "mean temperature".

FIG. 59



It seems to the writer that the maximum intensity of radiation is more likely to take place after the point of maximum pressure than before. The photographic records of Sections III and IV do not give any evidence of a condition of/

(1) Proc.Inst.Mech.Eng. Vol.II. 1924. p.763.

of intense radiation taking place previous to the point of maximum pressure. Nor is such a condition supported by the results of Hopkinson's measurement of temperatures during an explosion in a closed vessel. The highest temperature reached at any time during the explosion is at the core of the charge after the point of maximum pressure has just been passed. The gas is largely transparent to its own radiation and thus it is likely that this maximum temperature coincides with the point of maximum intensity of radiation.

In the curves for J1 in Fig. 58 p. 102 it will be noticed that the maximum value of T' is not much more than the maximum "mean temperature". In Hopkinson's experiments it would appear that the temperature of the centre of the charge is some 400° higher than the "mean temperature" at the point of maximum pressure. It may be that the turbulent condition of the gases when ignition takes place renders the combustion process in the engine even less comparable with the conditions in Hopkinson's closed vessel than has hitherto been supposed. This also applies to David's work on the same apparatus.

The assumption, which has been made in order to obtain the curve T' , however, is to be accepted with reserve. When the equation obtained in J1 is applied to, say, K5 the resulting temperature is unreasonable. The maximum temperature estimated from the ϕ values is $1890^{\circ}\text{C. abs.}$, as compared with a maximum "mean temperature" of $2030^{\circ}\text{C. abs.}$ By testing the results in this way, it is found that the relationship between ϕ and temperature is different in the different tests (J1 and Series K). The quality of the radiation, therefore, seems to change very considerably from/

(1) Proc. Roy. Socy. Vol. 77A. 1906.

(2) Callendar. B.A. Explosions Comm. Third Report. Append. A.

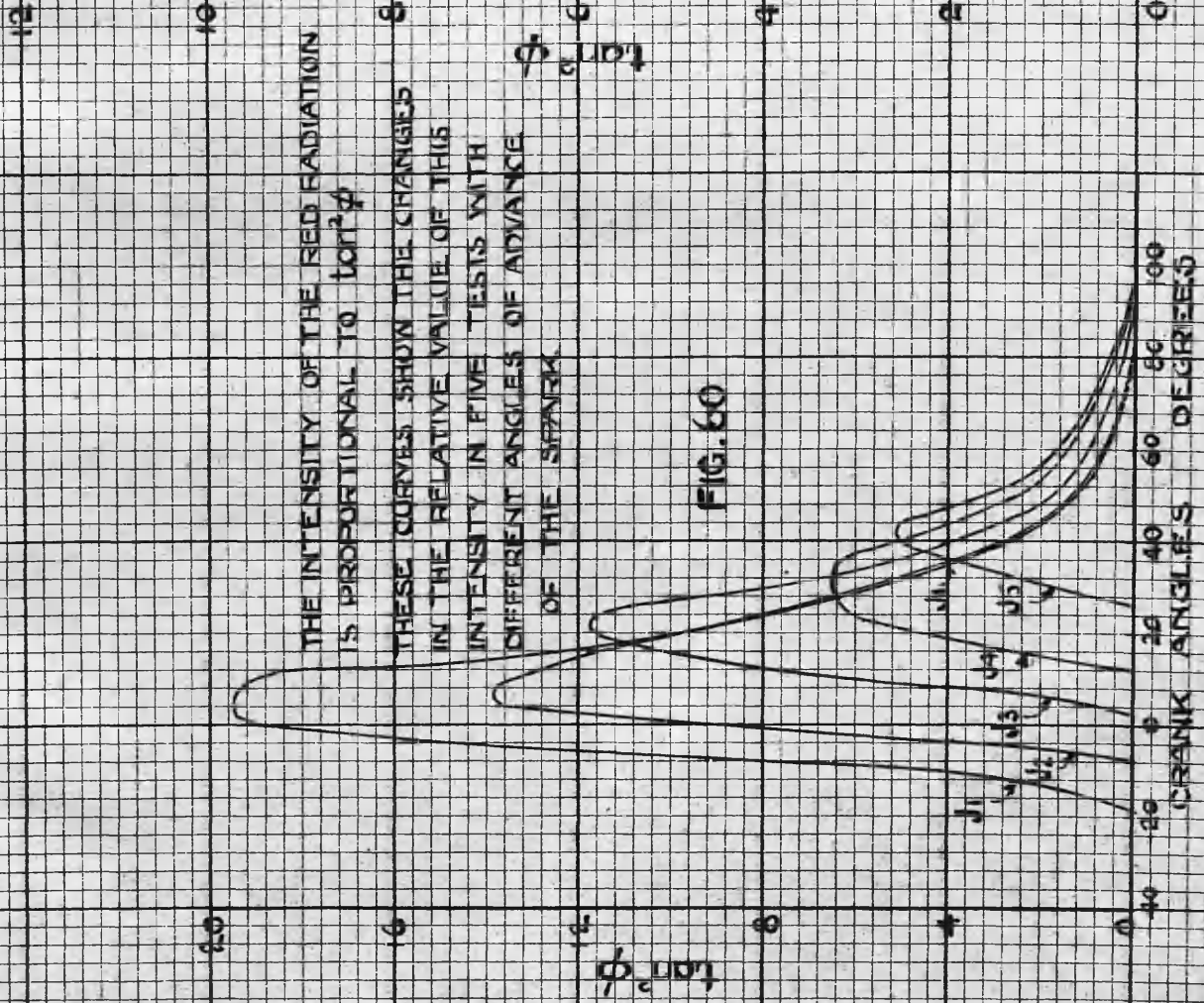


FIG. 60

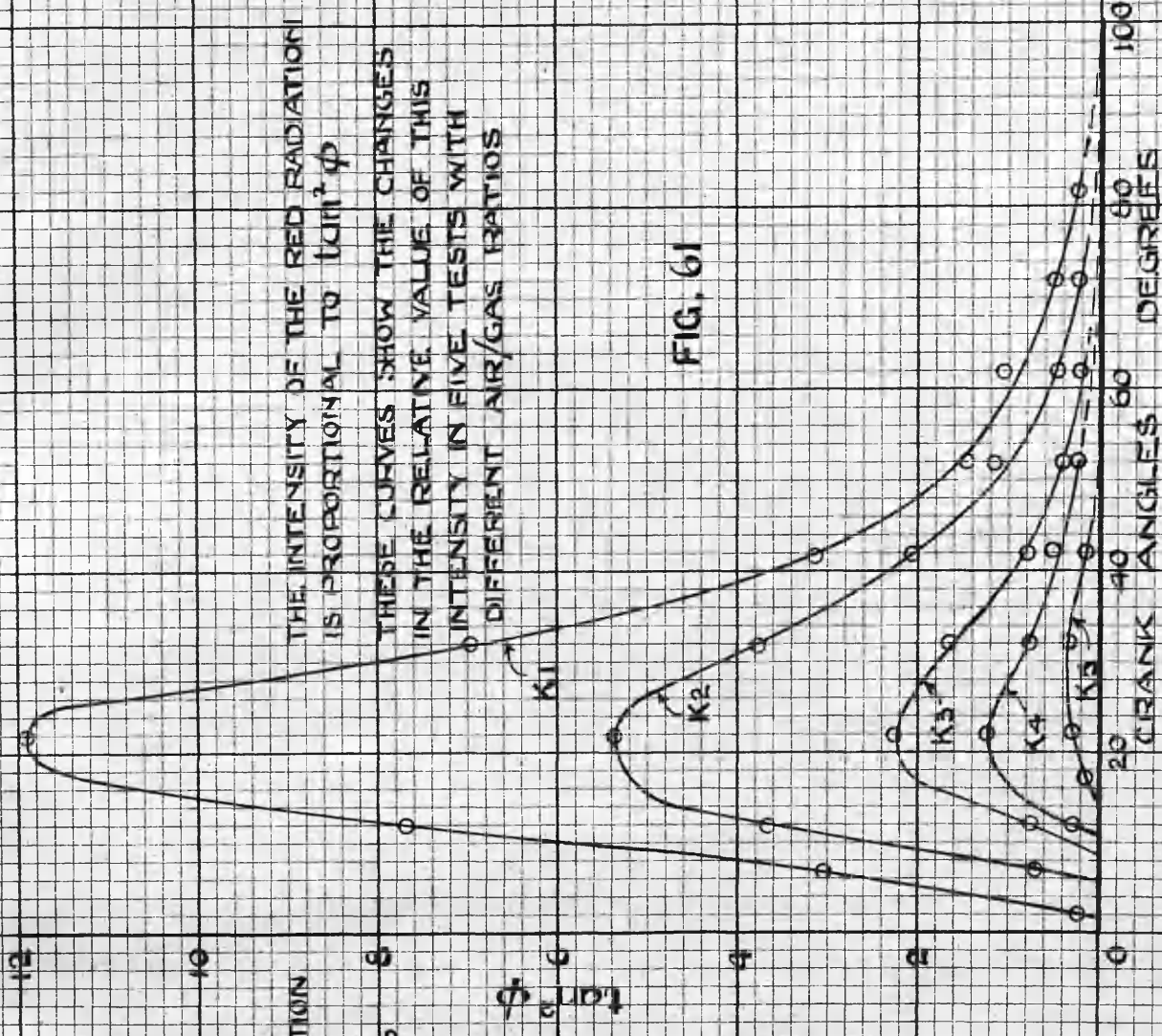


FIG. 61

from test to test, the chief factor no doubt being the air/gas ratio.

Variation in the total red radiation.

The tests of Series J were run at various angles of advance of the spark. Since the intensity of radiation is proportional to $\tan^2\phi$ it is of interest to note the variation of $\tan^2\phi$ with crank angle in the different cases. To this end the curves of Fig.60 p.104 were plotted. These curves are worthy of study in conjunction with the photographic record and the indicator diagrams obtained from a similar series of tests (D) pp.58 et seq. The same characteristics are discernible in both cases. As the spark is advanced the maximum intensity of the radiation goes up and the period of radiation is more prolonged. On expansion, however, the pressures, temperatures and intensities in those cases with an advanced spark are lower than in those with a later spark. This general characteristic is well sustained throughout all the tests dealt with in this report.

Now the intensity of radiation is a time-rate of dissipation of energy, and a scale of crank angles is really a scale of time. Hence the area under a curve of $\tan^2\phi$ is a measure of $\int E.dt$, or total energy radiated on the given wave-length during the radiant period.

Fig.62 is a curve of such areas taken from Fig.60 and plotted on a base of angle of advance of the spark. Here we see how excessive the radiated energy becomes at large angles of spark-advance.

In Fig.61 are plotted the $\tan^2\phi$ values for Series K and the areas under the curves are plotted on a base of air/gas in Fig.63. The very marked increase of radiated energy with increased strength of the mixture no doubt/

AREA UNDER INTENSITY CURVES IN²

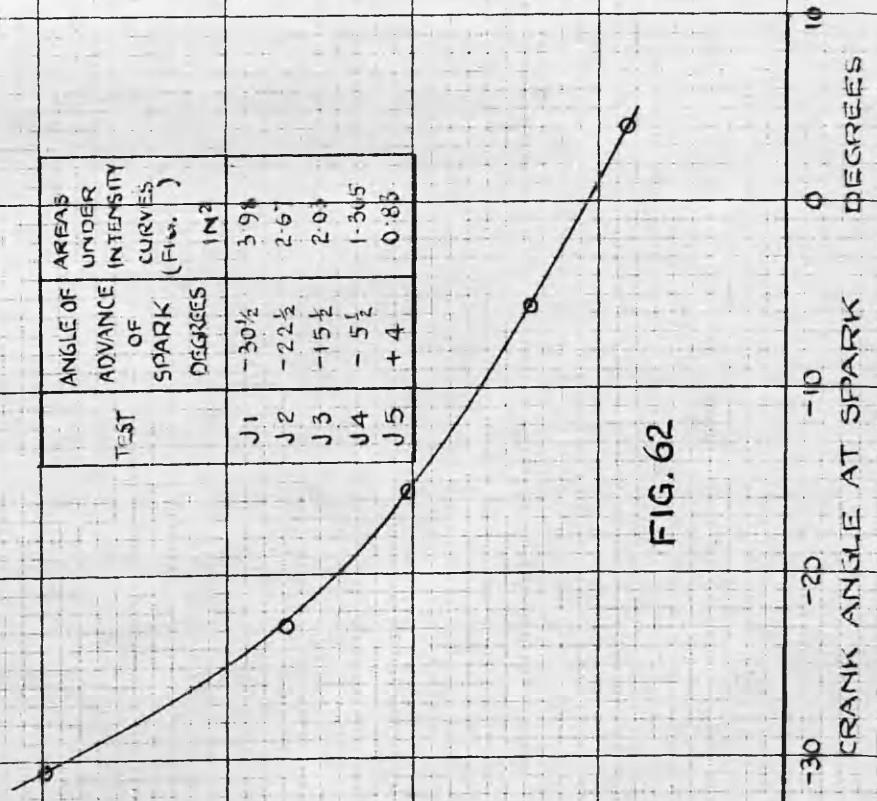


FIG. 62

AREA UNDER INTENSITY CURVES IN²

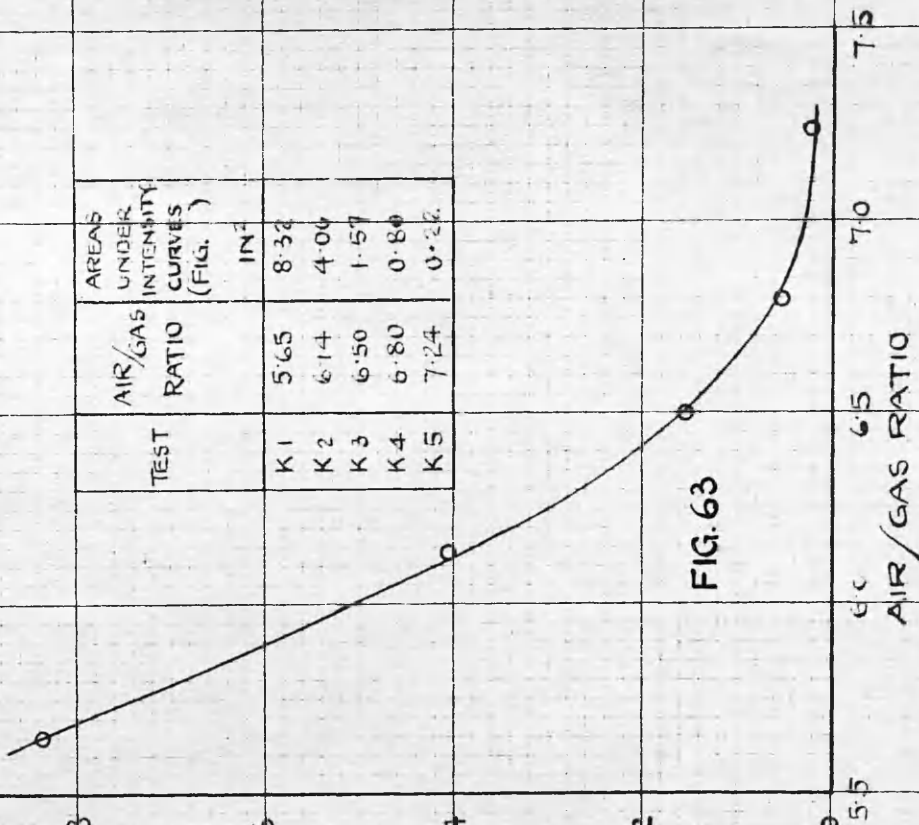


FIG. 63

AIR/GAS RATIO

doubt helps to explain the commonly accepted fact that weak mixtures give the best thermal efficiency.

It is scarcely permissible to generalise very broadly from the particular results of these tests, dealing as they do with only a narrow band of wave-lengths, but it is safe to assume that the intensity of radiation of any given wave-length increases and decreases along with - though not necessarily in proportion as - the total radiation on all wave-lengths.

Comment on theory of "after-burning".

It will be noticed that the curves of ϕ are very regular. Many of those who believe in the idea of "after-burning" support their belief with references to periods of an "isothermal" nature detectable on ordinary indicator cards at the beginning of the expansion curve. Here we have a property - the luminosity of combustion - capable of measurement by an instrument which is subject neither to friction nor to inertia, and in these tests it has afforded not the slightest evidence of a sustained chemical activity such as the "after-burning" theorists conceive.



The writer believes that these tests demonstrate that the repetitive nature of the engine-explosion can be used to measure the total radiation, and that they will lead to the construction of special apparatus for this purpose.



Acknowledgements.

The writer wishes to acknowledge the guidance and encouragement he has received from Professor W.J.Goudie, under whose supervision these tests were carried out. To Professor E.Taylor Jones he is indebted for the use of the polarising pyrometer and for the interest he has taken in the latter part of the work from the physicist's point of view. Thanks are due also to the mechanic, Mr. T. Paterson, not only for his efficient share in the making of the various special pieces of apparatus, but also for acting as the second observer in all the tests.